

DETECTION OF BOUND POLYCYCLIC AROMATIC  
HYDROCARBON RESIDUALS IN SOILS  
THROUGH DIRECT IMMUNOASSAY:  
A FEASIBILITY STUDY

BY

ALLEN G. TALLEY

Bachelor of Science

Kansas State University


Manhattan, Kansas

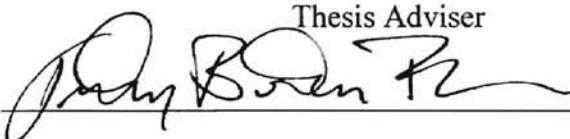
1969

Submitted to the Faculty of the  
Graduate College of the  
Oklahoma State University  
in partial fulfillment of  
the requirements for  
the Degree of  
MASTER OF SCIENCE  
May 1996

DETECTION OF BOUND POLYCYCLIC AROMATIC  
HYDROCARBON RESIDUALS IN SOILS  
THROUGH DIRECT IMMUNOASSAY:  
A FEASIBILITY STUDY

Thesis Approved:

  
\_\_\_\_\_  
Thesis Adviser

  
\_\_\_\_\_

  
\_\_\_\_\_

  
\_\_\_\_\_

  
\_\_\_\_\_  
Dean of the Graduate School

## PREFACE

Environmental immunoassay is the use of animal-derived antibodies that will specifically bind with targeted analytes, called antigens, to quantitatively measure levels of contamination of the analyte in the environment. Most commercially available forms of immunoassays require the analyte to be in solution. Therefore, for soil contaminants, the analyte must be extracted from the soil, usually by a strong solvent, prior to analysis. The potential inefficiency of the extraction process has led to the investigation of a method for direct detection in the solid phase.

This project deals strictly with testing potential assay procedures using monoclonal antibodies specific to naphthalene and polyclonal antibodies specific to pyrene. These antibodies were developed by Strategic Diagnostics, Inc. (SDI) under a joint agreement with Amoco Production Co. (APC). The testing of the antibodies for their ability to bind to the targeted analyte in solution and their cross reactivity, or ability to bind with other similar polycyclic aromatic hydrocarbons (PAH's), were tested exclusively by SDI, and only the results of these tests are discussed in this thesis.

Dextran, a chain of sugar molecules, was used as a surrogate antibody in establishing procedures. This was done because the newly developed antibodies used in this study were available in very small quantities. There would be few chances for adjusting procedures and re-testing, and careful preparation for testing was crucial.

## ACKNOWLEDGMENTS

I would like to express my gratitude to Dr. William McTernan for his support of me as a candidate for this project and his guidance throughout my graduate studies. His support inspired me to continue to pursue the degree of Masters in Environmental Engineering rather than to seek employment without completing the degree program.

I want to offer sincere thanks to Dr. John Veenstra for taking time out of his busy schedule to review my preliminary results and give me guidance in the direction of my research. His considerable knowledge of the mechanisms utilized in my research gave me confidence to continue in the direction I was going and to investigate new paths.

My appreciation goes to the many employees of Amoco Production Co. who graciously offered their time and interest to discuss my project and to offer help and advice. Dan Denham and John Corgan gave many suggestions and helped me with lab procedures. Dr. Lisa Sweeney's knowledge and reference material on immunology were invaluable. Dan Crosby instructed me on the use of the spectrophotometer, was a sounding board for ideas, and showed genuine interest in my project and its progress. Bruce Barnes performed many gas chromatography analyses. Dr. Marwin Kemp and Dr. Bob Harwood helped with my crude oil analysis. Paul Pettit's skill made it possible for me to continue my research when the spectrofluorometer lamp wouldn't ignite. I want to thank Dr. Nan Kemp, supervisor of the Environmental Research group, for supporting my research. To all of these individuals I extend my deepest appreciation.

A special thanks goes to Dr. Bert Fisher for serving as my thesis supervisor. His trust in me was greatly appreciated. He helped me set my goals but gave me my lead in

accomplishing them. We discussed my plans and he let me carry them out, offering suggestions along the way.

I would like to express my appreciation to the other graduate students working in the Environmental Research group. Their special help and camaraderie made this task a memorable experience. Donna Lautzenhiser gave me moral support and provided me with the benefit of her engineering knowledge and reference materials. Abhijeet Borole supported me with the benefit of his experience, knowledge, and friendship, and Miyoung Hammond kept us together as a group and our spirits high.

Finally, to my wife Louise, and my children Jenny and Ryan I give my love and thanks. Without their support this endeavor would not have been possible.

TABLE OF CONTENTS

CHAPTER I INTRODUCTION ..... 1

CHAPTER II LITERATURE REVIEW ..... 4

    Immunology ..... 4

    Fluorescence ..... 9

    Absorbance ..... 12

    Thermodynamics ..... 13

    Adsorption from Solution ..... 14

CHAPTER III EXPERIMENTAL APPARATUS ..... 22

    Introduction ..... 22

    Equipment ..... 22

CHAPTER IV EXPERIMENTAL MATERIALS AND METHODS ..... 28

    Adsorbents ..... 28

    Adsorbates ..... 30

    Solvents ..... 37

    Isotherm Procedure ..... 38

    Data Analysis ..... 41

    Spiking Procedures ..... 45

CHAPTER V RESULTS AND DISCUSSION ..... 48

    Non-specific Adsorption of Dextran-Eosin Conjugate on Clean Arkansas River  
         Sand and Arkansas River sand Spiked with Naphthalene ..... 48

    Non-Specific Adsorption of Dextran-Eosin Conjugate on Clean Ottawa Sand and  
         Ottawa Sand Spiked with Naphthalene ..... 52

Non-Specific Adsorption of Dextran-Eosin Conjugate on Arkansas River Sand Spiked with Arab Medium Crude Oil .....	56
Specific and Non-Specific Adsorption of Anti-Naphthalene Antibody on Clean Arkansas River Sand and Arkansas River Sand Spiked with Naphthalene .....	60
Specific and Non-Specific Adsorption of Anti-Pyrene Antibody and Negative Control Antibody on Arkansas River Sand Spiked with Pyrene .....	65
Evaluation of Commercially Available Immunoassay Field Test Kits Developed for Analysis of PAH Contamination to Soil .....	67
CHAPTER VI CONCLUSIONS .....	82
BIBLIOGRAPHY .....	85
APPENDIX A ISOTHERM DATA .....	87
APPENDIX B GAS CHROMATOGRAPH DATA.....	98
APPENDIX C ANTIBODY REACTIVITY DATA PROVIDED BY STRATEGIC DIAGNOSTICS.....	100

## LIST OF TABLES

TABLE I: CHARACTERISTICS OF SELECTED FLUOROPHORS.....	31
TABLE II: ANTIBODY CROSS-REACTIVITY COMPARISON.....	36
TABLE III: ANTIBODIES DEVELOPED BY STRATEGIC DIAGNOSTICS, INC. ....	37
TABLE IV: SPECTROFLUOROMETER SETTINGS .....	40
TABLE V: SAMPLE ISOTHERM DATA FOR CLEAN ARKANSAS RIVER SAND .....	49
TABLE VI: SAMPLE ISOTHERM DATA FOR CLEAN OTTAWA SAND.....	53
TABLE VII: COMPARISON OF QUANTIX SOIL IMMUNOASSAY RESULTS TO KNOWN SPIKED SAND LEVELS AND GC ANALYSES OF EXTRACTS....	71
TABLE VIII: COMPARISON OF QUANTIX SOIL IMMUNOASSAY RESULTS TO KNOWN PAH CONCENTRATIONS IN SOLUTION.....	72
TABLE IX: PAH RIS <sup>c</sup> ® SOIL TEST SENSITIVITY TO PAH COMPOUNDS.....	76
TABLE X: PYRENE ANALYSIS #1 AT 76 PPM.....	77
TABLE XI: PYRENE ANALYSIS #2 AT 76 PPM.....	78
TABLE XII: ANTI-NAPHTHALENE ANTIBODY ON CLEAN SAND .....	88
TABLE XIII: ANTI-PYRENE ANTIBODY ON PYRENE SPIKED SAND .....	92
TABLE XIV: NEGATIVE CONTROL ANTIBODY ON PYRENE SPIKED SAND.....	95
TABLE XV: CROSS REACTIVITY COMPARISON.....	107



LIST OF FIGURES

Figure 1.1: Flowchart showing the research structure ..... 3

Figure 2.1: The basic structure of IgG (Roitt, Brostoff, and Male, 1985) ..... 6

Figure 2.2: Good fit and poor fit between antigen and antibody ..... 7

Figure 2.3: Enzyme-Linked Immunosorbent Assay (ELISA) ..... 9

Figure 2.4: Langmuir model ..... 16

Figure 2.5: Linear plot of Langmuir model ..... 16

Figure 2.6: Brunauer, Emmett, and Teller multilayer adsorption model ..... 18

Figure 2.7: Linear plot of empirical data ..... 18

Figure 2.8: Freundlich empirical model ..... 19

Figure 2.9: Linear form of the Freundlich equation ..... 19

Figure 2.10: Schematic model of a region of a heterogeneous adsorbent showing equipotential surfaces ..... 20

Figure 2.11: Characteristic curve and isotherms ..... 20

Figure 3.1: Schematic drawing of the McPherson Instruments, FL-750 Spectrofluorescence Detector ..... 23

Figure 4.1: Background fluorescence produced by Arkansas River Sand tumbled in deionized water ..... 29

Figure 4.2: Comparison of particle size distributions of washed Arkansas River sand and washed Ottawa sand ..... 30

Figure 4.3: Calibration curve for Dextran-eosin conjugate ..... 32

Figure 4.4: Calibration curve for Ab-EITC conjugate ..... 32

Figure 4.5: Naphthalene molecular configuration ..... 33

Figure 4.6: Pyrene molecular configuration .....	33
Figure 4.7: Anthracene molecular configuration .....	34
Figure 4.8: Residual concentration of dextran-eosin with time when tumbled with Arkansas river sand. ....	39
Figure 4.9: DC bias is removed by subtracting the voltage values of the DC bias curve from the data curve. ....	42
Figure 4.10: Total recorded output of eosin at 300 ppb and background .....	43
Figure 4.11: Composite plot showing separate background and eosin emissions curves and the summation of the two .....	43
Figure 4.12: Composite plot showing converging backgrounds .....	44
Figure 4.13: Converged backgrounds - pure signal equals output signal .....	44
Figure 5.1: Combined Freundlich plots of four isotherms of DEC on Arkansas River sand .....	50
Figure 5.2: Combined Freundlich plot of two sets of isotherms on clean Ottawa sand and Ottawa sand spiked with naphthalene .....	53
Figure 5.3: Composite Freundlich isotherm plots comparing ARS adsorption to Ottawa sand adsorption .....	56
Figure 5.4: Freundlich isotherm plots of ARS spiked with Arab crude oil over a range of concentrations .....	57
Figure 5.5: Freundlich isotherm plots of ARS spiked with Arab medium crude oil over a range of concentrations .....	58
Figure 5.6: Crude oil content in percent by weight vs. Log of adsorbed concentration ...	59
Figure 5.7: Isotherm data for anti-naphthalene antibody on clean ARS .....	61
Figure 5.8: Composite Freundlich plots comparing three isotherms of Anti-naphthalene antibody on Arkansas River Sand .....	62
Figure 5.9: Cross plot of Anti-Naphthalene antibody isotherm data with lines of equal $\Delta G^\circ$ values in calories per mole .....	64

Figure 5.10: Freundlich isotherms of Anti-Pyrene antibody vs. Negative Control antibody on pyrene spiked ARS .....	66
Figure 5.11: Langmuir high plot of Anti-Pyrene antibody vs. negative control antibody on pyrene spiked ARS .....	66
Figure 5.12: Quantix immunoassay detector .....	69
Figure 5.13 Process flow diagram for the Quantix field test kit.....	70
Figure 5.14: Process flow diagram of the Ensis RIS <sup>c</sup> ® kit.....	74
Figure 5.15: EnSys RIS <sup>c</sup> ® test data for first pyrene sample at 76 ppm .....	78
Figure 5.16: EnSys RIS <sup>c</sup> ® test data for second pyrene sample at 76 ppm .....	79
Figure A.1: Cross plot of isotherm data for anti-naphthalene antibody on ARS.....	88
Figure A.2: Freundlich isotherm of anti-naphthalene antibody.....	89
Figure A.3: Langmuir high isotherm of anti-naphthalene antibody on ARS .....	89
Figure A.4: Langmuir low isotherm of anti-naphthalene antibody on ARS.....	90
Figure A.5: BET isotherm of anti-naphthalene antibody on ARS.....	90
Figure A.6: Polanyi adsorption theory characteristic curve of anti-naphthalene adsorption isotherm on ARS.....	91
Figure A.7: Cross plot of isotherm data for Anti-Pyrene antibody on pyrene spiked ARS.....	92
Figure A.8: Freundlich isotherm plot of Anti-Pyrene antibody on ARS spiked with pyrene .....	93
Figure A.9: High Langmuir isotherm of Anti-Pyrene antibody on ARS spiked with pyrene.....	93
Figure A.10: Low Langmuir isotherm of Anti-Pyrene antibody on ARS spiked with pyrene.....	94
Figure A.11: BET isotherm of Anti-Pyrene antibody on ARS spiked with pyrene .....	94
Figure A.12: Cross plot of isotherm data for Negative Control antibody on pyrene spiked ARS.....	95

Figure A.13: Freundlich isotherm plot of Negative Control antibody on ARS spiked with pyrene.....	96
Figure A.14: High Langmuir isotherm of Negative Control antibody on ARS spiked with Pyrene .....	96
Figure A.15: Low Langmuir isotherm of Negative Control antibody on ARS spiked with Pyrene .....	97
Figure A.16: BET isotherm of Negative Control antibody on ARS spiked with Pyrene .....	97
Figure B.1: Geochemistry Analysis of Arab Medium Crude Oil .....	99
Figure C.1: Antigen-Coated Plate Competition ELISA .....	102
Figure C.2: Labeled Analyte Competition ELISA .....	103
Figure C.3: Benzo(b)fluoranthene Inhibition ELISA .....	104
Figure C.4: Acenaphthene Inhibition ELISA .....	104
Figure C.5: Benzo(a)pyrene Inhibition ELISA.....	105
Figure C.6: Fluorene Inhibition ELISA .....	105
Figure C.7: Pyrene Inhibition ELISA .....	106
Figure C.8: Naphthalene Inhibition of N1 Monoclonal.....	108

## CHAPTER I

### INTRODUCTION

Polycyclic aromatic hydrocarbons (PAH's) are by-products of industrial and energy conversion processes. They are hazardous components of creosote and oil refinery wastes. Several of these hydrocarbons are carcinogenic in microbial and mammalian tests (National Research Council, 1983). Because some PAH's are known carcinogens, Federal and State regulatory agencies may require clean-up of many of these sites.

The use of immunoassays as rapid on-site indicators of hazardous contaminants in the environment is extremely attractive due to their low cost. There is a need for rapid, accurate and precise analytical methods to characterize contaminants, determine movement of contamination in the environment, and to monitor cleanup efforts as they proceed. The standard laboratory methods usually employed for PAH analysis, EPA methods 8270, Gas Chromatograph/mass spectrometry (GC/MS) and 8310, high pressure liquid chromatography (HPLC), are relatively expensive, typically \$200-\$500 per sample, and suffer from a long turnaround time.

Immunoassays are analytical techniques based on the specific and high affinity binding of animal-derived antibodies with particular target molecules called antigens (Miller *et al.*, 1992). Binding between antibodies and target antigens, coupled with the use of indicator compounds and simple instrumentation for reading the response, form the basis of the immunoassay.

A wide variety of immunoassay formats have been developed to allow either visual or instrumental measurement of antibody-antigen binding. With rare exception these

formats require soil analysis to be preceded by an extraction step (Miller *et al.*, 1992). The efficiency of these extraction processes varies between 75% to 100%. Extraction efficiency depends on extraction method and soil type and has a bearing on assay time and accuracy (Krahn *et al.*, 1991). For this reason alone, investigation of a method for direct immunoassay of soil-bound analytes is a logical step in improving the accuracy of an assay.

The objective of this research was to evaluate the ability of antibodies biologically engineered to be specific to naphthalene and pyrene to bind with these PAHs in the solid phase and, if feasible, design a solid phase assay that can be used on site. Adsorption isotherms were the investigative method chosen to evaluate specific and non-specific adsorption of the antibodies on a soil matrix. Arkansas river sand washed of clays and organic matter was used as a simple soil matrix for the investigation. Dextran, a chain of sugar molecules, was used as a surrogate antibody to establish isotherm procedures, to conserve antibody supply, and to study non-specific adsorption. Fluorescent compounds, eosin-5-isothiocyanate conjugated with dextran and erythrosin-5-isothiocyanate conjugated with the antibodies, were used as tags to measure their respective concentrations in solution.

An evaluation of two commercially available immunoassay kits for the detection of PAH's in soils and in water is included in this study. This evaluation was intended as an example of the current state of the art of this technology. Figure 1.1 is a flowchart itemizing the research structure.

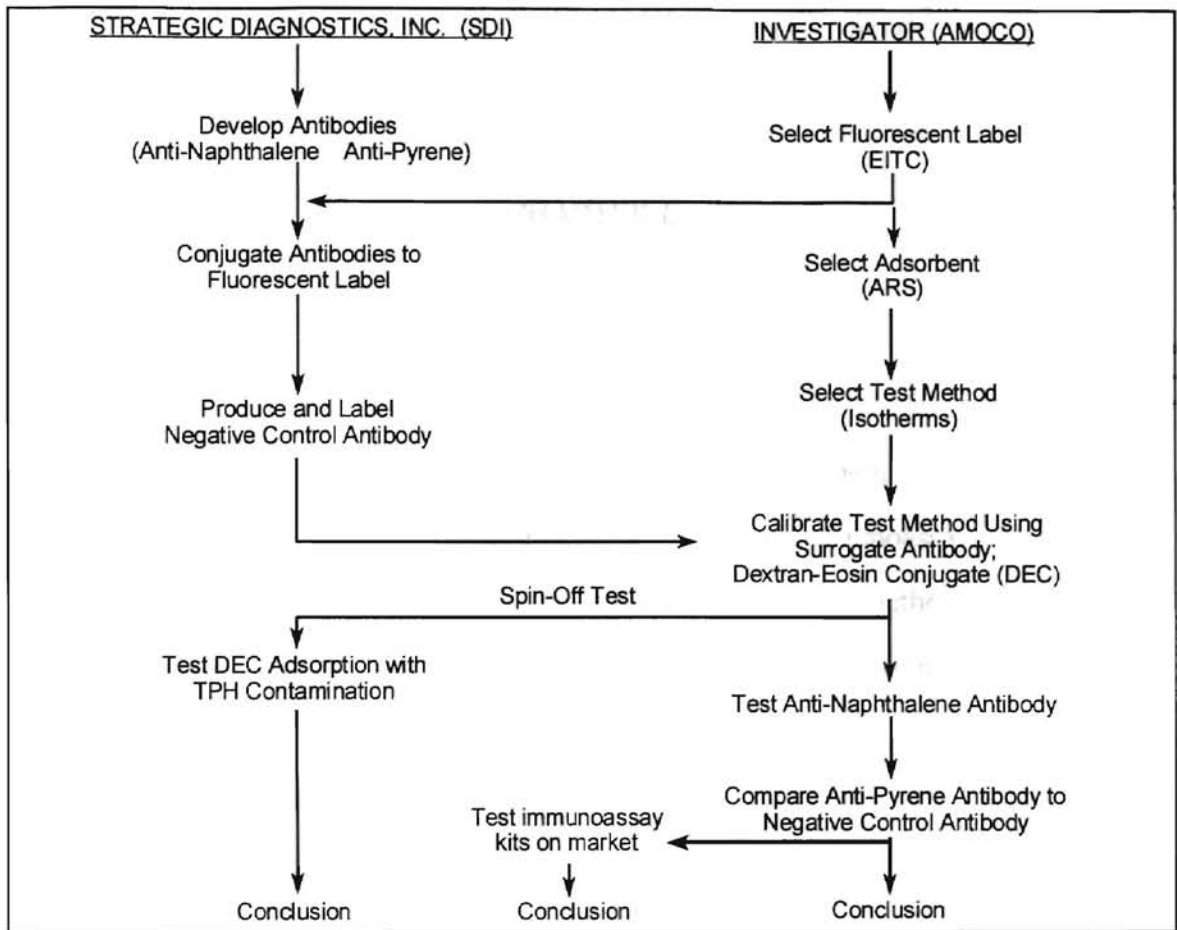


**Figure 1.1:** Flowchart showing the research structure. The spin-off test was an addition to the original structure.

## CHAPTER II

### LITERATURE REVIEW

The purpose of this section is to review the biological, chemical, and physical phenomena involved in quantifying an analyte substance by immunoassay. Fluorescence labeling, as used in this study, can be a highly sensitive detection method for determining concentrations of an analyte in solution, and is used in solid phase immunoassay (Stave, 1994). Fluorescence labeling is not the method currently used in field test kits by many major kit manufacturers, including Quantix, EnSys, and Millipore. Calorimetric detection is more commonly used due to the ability to utilize less sophisticated and less costly field equipment such as portable reflectometers, and is not hampered by the potential interferences to fluorescence measurements which are discussed in this chapter (EnSys, Inc., 1994). Absorbance measurement, which was used to measure concentrations in solution, is related to the calorimetric methods utilized by EnSys in their immunoassay kits. Adsorption isotherms were used as a developmental tool. They were chosen for this study as a means of comparing adsorption results while providing a method of determining the reliability of those results. Immunoassay methods in general rely on single sample data and are subject to variability. The user may average out random variability by repeating the test on one sample, however, this could become quite expensive, and highly accurate laboratory methods (gas chromatograph, mass spectrometer) are becoming faster and cheaper.



## Immunology

The immune system's principle function is to protect animals from infectious organisms and their toxic products (Harlow and Lane, 1988). The adaptive immune system produces a specific reaction to each infectious agent (antigen) (Roitt, Brostoff, and Male, 1985). A key feature of the immune system is its ability to synthesize a vast number of antibodies. Antibodies are proteins produced generally in response to an infection, with highly specific binding sites on which to bind and neutralize the infecting intruder. Bonding of the antibodies to foreign molecules provides the basis for the specificity of the immune response (Harlow and Lane, 1988) and is the basis for immunoassay techniques.

### Antibody Structure

The basic structure of all antibody molecules (immunoglobulins) is a unit consisting of two identical light polypeptide chains and two identical heavy polypeptide chains linked together by disulfide bonds. Five distinct classes of immunoglobulins (Ig) are recognized in most higher mammals (e.g. mice, rabbits), namely IgG, IgA, IgM, IgD and IgE. Each of these classes has a specific role in the immune response system. The IgG class accounts for 70-75% of the total antibody pool, is the major antibody of the adaptive immune system, and is the exclusive anti-toxin class (Roitt, Brostoff, and Male, 1985). The two regions that carry the antigen binding sites are known as Fab fragments, named for the *f*ragment having the *a*ntigen *b*inding site. The part that is involved in immune regulation is termed the Fc fragment for the *f*ragment that *c*rystallizes (Harlow and Lane, 1988). Figure 2.1 is a schematic of the structure of the IgG class antibody. The characteristic "Y" shape contains two antigen binding sites. The Fc region will readily bind to surfaces such as polystyrene, leaving the antigen binding sites free (Harlow and Lane, 1988).

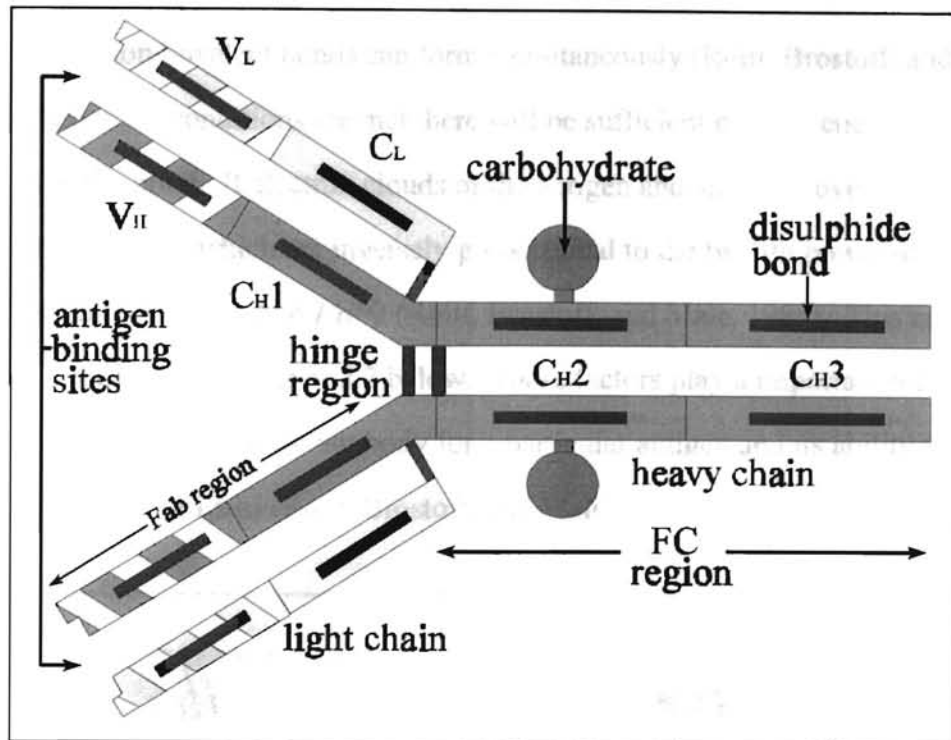


Figure 2.1 The basic structure of IgG. ( Roitt, Brostoff, and Male, 1985)

### Specific Binding

Antigens bind to antibodies by the formation of multiple non-covalent bonds. Although the attractive forces (hydrogen bonds, electrostatic, Van der Waals, and hydrophobic) involved in these bonds are weak by comparison with covalent bonds, the multiplicity of the bonds results in considerable binding energy (Roitt, Brostoff, and Male, 1985). The non-covalent bonds are dependent on the distance  $d$  between the interacting groups. The force is proportional to  $1/d^2$  for electrostatic forces and to  $1/d^7$  for Van der Waals forces; thus the interacting groups must be close in molecular terms, close enough to exclude water molecules, before these forces become significant (Roitt, Brostoff, and Male, 1985). The antibody and the antigen combining site must have complementary structures to be able to combine. In other words, two conditions must be met; (a) There must be suitable atomic groupings to form multiple non-covalent bonds on opposing parts of the antigen and antibody, and (b) the shape of the combining site must fit the antigen

so that several non-covalent bonds can form simultaneously (Roitt, Brostoff, and Male, 1985). When these conditions are met there will be sufficient binding energy to resist disruption of the bond. If electron clouds of the antigen and antibody overlap, repulsive forces come into play which are inversely proportional to the twelfth power of the distance between the clouds ( $F \propto 1/d^{12}$ ) (Roitt, Brostoff, and Male, 1985). This concept is schematically depicted in Figure 2.2 below. These factors play a important role in determining the specificity of the antibody for a particular antigen and its ability to discriminate between antigens (Roitt, Brostoff, and Male, 1985).

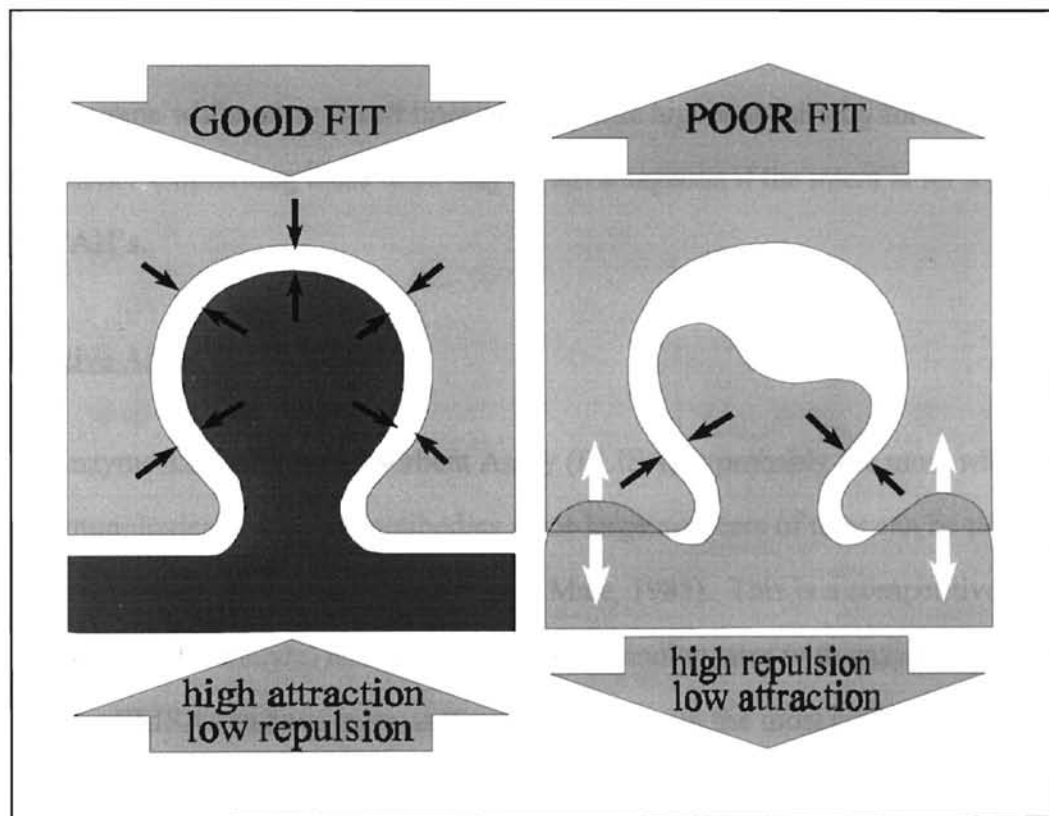


Figure 2.2 Good fit and poor fit between antigen and antibody (Roitt, Brostoff, and Male, 1985)

Since receptors on any one antibody can only bind to one antigen, it is easily seen how the immune system responds specifically to a particular antigen.

Antibodies are produced by B-cells. When B-cell surface antibodies bind to antigens, the B-cells are activated to secrete antibodies (Harlow and Lane, 1988). Antibodies develop complementary structures conforming to the shape of the antigen or to a side chain or protrusion called an epitope (Roitt, Brostoff, and Male, 1985). Through a screening process, B-cells that produce antibodies that are highly specific to a targeted antigen can be isolated (Stave, 1983). Antibodies isolated and reproduced in this way are called monoclonal because they are produced from a single line of B-cells (monogenetic) and their antigen specificity is the same. When several lines of B-cell are isolated because of their specificity to a variety of similar antigens they are called polyclonal. (Stave, 1983). For example, an antibody from one line of B-cells may have higher specificity for pyrene while other B-cell lines may provide higher specificity for naphthalene or anthracene. Combining these lines may be advantageous if the intent is for a general test for PAH's.

### Competitive Assay

Enzyme-Linked Immunosorbent Assay (ELISA) is probably the most widely used of all immunological assays for antibodies since large numbers of tests can be performed in a relatively short time (Roitt, Brostoff, and Male, 1985). This is a competitive assay where antigens (the analyte) compete for antibody binding sites with enzyme-labeled antigens. The ELISA can have many different protocols. In the most commonly used form (Figure 2.3), the antibody is immobilized on a surface, (e.g. polystyrene plates, inside test tubes, etc.) (Harlow and Lane, 1988). The analyte solution is mixed with an enzyme-labeled antigen, commonly a reactive antigen conjugated to either horseradish peroxidase (HRP), alkaline phosphatase (AP), or  $\beta$ -galactosidase (Brock and Madigan, 1991, Stave, 1994). This combined solution is introduced to the antibody. The analyte and the enzyme-labeled antigen compete for binding sites on the antibody. The binding sites are

taken up in proportion to the respective concentrations of the competing substances. A color developer is added that converts to a soluble colored product in the presence of the enzyme. The amount of color developed is inversely proportional to the amount of antigen present (or directly proportional to the amount of enzyme present).

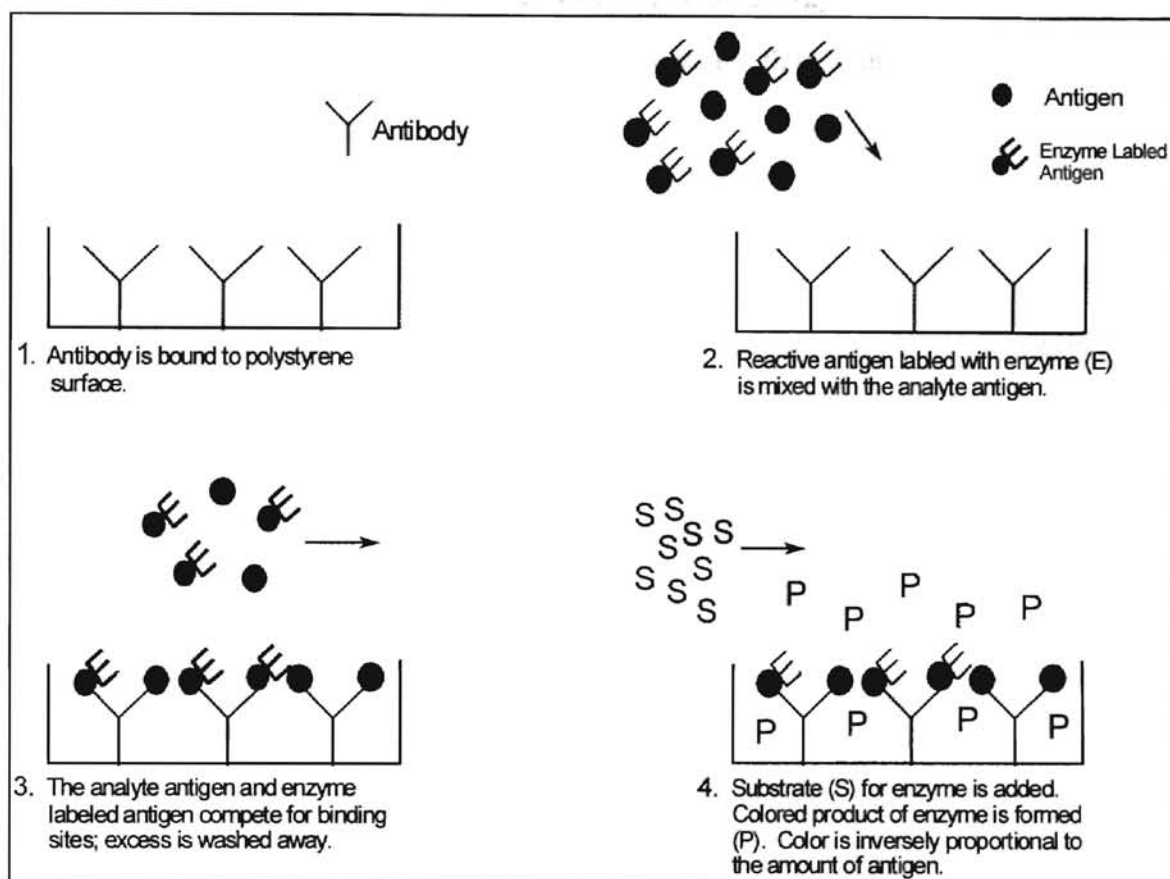


**Figure 2.3** Enzyme-linked immunosorbent assay (ELISA). Single antibody method. Adapted from Brock & Madigan (1988).

## Fluorescence

In any molecule, an electron can pass from a lower energy level to a higher one by absorbing an integral quantum of light which is equal in energy to the difference between the two energy states (Udenfriend, 1962). When electrons receive such energy promotions, the molecule is referred to as being in an excited state. During the time the mole-

cule can spend in the excited state, about  $10^{-4}$  second, some energy in excess of the lowest vibrational energy level is dissipated, through collision with other molecules. If all the excess energy is not dissipated the lowest vibrational level of the excited state is attained and the electron returns to the ground electronic state with the emission of energy. This phenomenon is called fluorescence. Because some energy is lost in the brief period before emission, the emitted energy is of longer wavelength than the energy that was absorbed (Guilbault, 1973).

### Rayleigh Scattering

Light, of a frequency which is incapable of producing a transition to an excited electronic state, is nevertheless capable of being absorbed by the molecule. An absorbed photon of energy excites an electron from its ground state to a higher vibrational level. Since there is no electronic transition, energy is entirely conserved and a photon of the same energy is re-emitted within  $10^{-15}$  second, while the electron returns to its original state. Since the absorbed and emitted photons are of the same energy, the emitted light has the same wavelength as the exciting light. Light emitted in this manner is referred to as Rayleigh scattering. It occurs at all wavelengths and its intensity varies inversely with the fourth power of the wavelength ( $I \propto 1/\lambda^4$ ). Vibrational excitation, leading to Rayleigh scattering, influences a large proportion of the molecules in a solution as compared to electronic excitation, which produces relatively few excited molecules (Udenfriend, 1962).

### Raman Effect

The Raman effect, discovered by C. V. Raman while determining why water appears blue, is related to Rayleigh scattering. An electron absorbs a photon of energy producing vibrational excitation. Vibrational energy may be added or subtracted to this pho-

ton depending upon the characteristic frequency of the electronic state. Energy is emitted at specific levels greater than and less than the exciting energy. The energy difference is characteristic of a given molecular structure and is independent of the energy of the exciting light. In liquids, the Raman bands are much fainter than the Rayleigh scatter peak (Guilbault, 1973).

### Fluorescence Quenching

True quenching is not related to absorption or light scattering, but is due to an interaction of the fluorescent molecule with solvent or with other solutes in such a manner as to lower the efficiency and or lifetime of the fluorescence process. Quenching is not random; each instance is indicative of rather specific chemical interactions.

The presence in solution of a second molecule which absorbs radiation at or near the wavelength emitted by the fluorophor will in some instances lead to a decrease in the fluorescence. This type of quenching is due to transfer of the energy from the fluorophor to the second absorbing species. The second molecule may re-emit the energy as heat, it may dissociate, or it may emit its own fluorescence (Udenfriend, 1962).

### Reabsorption Interference

When the fluorophor is present in high concentrations, a significant amount of the fluorescence radiation can be reabsorbed. Such reabsorption diminishes the observed fluorescence. This is termed the "inner filter" (Udenfriend, 1962). A plot of concentration versus strength of fluorescence radiation made from serial dilutions of a known concentration can indicate if inner filtering is a problem. Conjugation of a fluorophor to a protein can change this relationship do to interactions between the two molecules (Molecular Probes, 1994)

## Fluorescent Spectra

Fluorescent molecules have two distinct spectra called the absorption spectrum and the emission spectrum. The absorption spectrum is the range of excitation wavelength capable of producing fluorescence, while the emission spectrum is the relative intensity of fluorescence emitted at various wavelengths. The difference between these two spectra is called the Stokes loss and represents the energy dissipated during the lifetime of the excited state (Guilbault, 1973). Larger Stokes losses make possible observation of fluorescence spectra without interference from scattering effects. Since scattering effects occur at and on either side of the excitation wavelength, and the emission spectrum remains constant, greater separation can be achieved by setting the excitation wavelength toward the lower end of the absorption wavelength spectrum.

### Absorbance

Optical methods can be used to determine the concentration of many dissolved substances. The Beer-Lambert Law, better known as "Beer's Law" relates the amount of light transmitted by a solution to the concentration of a light absorbing substance in that solution:

$$\log \frac{I_0}{I} = A = \epsilon b C$$

where  $I_0$  = intensity of monochromatic light transmitted through the reference solution

$I$  = intensity of the same light transmitted through the test solution

$A$  = absorbance (dimensionless)

$\epsilon$  = absorptivity or molecular extinction coefficient, a constant for a given solute/solvent and a given wavelength (L/g•cm) or (L/mole•cm) (Veenstra, 1993).

$b$  = light path (cm)

$C$  = Concentration of solute (g/L) or (moles/L)



## Thermodynamics

Adsorption, a primary component of this study, involves many of the properties of thermodynamics. In the following discussion, each of the thermodynamic properties are related to adsorption. In Chapter V is a discussion of the change in free energy associated with naphthalene adsorption. This warrants a brief background discussion of thermodynamics.

### Enthalpy

Enthalpy is a concept developed for constant pressure systems like our environment. The quantity of heat absorbed by a system at constant temperature and pressure is equal to the change in system enthalpy (Sawyer & McCarty, 1978). A change in system enthalpy occurs during adsorption called the heat of adsorption.

### Entropy

The second law of thermodynamics is that all systems tend to approach a state of equilibrium. Entropy is concerned with the spontaneity of physical and chemical changes. It is a measure of the chaotic nature (disorder) of a system. As the system becomes more disordered the entropy increases. Entropy is at maximum at equilibrium (Look & Sauer, 1986). Adsorption isotherms represent a state of maximum entropy.

### Free Energy

Free energies can be used to determine the equilibrium state to which a reaction carries the system, as well as the reaction direction (Sawyer and McCarty, 1978). The change in free energy ( $\Delta G$ ) is defined as:

$$\Delta G = \Delta H - T\Delta S$$

where  $\Delta H$  is the change in enthalpy,  $T$  is absolute temperature, and  $\Delta S$  is the change in entropy. Sawyer and McCarty (1978) describe the change in free energy from an equilibrium reaction as follows:



At equilibrium the rate of the forward reaction is equal to the rate of the reverse reaction and the concentration of reactants and products is constant. The change in free energy of this reaction, is given by the equation

$$\Delta G^\circ = -RT \ln \frac{\{C\}^c \{D\}^d}{\{A\}^a \{B\}^b} \text{equilibrium}$$

where  $\Delta G^\circ$  is the standard free energy change,  $R$  is the universal gas constant, and  $T$  is the absolute temperature. The concentration of the various reactants and products can be expressed as

$$\frac{\{C\}^c \{D\}^d}{\{A\}^a \{B\}^b} = K$$

where  $K$  is the equilibrium constant. Thus

$$\Delta G^\circ = -RT \ln K.$$

### Adsorption from Solution

Adsorption is transfer of material from a gas or liquid phase to a surface. The surface may be a liquid or a solid. The substance being concentrated on the surface is termed the *adsorbate*; the material on which the adsorbate accumulates is termed the *adsorbent* (Hines & Maddox, 1985). Adsorbate is bound to adsorbent by intermolecular forces. Physical adsorption results when the adsorbate adheres to the surface by Van der Waals (Hines & Maddox, 1985), hydrophobic, and electrostatic forces. A displacement of the electron cloud occurs and a quantity of heat is given off called the *heat of adsorption*. Chemical adsorption involves the sharing of electrons between the adsorbate and

the adsorbent. In this case the quantity of heat released approximately equals the heat of reaction (Hines & Maddox, 1985).

### Isotherms

An isotherm is an equilibrium relationship between the amount of solute adsorbed on the surface of a solid and the concentration of solute remaining in solution at a given temperature (Adamson, 1976). Four isotherm models will be discussed, (a) the Langmuir isotherm which is a monolayer adsorption model limiting the amount of solute that can be adsorbed, (b) the BET isotherm after Brunauer, Emmett, and Teller, which is characteristic of the formation of multiple layers of adsorbate molecules, (c) the Freundlich isotherm which, according to some authors, is not limited to a monolayer and does not fit any particular mechanism (Adamson, 1976 and Hiemenz, 1977) but is widely used in low to intermediate concentration ranges, and (d) Polanyi adsorption potential which is a multilayer approach, but differs from the other models because of its thermodynamic approach (Hines & Maddox, 1985). These models represent a means of interpreting the isotherm data. If there is a good fit to a particular model, the empirical constants used in the model may have physical meaning. The environmental isotherms in this study are not definitive enough to fit any one model particularly well. Therefore, they are just a convenient way to compare adsorption results.

### Langmuir Isotherms

Langmuir (1918) proposed a model that quantitatively described the volume of gas adsorbed onto an open surface. His model includes the following assumptions:

1. All the sites of the solid have the same activity for adsorption.
2. There is no interaction between adsorbed molecules.

3. All of the adsorption occurs by the same mechanism, and each adsorbent complex has the same structure.
4. The extent of adsorption is no more than one monomolecular layer on the surface (Hiemenz, 1977).

Veenstra (1993) derives the Langmuir equation as

$$q = \frac{Q_o bC}{1 + bC}$$

where  $q$  equals mass of solute adsorbed per mass of adsorbent,  $Q_o$  is the maximum monolayer adsorption capacity,  $b = K_1/K_2$  and is the ratio of the forward reaction constant to the reverse reaction constant, and  $C$  is the concentration of the solute in solution.

The linear form becomes

$$\frac{C}{q} = \frac{1}{bQ_o} + \frac{1}{Q_o}C.$$

Figure 2.4 is a graphical presentation of the Langmuir model.  $Q_o$  is the limiting concentration determined by the forming of a single layer of adsorbate on the adsorbent surface. Figure 2.5 is the linear presentation of the model.

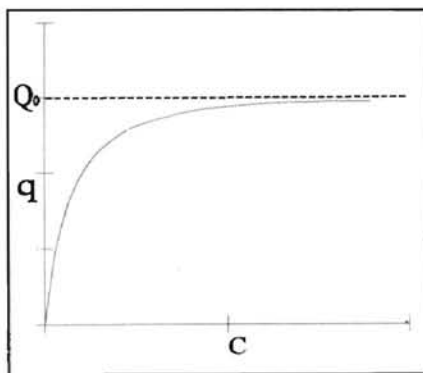


Figure 2.4: Langmuir model

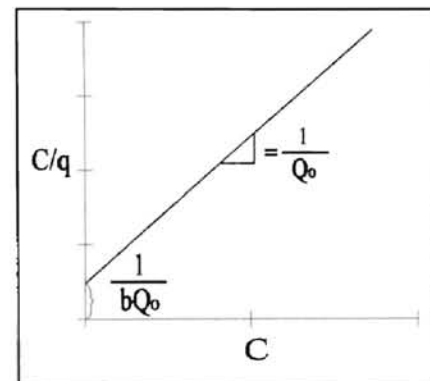


Figure 2.5: Linear plot of Langmuir model

The Langmuir derivation describes the adsorbed molecules interacting with the surface but not with each other. The adsorbed layer is assumed to be ideal. Once the surface is covered with adsorbed molecules, the surface has no further influence on the system.

### BET Isotherms

Brunauer, Emmett, and Teller extended Langmuir's approach to multilayer adsorption common to many nonporous solids. Their derivation became known as the BET equation. The basic assumption is that the Langmuir equation applies to each layer (Adamson, 1976). Adamson (1976) does an extensive treatment of the derivation of the BET equation. The derivation by Veenstra (1993) is more convenient since the terms are consistent with the previous model.

$$q = \frac{Q_o K_B C}{(C_s - C)[1 + (K_B - 1)(C/C_s)]}$$

where  $K_B$  is a constant related to energy of adsorption,  $C$  is the concentration of the solute at equilibrium,  $Q_o$  is the monolayer adsorption capacity, and  $q$  is the equilibrium adsorption capacity at concentration  $C$ , and  $C_s$  is the concentration at saturation. The linear form of this equation follows.

$$\frac{1}{(C_s - C)q} = \frac{1}{K_B Q_o} + \frac{K_B - 1}{K_B Q_o} \frac{C}{C_s}$$

If adsorption fits the multilayer BET model, a plot of  $1/(C_s - C)q$  versus  $C/C_s$  using  $C_o$ , the initial concentration of the solute, in place of  $C_s$  will yield a straight line from which the constants  $K_B$  and  $Q_o$  can be empirically derived from the slope and the intercept. Figures 2.6 and 2.7 are the graphical representations of these forms.

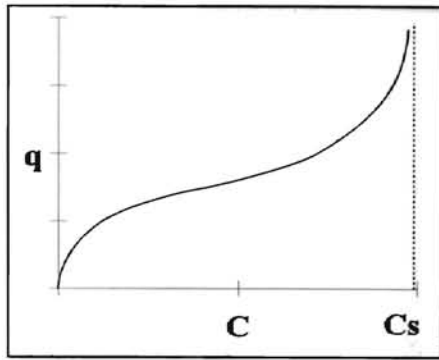


**Figure 2.6:** Brunauer, Emmett, and Teller multilayer adsorption

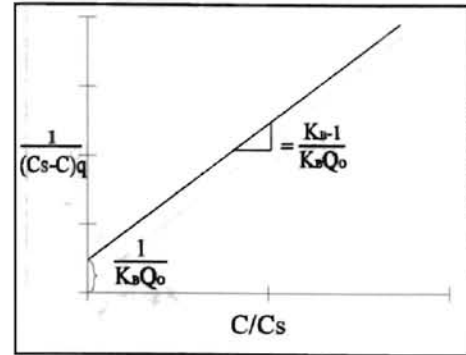


**Figure 2.7:** linear plot of empirical data

### Freundlich Isotherms

The Freundlich isotherm is an empirical model that was in use long before the interpretation of a certain distribution of sites was assigned to it. It does not presume a limit to adsorption capacity imposed by the formation of a monolayer (Hiemenz, 1977).

The Freundlich isotherm is given by the expression

$$q = KC^{1/n}$$

in which  $q$  is the mass of solute adsorbed per mass of adsorbent,  $C$  is the concentration of solute, and  $K$  and  $n$  are constants with  $n > 1$  (Figure 2.8). The constants may be evaluated from the slope and intercept of a log-log plot of  $q$  versus  $C$  (Veenstra, 1993) (Figure 2.9). The Freundlich equation, unlike the Langmuir equation, does not become linear at low concentrations but remains convex to the concentration axis; nor does it show a saturation or limiting value (Adamson, 1976). Benefield, *et al.* (1982) have suggested that the system that can be modeled by the Freundlich equation may be an example of monolayer adsorption at heterogeneous sites.

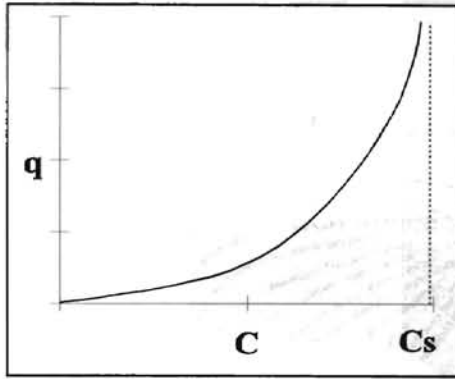


Figure 2.8: Freundlich empirical model

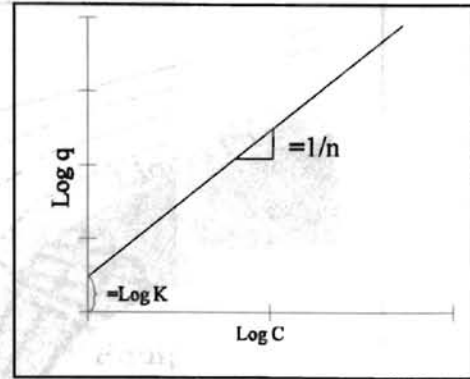


Figure 2.9: Linear form of the Freundlich equation.

### Polanyi Adsorption

The Polanyi adsorption potential theory for gases is summarized by Manes (1980) as follows: The adsorption potential,  $\epsilon$ , of any molecule within the attractive force field of the solid surface is the work required to remove the molecule to infinity from its location in the adsorption space. The value of  $\epsilon$  varies continuously in the adsorption space from some maximum value to zero. When the adsorbent is exposed to increasing pressures of gas, the attractive forces of the solid for the gas molecules enforce their attraction for each other, with the result that the gas liquefies between the solid surface and that equipotential surface for which

$$\epsilon = RT \ln p_s / p$$

where  $R$  is the universal gas constant,  $T$  is temperature in degrees Kelvin,  $p$  is the equilibrium pressure of the gas, and  $p_s$  the vapor pressure of the corresponding liquid at the equilibrium temperature (Manes & Hofer, 1968). Figure 2.10 schematically depicts a solid surface with equipotential surfaces grading from a liquid to a gas phase.

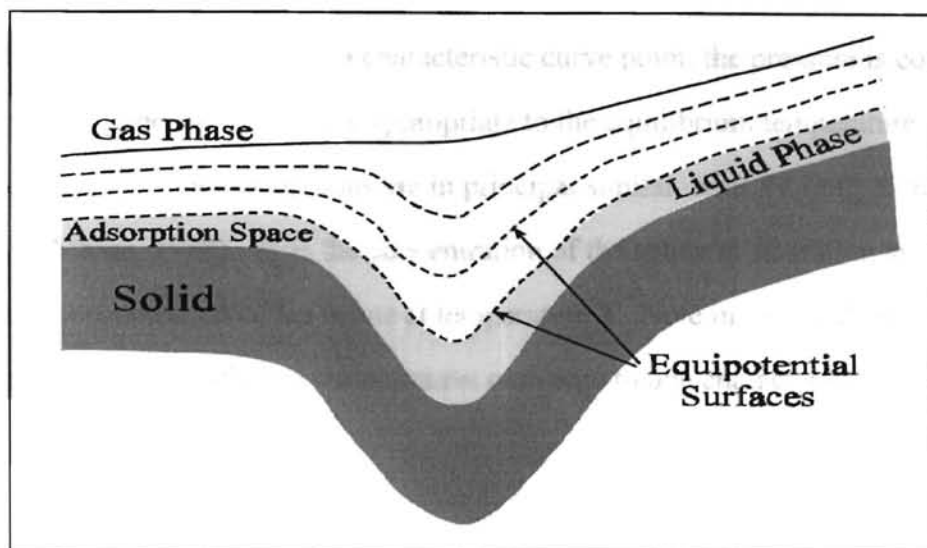


**Figure 2.10:** Schematic model of a region of a heterogeneous adsorbent, showing equipotential surfaces (Manes, 1980)

Given an adsorption isotherm over some capacity range, one can calculate what is defined as the characteristic curve over the same capacity range. (Manes, 1980). The curve is characteristic to all isotherms of the same components over the same range. An example is shown in figure 2.11.

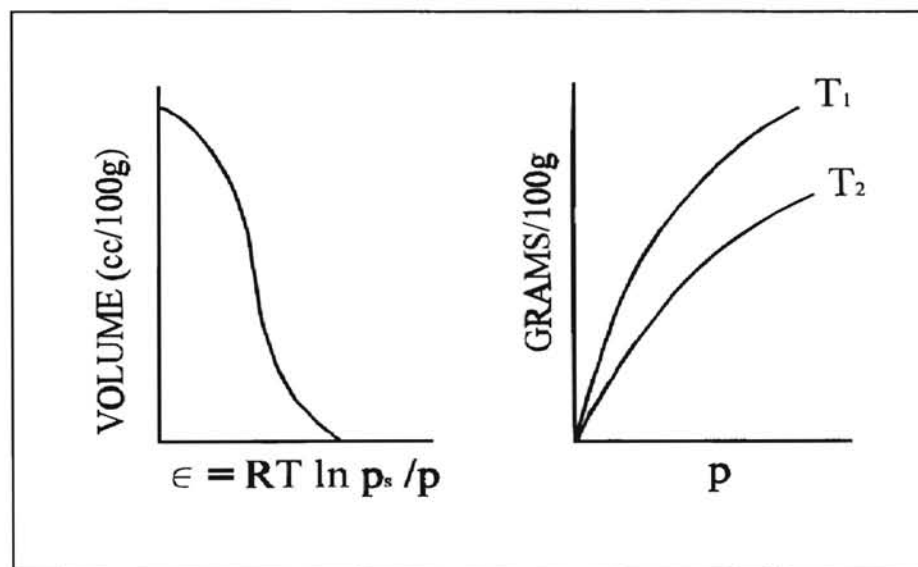


**Figure 2.11:** Characteristic curve and isotherms. The lines on the right represent two gas phase isotherms of the same solvent on one carbon taken at two different temperatures,  $T_1$  and  $T_2$ . The line on the left is the characteristic curve of the two isotherms (Manes, 1980).



To transform an isotherm point to a characteristic curve point, the pressure is converted to  $RT \ln p_s/p$ , using the vapor pressure appropriate to the equilibrium temperature. For liquid-phase adsorption the calculations are in principal similar, with  $RT \ln C_s/C$  replacing  $RT \ln p_s/p$  (Manes, 1980).  $C_s$  is the concentration of the solute at saturation and  $C$  is the equilibrium concentration of the solute at temperature  $T$ . Note in Figure 2.10 that the two isotherms taken at two different temperatures converge to one characteristic curve.

## CHAPTER III

### EXPERIMENTAL APPARATUS

#### Introduction

This investigation required the use of several laboratory instruments that were operated either by this investigator or by Amoco employees skilled in the use of the particular apparatus. The majority of the investigative work required the use of a McPherson Instruments FL-750 HPLC spectrofluorescence detector. This instrument was used to measure the change in concentration of the assay solutions through detection of the strength of the fluorescent response from the fluorophor label. The use of this instrument and the development of analytical tools for analyzing the output data, was critical to this study and is discussed here.

#### Equipment

##### FL-750 Spectrofluorometer

The McPherson Instruments FL-750 HPLC spectrofluorescence detector (FL-750) is a single beam detector consisting of a 150W xenon arc ultraviolet and visible light source, two optical gratings for excitation and emission wavelength selection, and a photomultiplier tube (PMT) for converting the fluorescence to a voltage output. The sample holder consists of fused quartz cuvettes placed in a holder at the front of the detector. The light source focuses at the center of the cuvette where the emissions can be read by

the PMT. The light passes through adjustable band width slits (0, 2, 8, & 16 nm) at four locations; the source, at the entrance of the sample holder, the exit of the sample holder, and at the PMT. Wavelength filters can be placed either at the entrance to the sample holder or at the exit. Figure 3.1 illustrates the configuration of the FL-750.

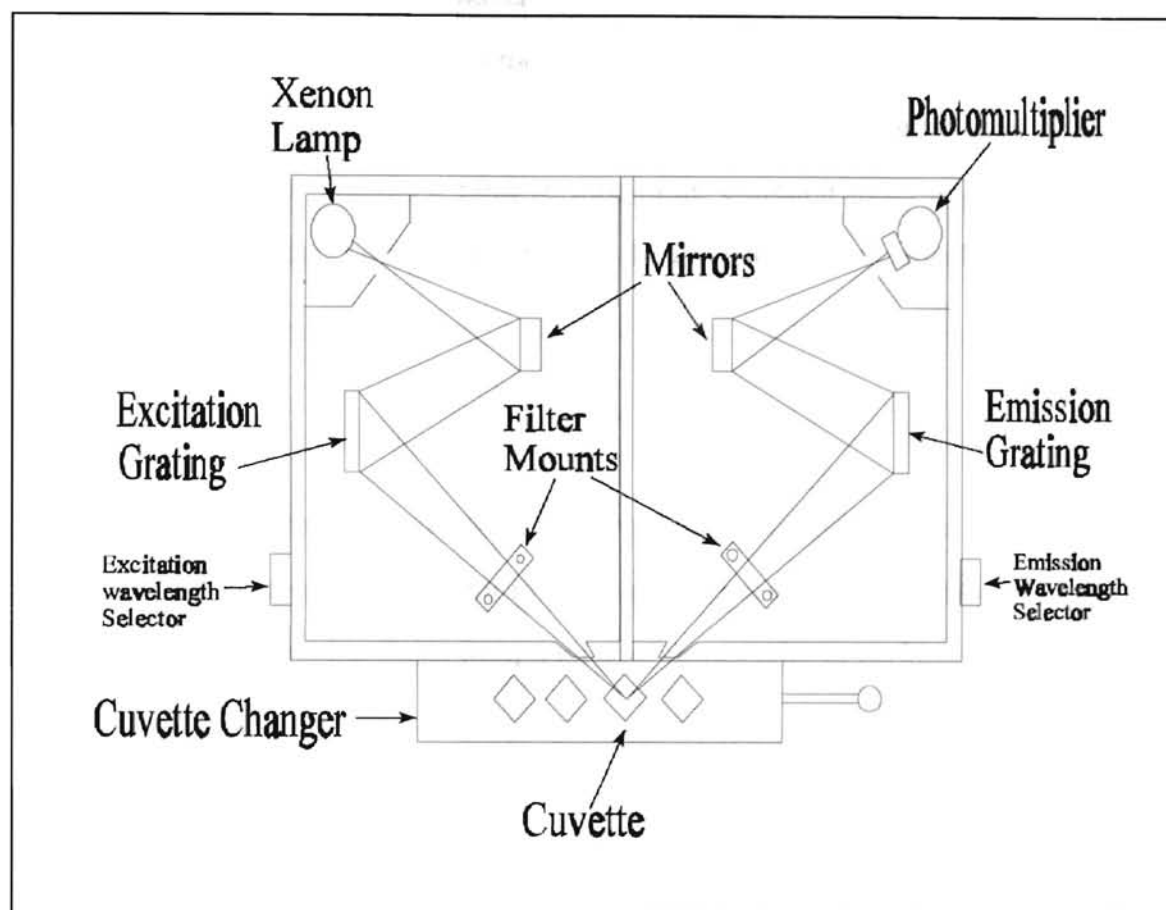


**Figure 3.1:** Schematic drawing of the McPherson Instruments, FL-750 Spectrofluorescence Detector.

The PMT converts the fluorescent emissions to a DC voltage output. The emission voltage varies as the emission wavelengths are scanned via the emission grating. A McPherson model 789B controller controls the wavelength scanning rate of the motor-driven emission and excitation gratings in the FL-750. The PMT voltage output is received by an analog-to-digital converter adapted for use with the FL-750 by the Amoco Services department. Here the analog voltage signal is converted to digital values at pre-

cise time intervals. The digital signal is then received by an IBM AT personal computer where it is processed by a Basic program written by Paul Pettit of the Amoco Services Department. This program triggers a scan controller and creates an abscissa for the incoming voltage ordinates in units of nanometers wavelength, based on the relationship of the starting point of the scanning wavelength, the time interval between the digitized voltages, and the scanning rate set at the 789B controller. The data is then output to an ASCII file as nanometers versus voltage. Data files contain 1800 digital pairs at intervals of 0.1726 nanometers. Quality control viewing of the emission spectrum is made possible by routing secondary voltage outputs from the PMT to a Soltec model 1242 chart recorder.

### Centrifuge

A Baxter Scientific Products Omnifuge model RT centrifuge was utilized to settle silts and colloids out of solution prior to fluorometric measurements. The centrifuge was also used to extract spiking fluids from sand pore spaces prior to performing isotherms with the spiked samples.

### Eppendorf Pipettes

Eppendorf positive displacement pipettes with disposable tips were used to transfer liquids. Pipette tips were discarded after each transfer to prevent cross contamination of samples. Pipetted volumes were weighed for greater accuracy.

### Vials

Borosilicate vials (6 dram) model N-51A from Kimble Manufacturing, with Teflon-lined screw caps were used for all adsorption isotherms and samples for GC analysis. A new vial was used for each sample to prevent the possibility of cross con-

tamination. These vials stand 3.3 inches tall and are approximately 3/4 inch in diameter. This shape vial is ideal in that it makes a good continuous mix batch reactor when tumbled end over end, it will fit in available test tube racks and centrifuge buckets, and will withstand the g-loading at 2000 rpm.

#### Tyler Rotap Sieve Shaker

Particle Sizing was performed with a Tyler Manufacturing Rotap model RX-29 soil shaker. The Tyler nest of sieves #45, #60, #120, #140, #200, #230, and pan were used in the sizing. This corresponds to particle sizes of 0.0139, 0.0098, 0.0049, 0.0041, 0.0029, 0.0025 inches (0.0353, 0.0249, 0.0124, 0.0104, 0.0074, 0.0064 cm).

#### Millipore Water Purification

A Millipore Milli-Q Plus water system was used as the source of deionized water. The system contained carbon filters, an ion exchange unit and a .22  $\mu\text{m}$ -rated filter. Deionized water was used for rinsing in all cleaning procedures and as the solvent in all solutions.

#### IBM Instruments' UV-VIS Spectrophotometer

An IBM Instruments' ultraviolet and visible spectrum spectrophotometer model number 9430 was used to measure the concentration of the antibody solutions. This is a dual beam system that compares the sample with a reference (the solvent). The absorbance, measured at the peak absorption wavelength of the fluorophor tag, was utilized with the Beer-Lambert law to compute concentration. The desired concentration was achieved by adjusting solute and solvent to obtain the required absorbance. This instrument was considered accurate enough (.001 absorbance units) to measure the starting concentration of the solute prior to performing adsorption isotherms, however, it was not

accurate enough to measure some of the very small changes in concentration that occurred with the isotherms. The absorbance method proved to be more accurate than gravimetric measurement due to the exceptionally small amounts of solute required for each solution, and the need to conserve samples.

#### Mettler AT261 Balance

A Mettler AT261 balance is an electronic balance with two accuracy settings, 0.1 or 0.01 mg. The motorized canopy allows for ease of opening and closing to shield the sample from air currents while weighing. All samples were weighed to .1 mg accuracy. The 0.01 mg accuracy required more time to stabilize.

#### Denver Instruments IR-100 Moisture Balance

A Denver Instruments IR-100 moisture balance was used to measure the moisture content of the spiked samples. The percent moisture content by weight is determined by monitoring the change in weight as the sample is dried by a quartz infrared heating system. When less than 0.05% change in weight occurs over a one minute time interval, the heater shuts off and the data is printed.

#### Rotating Tumbler

A rotating tumbler, model no. 3748-8-BRE, by Associated Design and Manufacturing Co., Alexandria, Virginia, was used to create continuous mixing in the vials used for isotherms. The tumbler contains holders for eight plastic-coated two liter jars and rotates at thirty revolutions per minute.

### Thermolyne Maxi Mix 1

The Thermolyne Maxi Mix 1 has a three inch diameter padded surface that revolves in a rapid circular motion in the horizontal plane. Holding a vial of solution against the padded surface while in operation causes a circular vibration ideal for short mixing periods.

### Computer Equipment and Software

Microsoft Excel (version 4.0a) spread sheet program on a IBM compatible personal computer, was applied to analyze ASCII output data from the FL-750. The spread sheet capabilities were used to develop a method to remove background noise and DC bias and to calculate the area under the emissions curve using Simpson's rule.

## CHAPTER IV

### EXPERIMENTAL MATERIALS AND METHODS

#### Adsorbents

##### Arkansas River Sand

Arkansas River Sand (ARS) was chosen as an adsorbent because of its abundance in the Tulsa area, and because it was necessary to select a soil matrix that could be washed free of organics and be consistent from sample to sample.

Two five-gallon buckets of ARS were collected and washed with water in a hydrocyclone to remove most of the bound clays. This partially cleaned sand was washed further in a large bucket with copious amounts of water, stirring while allowing it to overflow, until the remaining sand would settle rapidly. The goal was to bring the sand to a particle size distribution that could be settled quickly by centrifuge, leaving a clear supernatant. It was then washed with Clorox to remove organics, rinsed thoroughly in deionized water, and oven dried at 105° C for 24 hours. A sample of the dried sand was sieved to determine the particle size distribution.

The supernatant from tumbling this sand in deionized water was found to produce a broad fluorescent response with a peak in the lower end (about 465 to 525 nm) of the emission spectrum of the fluorophors to be used in this investigation. This background



fluorescence is shown in Figure 4.1. The technique developed to remove the background is discussed later in this chapter.

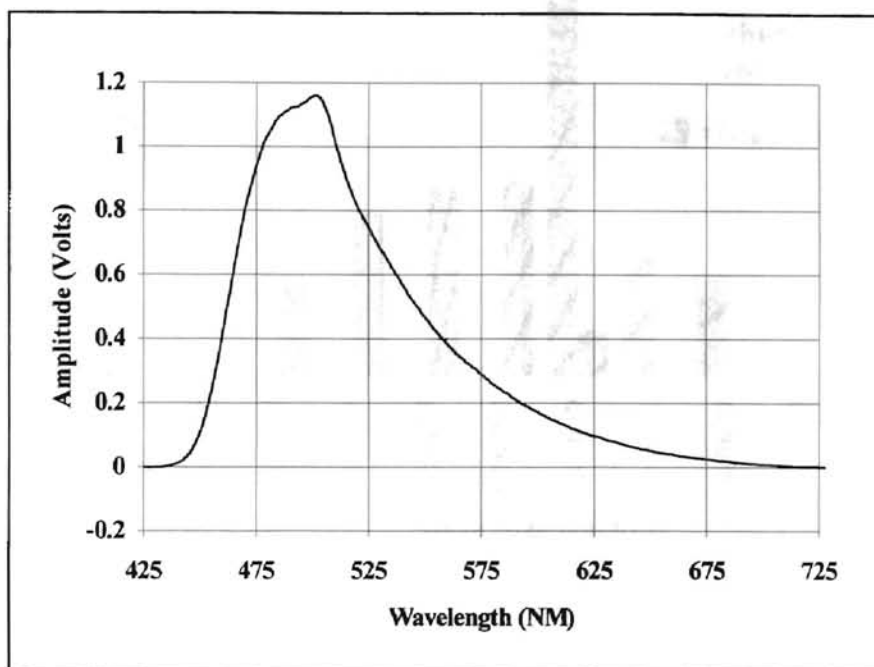


**Figure 4.1:** Background fluorescence produced by ARS tumbled in deionized water.

### Ottawa Sand

Standard Ottawa sand (washed and ignited) was purchased from EM Science. After washing and drying in the same manner as the ARS, the background fluorescence was tested and found to be similar to that of the ARS, however, of lesser amplitude for equivalent amount of sands. This sand was also sieved to determine the particle size distribution. A comparison of the size distributions of the two sands is shown in Figure 4.2.

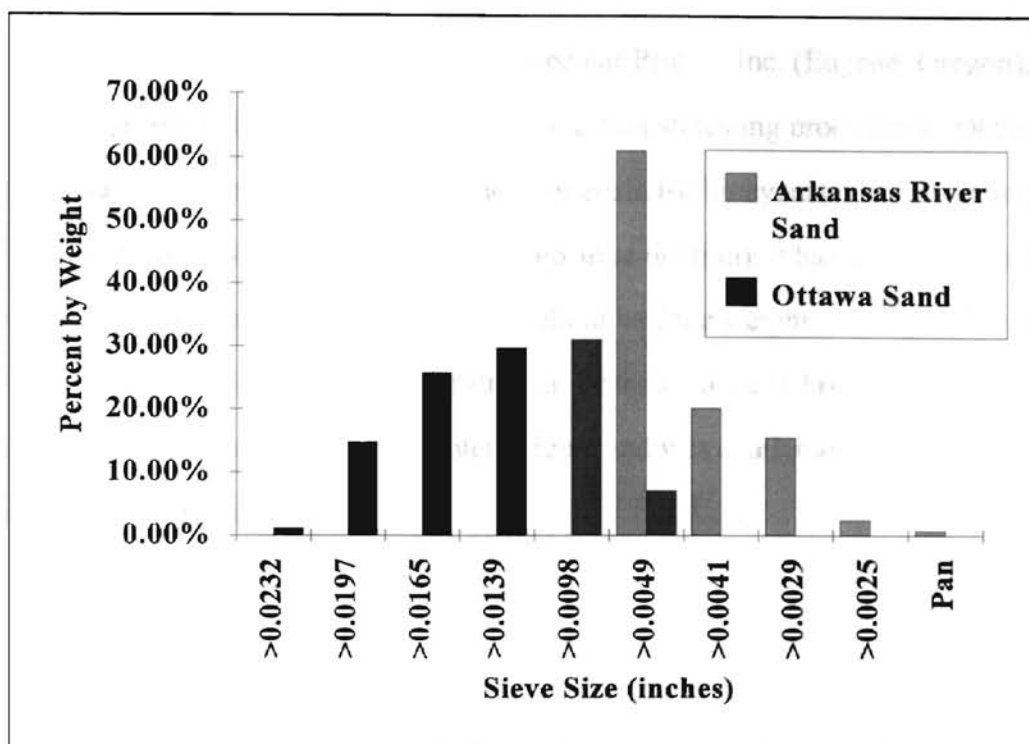


**Figure 4.2:** Comparison of particle size distributions of washed ARS and washed Ottawa sand.

On the basis of this particle size distribution, Ottawa sand should have less surface area per unit weight than ARS. This was confirmed with a surface area analysis performed by Micromeritics Instrument Corporation. A BET surface area analysis using Krypton gas adsorption showed 0.574 m<sup>2</sup>/g for ARS versus 0.039 m<sup>2</sup>/g for Ottawa sand. This is a ratio of 14.7 to 1. The theoretical ratio, based on spherical particles, gives a ratio of 2.5 to 1. Kolodziej (1993) showed through scanning electron microscope images that ARS is highly pitted, creating a significant increase in surface area.

#### Adsorbates

##### Dextran-Eosin Conjugate

The antibodies used in this investigation were available in very small quantities. Consequently, additional effort was required to conserve the available samples. Dextran-

eosin conjugate (DEC), available through Molecular Probes, Inc. (Eugene, Oregon), was chosen as a surrogate to the antibody in order to establish testing procedures. Dextran is a chain of sugar molecules while eosin, short for eosin isothiocyanate, is a fluorescent label. Conjugated at a mole ratio of 6.6 to 1 (eosin to dextran), it has a combined molecular weight of 75,000 grams per mole. This is about half the weight of an IgG-class antibody. Eosin has similar properties to erythrosin isothiocyanate (EITC), the fluorophor used to label the antibodies. DEC is water soluble and was available in solid form in quantities of 25 milligrams.

#### Eosin and Erythrosin Isothiocyanate

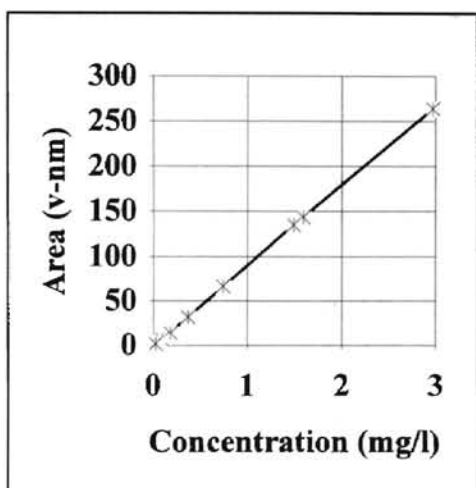
Eosin and EITC are commonly useful as phosphorescent or fluorescent probes (Molecular Probes, Inc., 1994). Fluorescein isothiocyanate (FITC) is more commonly used to prepare proteins because it has a higher quantum yield (Molecular Probes, Inc., 1994). However, the peak emission wavelength coincides more closely with the peak background emission of the adsorbents (500 nm) used in this investigation, making it less useful as a fluorescent label. The following table compares the characteristics of the three fluorophors.

TABLE I  
CHARACTERISTICS OF SELECTED  
FLUOROPHORS

	Absorbance Wavelength (nm)	Emission Wavelength (nm)	Molecular Extinction Coefficient ( $\epsilon \times 10^{-3}$ )	Molecular Weight (grams/mole)
Eosin	522	543	100	705
EITC	528	553	86	893
FITC	495	519	76	389

From Molecular Probes 1994 catalogue

Figures 4.3 and 4.4 are plots of the area under the emissions curve versus concentration for eosin and EITC. The plots were generated from serial dilutions of the two fluorophors in their conjugate form in order to verify that inner filtering effects would not be a factor in relating the fluorescent energy to concentration.



**Figure 4.3:** Calibration curve for Dextran-eosin conjugate

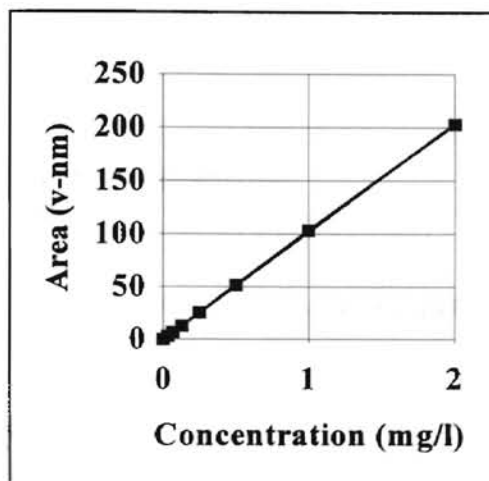


**Figure 4.4:** Calibration curve for Ab-EITC conjugate

These plots verify that area versus concentration is linear at low concentrations for both fluorophors, and that concentration can easily be computed as a function of the curve area.

### Polycyclic Aromatic Hydrocarbons

Naphthalene. Naphthalene (CAS no. 91-20-3) is a product of petroleum refining and coal tar distillation and is best known for its use in moth balls. Its solubility is 31-34 mg/l in distilled water at 25° C (Verschuere, 1983). It was purchased from Fluka chemical company as white flakes. Figure 4.5 is the structure of the naphthalene molecule.

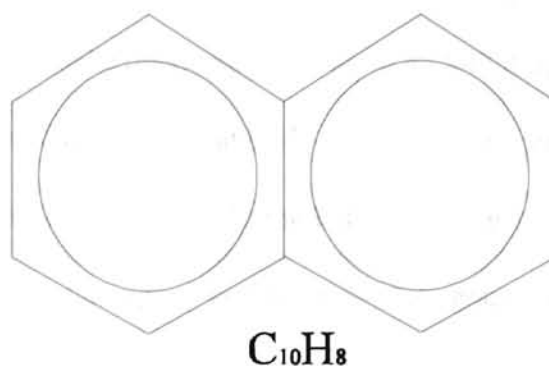


**Figure 4.5:** Naphthalene molecular configuration (reproduced from Verschueren, 1983).

**Pyrene.** Pyrene (CAS no. 129-00-0) is present in crude oil at 3.5 to 4.5 ppm. Air pollution sources are numerous. Some man made sources are tail pipe emissions from gasoline engines at 63-484  $\mu\text{g}/\text{cu m}$  and coke oven emissions at 206-4627  $\mu\text{g}/\text{g}$  of sample (Verschueren, 1983). Its solubility is 0.16  $\text{mg}/\text{l}$  at 26° C (Verschueren, 1983). It was purchased from Fluka chemical company in the form of yellow flakes. Its structure is shown in Figure 4.6.

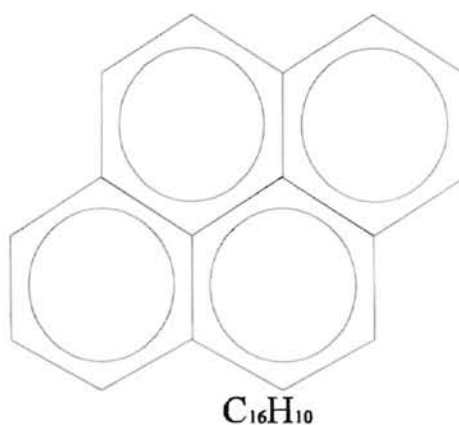


**Figure 4.6:** Pyrene molecular configuration (reproduced from Verschueren, 1983).

Anthracene. Anthracene (CAS no. 120-12-7) has many man-made air pollution sources. Among them are coke oven emissions at 46.4 - 942.8  $\mu\text{g/g}$  of sample, and exhaust condensates of gasoline engines, at 0.53 - 0.64 mg/l gasoline consumed (Verschueren, 1983). Its solubility is 1.29 mg/l at 25° C in distilled water. It was purchased from Fluka chemical company as fine gray-white granules. The structure of anthracene is shown in Figure 4.7 below.

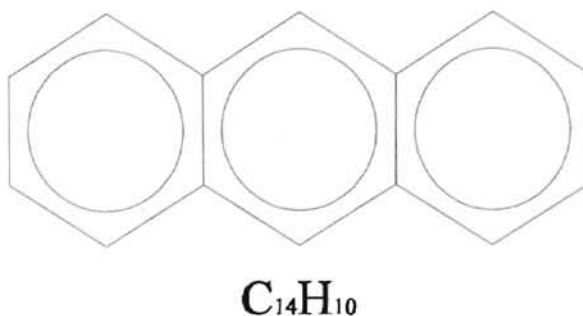


**Figure 4.7:** Anthracene molecular configuration (reproduced from Verschueren, 1983).

#### Arab Medium Crude Oil

Arab Medium Crude oil was used for spiking ARS to simulate crude oil contamination in soil. A GC analysis of the crude oil is displayed in the appendix. ARS spiked with crude oil was used to study the effect on DEC adsorption at various spiking levels.

## Antibodies

This project was executed under a joint agreement with Strategic Diagnostic, Inc. (SDI), Newark, Delaware, and Amoco Production Company (APC), Tulsa, Oklahoma. Under this agreement, SDI developed monoclonal mouse antisera which binds specifically with naphthalene while also possessing cross-reactivity characteristics to other similar PAH molecules. SDI also provided polyclonal rabbit antisera reactive to pyrene. Cross-reactivity characteristics of the polyclonal rabbit antibody are shown in Table II. Reactivity and cross-reactivity characteristics of both antibodies were verified by SDI using standard ELISA protocol.

The Anti-Pyrene Antibody was reacted with 18 different PAH's, establishing 100% as the baseline reactivity to pyrene. Four different PAH's conjugated with the enzyme alkaline phosphatase (AP) were used as indicator compounds in a standard ELISA protocol. The indicator conjugate competes for binding sites on the antibody with the material being assayed. The cross reactivity percentages varied, depending on which PAH was used with the enzyme as the indicator.

Table II shows how changing the PAH-AP indicator conjugate changes the cross-reactivity, thus changing the selectivity of the assay (Stave, 1994). For example, using pyrene-AP as the indicator conjugate will produce an assay that is highly specific to pyrene, with 10 fold less reactivity to fluoranthene and very little reactivity to the remaining listed PAH's. With Chrysene-AP as the indicator compound, the assay is less specific to pyrene and becomes more of a general assay for the listed PAH molecules.

Table II

## ANTIBODY CROSS-REACTIVITY COMPARISON

(Units of Percent Reactivity where  
Pyrene with Pyrene-AP = 100%)

PAH	Pyrene-AP	Anthracene-AP	Fluorene-AP	Chrysene-AP
Pyrene	100	100.0	25	33
Fluorene	1	2.8	100	22
Fluoranthene	10	200.0		
Naphthalene	< 1	25.0	1	28
Acenaphthylene	1	10.0	40	100
Benzo(a)anthracene*	1	1.0	3.3	16
Anthracene	< 1	6.6	33	25
Benzo(a)Pyrene*	2.5	100.0	160	20
Indenopyrene*	1	7.5	250	100
Benzo(k)Fluoranthene*	< 1	6.6	< 1	< 1
Dibenz(a,h)anthracene*	< 1	ND	10	9
Benzo(g,h,i)Perylene	< 1	100.0	66	50
Chrysene*	< 1	7.5	140	10
Benzo(b)fluoranthene*	< 1	15.0	50	10
Acenaphthene	1	10.0	40	100
Phenanthrene	ND	ND	ND	ND
Dimethylnaphthalene				
Tetrahydroxynaph.				

\* Carcinogenic PAH's

A third antibody, a negative control antibody, was used in this investigation. The negative control antibody was identical to the other antibodies in class and molecular weight. However, it was selected by SDI specifically to be non-reactive with PAH molecules. SDI provided these antibodies conjugated with the fluorescent label EITC. The following table summarizes the quantities and the form in which the three antibodies were received.



TABLE III

## ANTIBODIES DEVELOPED BY STRATEGIC DIAGNOSTICS, INC.

Antibodies	Type	Quantity (ml)	Degree of Substitution (DOS) EITC:Ab	Buffer Solution	Antibody Concentration (mg/ml)
Anti-Naphthalene	Monoclonal Mouse	4.4	4:1	0.1 M Bicarbonate pH = 9	2.0
Anti-Pyrene	Polyclonal Rabbit	4.0	1.2:1	Phosphate Buffered Saline, 0.05% azide pH = 7.4	1.6
Negative Control	Polyclonal Rabbit	3.0	1.5:1	Phosphate Buffered Saline, 0.05% azide pH = 7.4	1.7

## Solvents

Deionized Water

Deionized water was used in all solutions containing water soluble solutes. The Millipore Milli-Q Plus Water System was the source for all deionized water. The system contained carbon filters, an ion exchange unit and a .22  $\mu\text{m}$ -rated filter.

Phosphate-Buffered Saline

Phosphate-buffered saline (PBS) with a pH of 7.5 was used to dilute the antibody solutions to perform isotherms (Stave, 1994). PBS was prepared using 1.149 grams of dibasic potassium phosphate, 0.262 grams of monobasic potassium phosphate, and 8.33 grams of NaCl in one liter of deionized water. This formulation was adapted from Dulbecco's Phosphate-Buffered Saline advertised in GIBCO BRL, Life Technologies, Inc. catalogue (1994). Since the pH of this adapted formulation tended to rise over a period of 24 hours, it was mixed for immediate use and then discarded.

## Isotherm Procedure

The following is a standardized isotherm procedure, followed with the isotherms performed in this study. This procedure is a constant concentration, variable mass method and was established through several trial isotherms with the goal of conserving adsorbates while staying safely above the lower fluorometric detection limits. Variations or additions to the procedure required for a particular test are discussed in the chapter dealing with that test.

### Standardized Isotherm Procedure

1. Adsorbent was placed in 8 25-ml vials by placing a vial on the balance, taring, and placing the target mass of adsorbent in the vial with a clean stainless steel spatula. Target masses were 2.4, 2.1, 1.8, 1.5, 1.2, 0.9, 0.6, and 0.3 grams. A tolerance of + 0.08 gram was allowed. Actual masses were recorded, the vials sealed with a Teflon lined screw cap, and numbered 1 through 8.
2. Twenty five milliliters of adsorbate were prepared at a specific concentration either gravimetrically by adding an aliquot of the antibody solution to PBS on a laboratory balance, or by adding a solid solute to deionized water until a specific absorbance value was achieved according to the following adaptation of the Beer-Lambert law:

$$\frac{\epsilon_{\text{fluorophor}} \times [\text{fluorophor}] \times l}{MW_{\text{fluorophor}}} = \text{Absorbance}$$

where  $l$  is the length of the travel path through the solution (cuvette inside thickness). The remainder of the adsorbate solution was retained for spectrofluorometer calibration.

3. The screw caps were removed from the vials containing the adsorbent, individually placed on the balance, and tared. Approximately three milliliters of adsor-

bate were placed in each vial using a 1000  $\mu$ l Eppendorf pipette. The masses of the solutions were recorded and the screw caps replaced. The volumes were computed at one milliliter per gram. A tolerance of  $\pm 0.05$  milliliter was considered acceptable.

4. The vials were placed upright in the rotating tumbler jars with padding around the vials and filling the remainder of the jar. Adsorption equilibrium tests indicated that most of the adsorption occurred in 1.5 to 2 hours of tumbling. Figure 4.8 is a plot of the residual concentration of dextran-eosin with time when tumbled with ARS. The decline becomes essentially flat after 1.5 hours. As a safety factor, all isotherms were tumbled for a minimum of three hours.

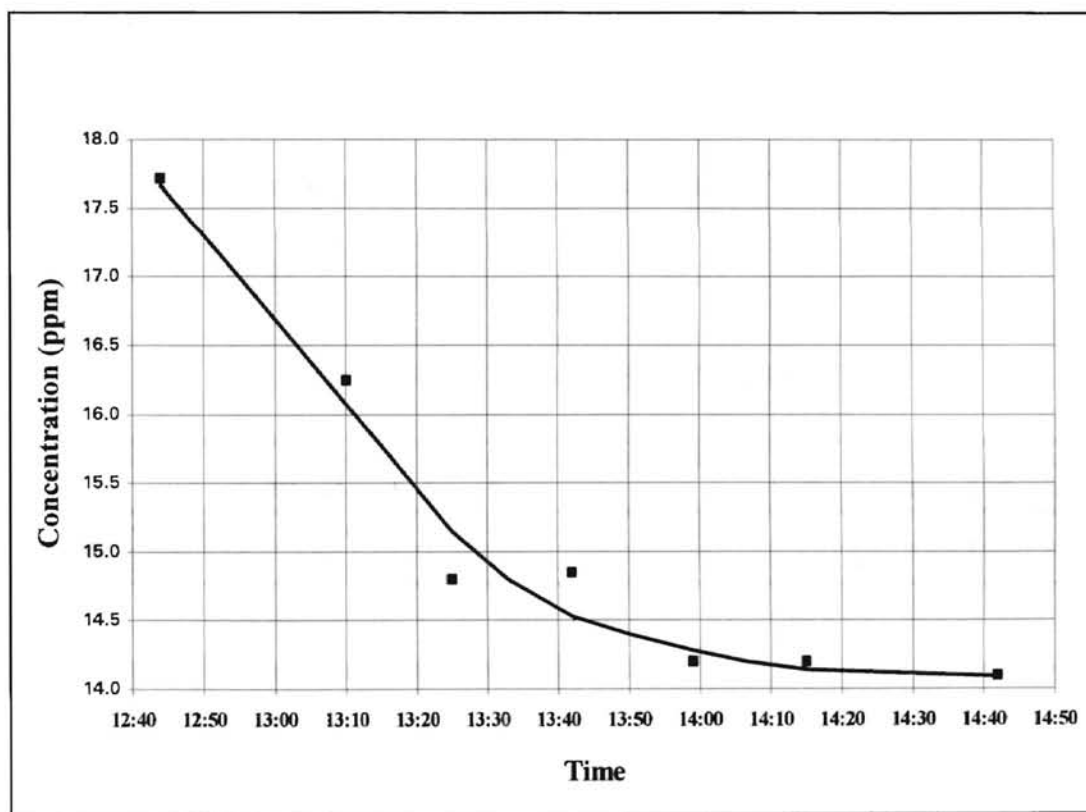


Figure 4.8: Residual concentration of dextran-eosin with time when tumbled with ARS.

5. After tumbling for three hours the vials were subjected to centrifugation for ten minutes at 2000 RPM.
6. Spectrofluorometer calibration was achieved by scanning a portion of the adsorbate solution retained in step two and recording the output voltage versus wavelength in a computer file. A plot of curve area versus concentration projected through the origin constitutes a calibration curve as long as the concentrations are below the range of inner filtering effects. A second scan of the retained starting concentration was performed after scanning all of the isotherm supernatants. This was necessary when more than one isotherm was being run at the same time to adjust for photodegradation that occurred over the extended scanning period. The change in amplitude of the two calibration scans and the time of each scan as recorded in the computer file, provided the basis for an amplitude decay correction linear with time. A 10% decay in amplitude was observed over a seven hour period. Spectrofluorometer settings are shown in Table IV.

TABLE IV  
SPECTROFLUOROMETER SETTINGS

Adsorbate	Excitation Wavelength	Emission Scan	Sensitivity	Background Suppression	Time Constant
Dextran-Eosin	341 nm	425-725 nm	0.1-0.3	none	1
Ab-EITC	355 nm	425-725 nm	0.1-0.3	none	1

7. Two milliliters of the supernatant from the centrifuged vials were placed into clean cuvettes and scanned for residual fluorescent emissions. Output voltage versus wavelength of the fluorescent emissions were recorded for each vial in separate computer files. The residual concentrations were then computed as a function of the area of the emissions curve with background emissions removed,

and the slope of the fluorophor calibration curve. The computer methods used in computing the concentrations are discussed in detail later in this chapter.

8. Freundlich, Langmuir, and BET isotherm plots were constructed for each isotherm.

### Data Analysis

The Microsoft Excel spreadsheet program was used to analyze the recorded fluorescent emissions data. Emissions curves are digital recordings of the fluorescent radiation in terms of voltage, monitored over a range of wavelengths. Interferences from Rayleigh scatter and Raman effect were avoided by setting the excitation wavelength at the lower end of the excitation spectrum. This shifted these interferences outside of the range of the emissions spectrum. The recorded data contain two components that interfere with data analysis. These are (a) a shift in voltage from a zero baseline called DC bias, and (b) background emissions from various dissolved components that come from mixing the adsorbate solution with the adsorbent. These two components must be removed before the area under the emissions curve can be calculated.

#### DC Bias Removal

DC bias removal was accomplished by computing a straight line tangent to the base of the total emissions curve. To do this, an average amplitude over ten nanometers was computed at the low wavelength and high wavelength ends of the curve where the voltage was at a minimum, and a straight line was computed connecting the two points with matching values for each data point on the emissions curve. The line was then subtracted from the emissions curve.

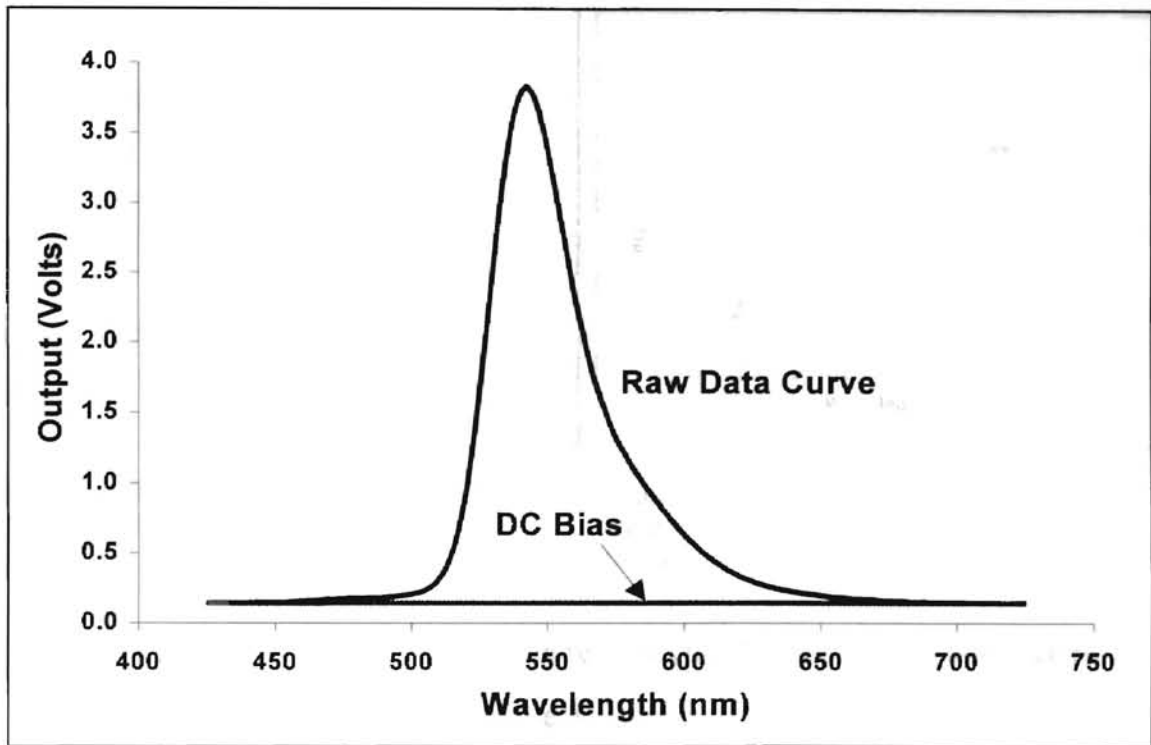
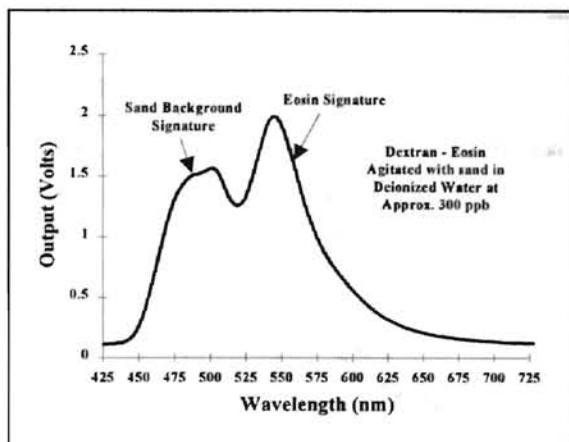


Figure 4.9: DC bias is removed by subtracting the voltage values of the DC bias curve from the data curve, causing the data curve to be shifted to the zero line.

### Background Removal

Background emissions (background) were often of greater magnitude than the eosin or EITC emissions (signal). However they proved to be additive, and although a nuisance, did not obscure the signal. Figures 4.10 and 4.11 illustrate the additive nature of these signals.



**Figure 4.10:** Total recorded output of eosin at 300 ppb and background.

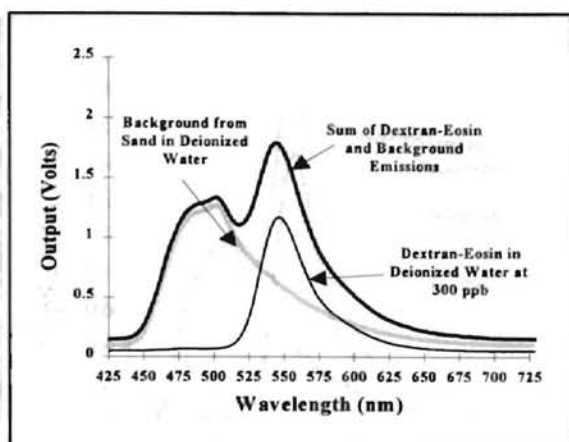


**Figure 4.11:** Composite plot showing separate background and eosin emissions curves and the summation of the two.

Figure 4.9 is a composite plot of eosin fluorescence and background fluorescence recorded separately, and a summation of the two curves. The summation closely approximates Figure 4.10 which is a single recording of eosin and background.

The background emission, as labeled in Figure 4.11 above, was somewhat variable between isotherms. With the exception of amplitude variations, the shape of the eosin signature (signal) curve (Figure 4.11) proved to be consistent. Therefore, it was more accurate to subtract pure signal from the total output creating a computed background than to subtract background.

Pure signal was scaled with a multiplication factor to approximate the signal in the recorded total emissions (output) curve. This was done by trial and error and the help of composite plots of the output and pure signal as shown in Figures 4.12 and 4.13 below.

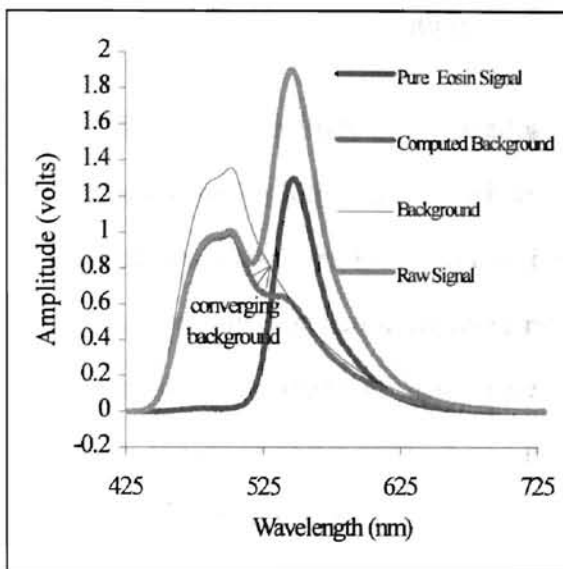


**Figure 4.12:** Composite plot showing converging backgrounds.

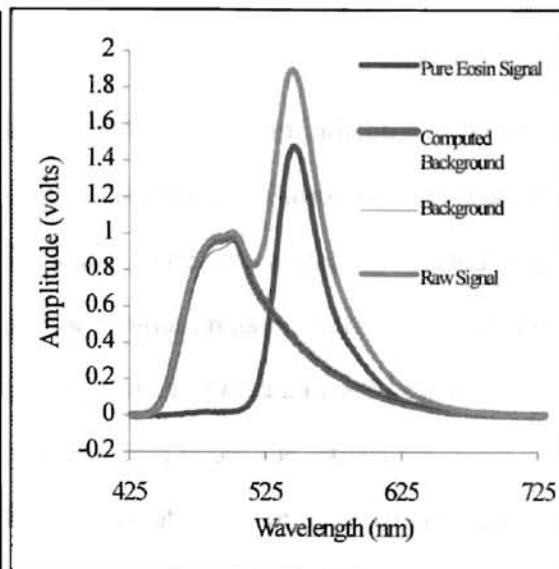


**Figure 4.13:** Backgrounds have converged and pure signal equals signal in the output data.

Including a plot of the computed background and a plot of pure background for comparison made a very convenient way of observing when the correct signal amplitude was reached. The amplitude of the sample background was adjusted by an automatically computed scale factor that would force the pure background and computed background curves to intersect at the wavelength of maximum signal amplitude. As pure signal amplitude was adjusted, the two background curves converged. At maximum convergence, all signal was removed leaving only background. The amplitude-adjusted pure signal curve then became the sought after signal from the residual concentration separated from background. It was found to be helpful to substitute computed background from the previous analysis for pure background in the subsequent analysis. In Figure 4.13 the two backgrounds have converged, however the crests at 475 to 500 nanometers are not perfectly matched. This is where the backgrounds tended to vary between samples.



### Computing Residual Concentration

The peak amplitude of the residual fluorescent signal as an indicator of concentration tended to be slightly unstable, while the area under the emissions curve averaged out local amplitude variations for a more stable indicator. The area under the residual signal curve was computed by summing incremental trapezoidal areas between sample points. Since the calibration curve for low concentrations proved to be a straight line intersecting the origin, the slope of the calibration curve was the area under the emissions curve of the starting isotherm concentration divided by the concentration. The residual concentration was computed as the area under the residual emissions curve divided by the slope.

DC bias and background removal, integration, and calculation of concentration were handled simultaneously in one spreadsheet. Each emissions output curve was retrieved individually and pasted into the spreadsheet preset with the necessary computations. Once the slope of the calibration curve was determined and a suitable starting background sample pasted into the spreadsheet, analysis proceeded by adjusting the amplitude factor until the background curves converged. The residual concentration was then recorded in another spreadsheet where it was used to create isotherm plots. Photodegradation adjustments were handled within the same spreadsheet by entering a "time factor" computed from the computer's directory information showing the time of recording. The "time factor" is a function of the elapsed time between the scanning of the data and the scanning of the known sample. The amplitude was observed to decay approximately 10% after seven hours.

### Spiking Procedures

Specific adsorption is defined for the purposes of this investigation as specific binding of the antibody to the antigen while the antigen is in solid phase adsorbed to the soil surfaces. Testing for specific adsorption required that the soil (ARS) be spiked with

the antigen (naphthalene or pyrene) at known concentrations. Two slightly different spiking procedures were employed for naphthalene and pyrene.

#### Naphthalene Spiking Procedure

A one-pint Kerr jar was filled with deionized water, leaving a small headspace. Naphthalene sufficient for greater than a 30 ppm solution, the maximum solubility (Verschueren, 1983), was added to the deionized water. A Teflon-coated magnet was placed in the bottom of the jar, and the jar was sealed and placed on a magnetic stirrer for 24 hours, sufficient time to reach the concentration maximum solubility. After 24 hours, the jar was removed from the stirrer and the remaining undissolved naphthalene allowed to settle. Approximately ten milliliters of the solution was drawn off, taking care not to include undissolved naphthalene, and sealed in a 25 ml vial for later analysis. The remaining solution was combined with ARS in a clean Kerr jar at known quantities of each and tumbled overnight. After settling, approximately ten milliliters were placed in a 25 ml vial and sealed. The two samples were taken to the Amoco analytical group for gas chromatograph (GC) analysis along with three samples of naphthalene in hexane at known concentrations. The GC analysis, with the help of the three calibration samples, provided the concentrations of naphthalene in deionized water before and after tumbling with ARS. From the difference in concentration of these two solutions the spiked concentration was computed. The sand was centrifuged to a 2% moisture content and stored in sealed vials with minimal headspace for later use. Greater spiking concentrations were achieved by combining less sand with the naphthalene solution. Confirmation by extraction from the solid phase was not performed.

### Pyrene Spiking Procedure

Pyrene, with a solubility of 0.16 mg/l, is much less soluble in water than naphthalene (Verschueren, 1983). Consequently a different approach had to be taken in spiking ARS at a significant level. Known quantities of ARS, deionized water and pyrene were placed in a Kerr jar together and tumbled for 48 hours. The amount of pyrene and deionized water represented a theoretical starting concentration. After tumbling, the supernatant was sent to the APC analytical group for GC analysis and the sand was centrifuged to a 2% moisture content and stored in 25 ml vials with minimal head space. For comparison purposes, a measured quantity of the spiked ARS was mixed with a measured quantity of methylene chloride, a solvent often used in hydrocarbon extraction. The supernatant was also taken to the analytical lab for GC analysis. The extraction efficiency using methylene chloride is unknown, but assumed to be less than 100% (Krahn et al., 1991). If the two methods are within 20% of each other and the extraction method shows slightly less concentration, then this is a logical relationship and the residual concentration method is taken as the correct amount. If the two methods are within 20% and extraction is greater, then random error is assumed and the two are averaged. If a difference greater than 20% was obtained, the procedure was repeated.

### Crude Oil Spiking Procedure

ARS was spiked with Arab Medium Crude oil to 10.6% by weight by mixing the crude oil directly with the sand. This entire sample was analyzed in parts for moisture content using a Denver Instruments Moisture Balance. The purpose was to evaporate most of the lighter volatiles while measuring the weight loss percentage and averaging the results. The resulting spiking level computed to be 8.7% by weight. This sample was cut with clean ARS serially to obtain five spiked samples ranging from 1.07 to 0.07% by weight.

## CHAPTER V

### RESULTS AND DISCUSSION

The adsorption isotherm provides a statistical method for evaluating changes in adsorption characteristics of antibodies, to determine if the specificity of an antibody for its antigen changes those characteristics. Dextran-eosin conjugate (DEC) was used as a surrogate antibody to establish the isotherm procedures without wasting the antibodies. The adsorption characteristics of a negative-control antibody (antibody non-reactive to PAH's) were compared to adsorption of a reactive antibody to determine if there were any measurable difference contributable to specific binding. It was assumed from the reactivity data provided by SDI that antigens desorbed during the isotherm procedures would specifically bind with the antibodies in solution. This was not considered a factor in the solid phase adsorption, since the weak attractive forces of antibody-antigen binding did not influence antigen desorption (Roitt, Brostoff, and Male, 1985). Following are the results and discussions of the significant isotherms that were run.

#### Non-Specific Adsorption of Dextran-Eosin Conjugate on Clean Arkansas River Sand and Arkansas River Sand Spiked with Naphthalene

Arkansas River Sand (ARS), abundantly available in the Tulsa area, was used as the adsorbent. The sand was prepared as described in Chapter IV. Approximately 16 grams of ARS was spiked with naphthalene to a concentration of 22 mg/kg. For the second test, the spiking level was raised to 128 mg/kg.

DEC was mixed with deionized water to a concentration of approximately 4.85 mg/l using the absorbance method described in Chapter IV. The equivalent concentration of eosin is 0.3 mg/l. Since the absorbance method was used to mix most solutions, it became standard to express solution concentrations in terms of the amount of fluorescent label present. The ratio of DEC to eosin is 16.18 to 1.

## Results

Table V is a sample of isotherm data from DEC adsorption on clean ARS. The remainder of the isotherm data are displayed in appendix A.

Table V

SAMPLE ISOTHERM DATA FOR CLEAN  
ARKANSAS RIVER SAND

Sample No.	Dextran-Eosin Sol. (grams)	Dextran-Eosin Sol. (ml)	ARS Sand Dosage (grams)	Emissions Curve Area (v-nm)	Residual Concentration (mg/l Eosin)	Adsorbed Concentration (gm/gm)
Co	0		0	25.73	0.287	
1	2.9887	2.9887	2.4312	18.11	0.202	1.044E-07
2	2.9738	2.9738	2.1519	15.625	0.174	1.556E-07
3	2.9735	2.9735	1.8266	16.505	0.184	1.673E-07
4	2.9822	2.9822	1.5194	17.168	0.191	1.872E-07
5	2.9804	2.9804	1.2448	16.314	0.182	2.512E-07
6	2.99	2.99	0.9371	18.711	0.208	2.495E-07
7	2.9906	2.9906	0.6373	20.048	0.223	2.971E-07
8	2.989	2.989	0.3391	20.831	0.232	4.812E-07

The combined Freundlich plot of four isotherms is shown in Figure 5.1. Two clean sand isotherms were run five days apart showing good repeatability, followed by two isotherms on naphthalene-spiked sand. Clean sand isotherms were generated using starting eosin concentrations of 5, 1, and 0.3 mg/l. Freundlich plots of the clean sand isotherms had slightly higher  $r^2$  values than did the Langmuir high and low plots. This

suggests that adsorption is proceeding past the point of forming a monolayer. The Langmuir plots are included in the appendix. The concentration of 0.3 mg/l was extrapolated from the earlier tests as a level that would be low enough to conserve resources and still have a residual concentration easily detectable above background fluorescence. Fluorescent dyes conjugated with proteins such as antibodies will be partially quenched due to partial absorption from the large mass of the antibody (Udenfriend, 1962, Molecular Probes, Inc. 1993). This was anticipated in not choosing an even lower concentration. The isotherms on naphthalene-spiked sand exhibited inhibition of DEC adsorption. The inhibition increased as the spiking level increased. In Figure 5.1, adsorption potential decreases to the lower right on the graph. With decreased adsorption potential comes more random variability of the isotherm data.

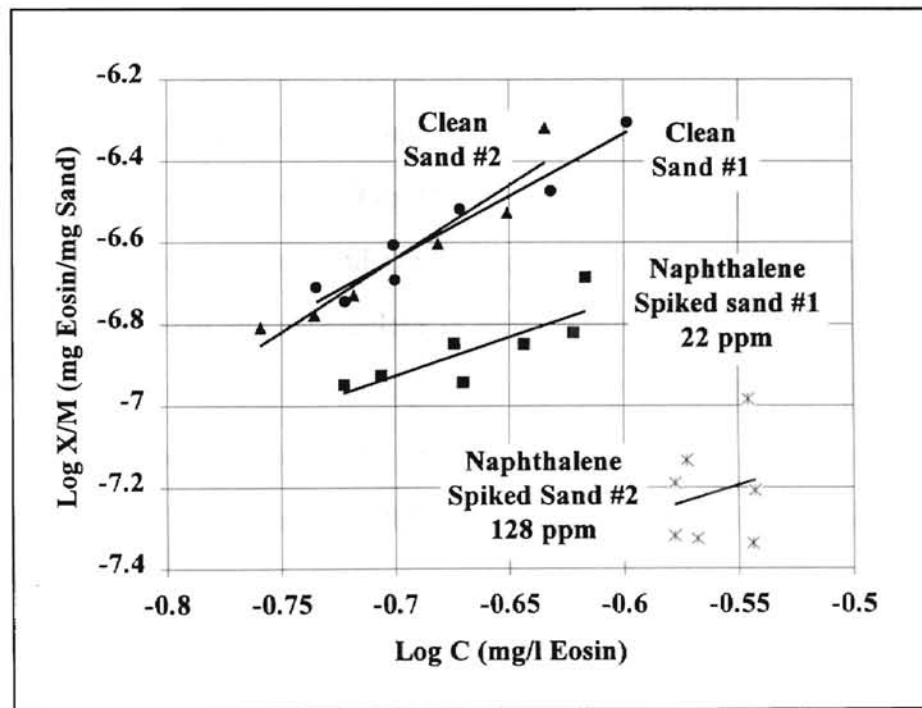


**Figure 5.1:** Combined Freundlich plots of four isotherms of DEC on Arkansas River Sand. The two clean sand isotherms exhibit good repeatability while the isotherms using naphthalene-spiked sand exhibit increased inhibition of DEC adsorption as the naphthalene spiking level increases.

## Discussion

The adsorption isotherms in Figure 5.1 indicate a competition for free surface area on the sand. The more naphthalene that was adsorbed to the surface of the sand grains, the less area available for DEC adsorption. While this may seem somewhat contradictory to the multilayer adsorption model, according to Hiemenz (1977), naphthalene adsorption fit closely to the monolayer adsorption model. Further support for this was found by generating a naphthalene adsorption isotherm with data from a DEC isotherm on naphthalene-spiked sand. GC analysis of the supernatant gave the residual naphthalene concentration  $C$  and, since the spiking level of the sand was known, the equilibrium concentrations of naphthalene on the sand could be calculated. Freundlich and Langmuir plots were generated from the data. The Low Langmuir plot ( $C$  vs.  $C/q$  where  $q$  is the solid phase concentration) had an  $r^2$  value of essentially unity from the regression analysis. This was expected since  $q$  was a function of  $C$  only. The Freundlich plot, had an  $r^2$  value of 0.4, which was much lower than for the Freundlich plots of the DEC isotherms on clean sand, which range from 0.7 to 0.9. The high Langmuir plot gave an  $r^2$  value of 0.48. These values are both low and support for one model or the other cannot be confirmed. The presence of any naphthalene in solution is enough to indicate that some desorption of naphthalene was occurring simultaneously with DEC adsorption. PAH molecules such as naphthalene adsorb primarily hydrophobically, as evidenced by its low solubility of 30 ppm (Verschueren, 1983). They are fairly neutral electrostatically, thus forming a barrier to adsorption by electrostatic bonding (Verschueren, 1983).

These findings suggest that competition for free surface by DEC or similar compounds on contaminated soils could be the basis of a very inexpensive qualitative assay for total petroleum hydrocarbon (TPH) contamination. Potentially the relative concentrations might be predicted in the field on this basis. The complexity of TPH's, as op-

posed to just PAH's, and soil with organic content as opposed to washed river sand add complexity beyond the scope of this investigation. Further investigation is warranted.

#### Non-Specific Adsorption of Dextran-Eosin Conjugate on Clean Ottawa Sand and Ottawa Sand Spiked with Naphthalene

When a fluorescent material is conjugated with a protein such as an antibody, quenching of the fluorescent signal occurs (Molecular Probes, Inc., 1993). To enhance the signal-to-background ratio while performing adsorption experiments, an adsorption media was sought that would produce a minimum of fluorescent background when agitated with deionized water. As discussed in Chapter IV, standard Ottawa sand produced less background than ARS. The following experiment was designed to test its ability as an adsorbent.

Standard Ottawa sand purchased from EM Science was prepared as described in Chapter IV. A portion of the sand was spiked with naphthalene at a concentration of approximately 34 ppm.

A solution of DEC in deionized water at an eosin concentration of 0.3 mg/l ( $\pm$  3%) was prepared as the adsorbate. Two isotherms were run in parallel using clean sand and naphthalene-spiked sand. The experiment was duplicated later using the same batch of naphthalene-spiked sand.

#### Results

Table VI shows a sample of the data from the clean sand isotherm. Figure 5.2 is a combined Freundlich plot of the four isotherms. The heavy arrows indicate increasing sand dosage.



Table VI

SAMPLE ISOTHERM DATA  
CLEAN OTTAWA SAND

Sample No.	Dextran-Eosin Sol. (grams)	Dextran-Eosin Sol. (ml)	Sand Dosage (grams)	Emissions Curve Area (v-nm)	Residual Concentration (mg/l Eosin)	Adsorbed Concentration (gm/gm)
Co				157.558	0.297	
1	2.9495	2.9495	2.4701	104.909	0.198	1.185E-07
2	2.9453	2.9453	2.1885	99.919	0.188	1.462E-07
3	2.9487	2.9487	1.8206	112.281	0.212	1.382E-07
4	2.9436	2.9436	1.5217	123.846	0.233	1.229E-07
5	2.9332	2.9332	1.2462	131.092	0.247	1.174E-07
6	2.9439	2.9439	0.9133	135.899	0.256	1.316E-07
7	2.9428	2.9428	0.6477	137.764	0.260	1.695E-07
8	2.9429	2.9429	0.3138	143.339	0.270	2.514E-07

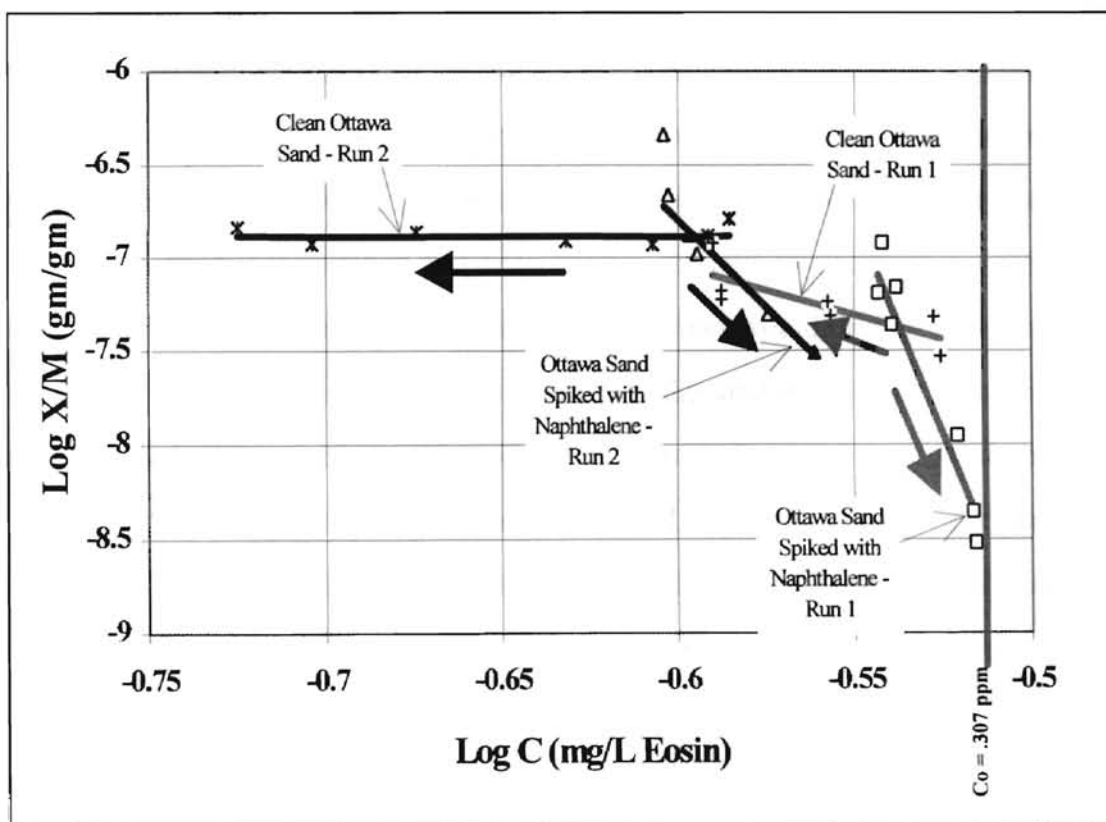


Figure 5.2: Combined Freundlich plot of two sets of isotherms on clean Ottawa sand and Ottawa sand spiked with naphthalene. The heavy arrows indicate the direction of increasing sand dosage. The presence of naphthalene on the sand inhibited DEC adsorption.

Run 2, displayed as black regression lines (Figure 5.2), indicated increased adsorption efficiency over Run 1, shown in gray, yet the relationship between clean sand and spiked sand isotherms was duplicated. The two spiked sand isotherms showed a greater adsorption capacity for DEC as the residual concentration of DEC in solution decreased. This is reversed from the norm. The residual concentration of DEC is also decreasing as the sand dosage decreases. GC analysis of the supernatant indicated that the concentration of naphthalene remaining on the sand decreased as the sand dosage decreased. The clean-sand isotherms showed relatively little change in adsorption with changing sand dosage.

### Discussion

The trend of adsorbed concentration versus residual concentration was reversed with the spiked sand isotherms. This trend reversal can be explained by understanding what happened to the adsorbed naphthalene as the sand dosage changed and by understanding the effect of the relative size differential in the DEC molecule versus the naphthalene molecule. The many times larger DEC molecules would likely need to find areas large enough to fully contain it in order to adsorb to the sand surface. GC analysis verified that naphthalene repartitioned into solution and was also seeking equilibrium, creating a reverse isotherm. As the sand dosage decreased more naphthalene, on a gram per gram basis, desorbed into solution. This created a greater potential for DEC adsorption as more contiguous surface area became free, reversing the normal adsorption trend. Competition for surface area was not a factor with clean sand. The adsorbed concentration was relatively constant at all sand dosages.

Polanyi adsorption theory (Manes, 1980) was applied in an attempt to determine if a change in ambient laboratory temperature could explain the apparent increase in adsorption efficiency of Ottawa sand in Run 2. It was possible to merge the characteristic

curves from Run 1 and 2 by adjusting the temperature parameter in the calculation. However, this required a change in the ambient laboratory temperature of  $-117^{\circ}$  centigrade, which was not a possible condition.

The Freundlich isotherm of the two tests could also be made to nearly coincide by increasing the starting concentration ( $C_0$ ) in the first test by 3% and decreasing the area under the  $C_0$  emissions curve by 9%. This did not affect the area under the emissions curves for the isotherm samples, however, it did change the computed residual concentrations and consequently the adsorbed concentrations. This amount of change is within the realm of possibility. A slight change in gain in the spectrofluorometer after the calibration scan could cause such a reduction in curve area. This apparent error did not influence the conclusions concerning adsorption mechanisms since that conclusion was based on the relationship between clean sand and spiked sand isotherms. That relationship was consistent between Run 1 and Run 2.

Figure 5.3 is a composite Freundlich plot comparing ARS and Ottawa sand isotherms. ARS is clearly the more efficient adsorbent as evidenced by larger values of X/M (gram per gram adsorption) under the same isotherm conditions. The BET analysis indicated ARS as having more surface area per gram than Ottawa sand ( $0.574 \text{ m}^2/\text{g}$  vs.  $0.039 \text{ m}^2/\text{g}$ ), which explains its superior ability as an adsorbent. The positive slope of the ARS regression lines indicate that residual concentration was the primary driving force for DEC adsorption. The repartitioning of naphthalene into solution tended to flatten the slope, but did not reverse it. These characteristics made ARS the preferred choice for antibody testing.

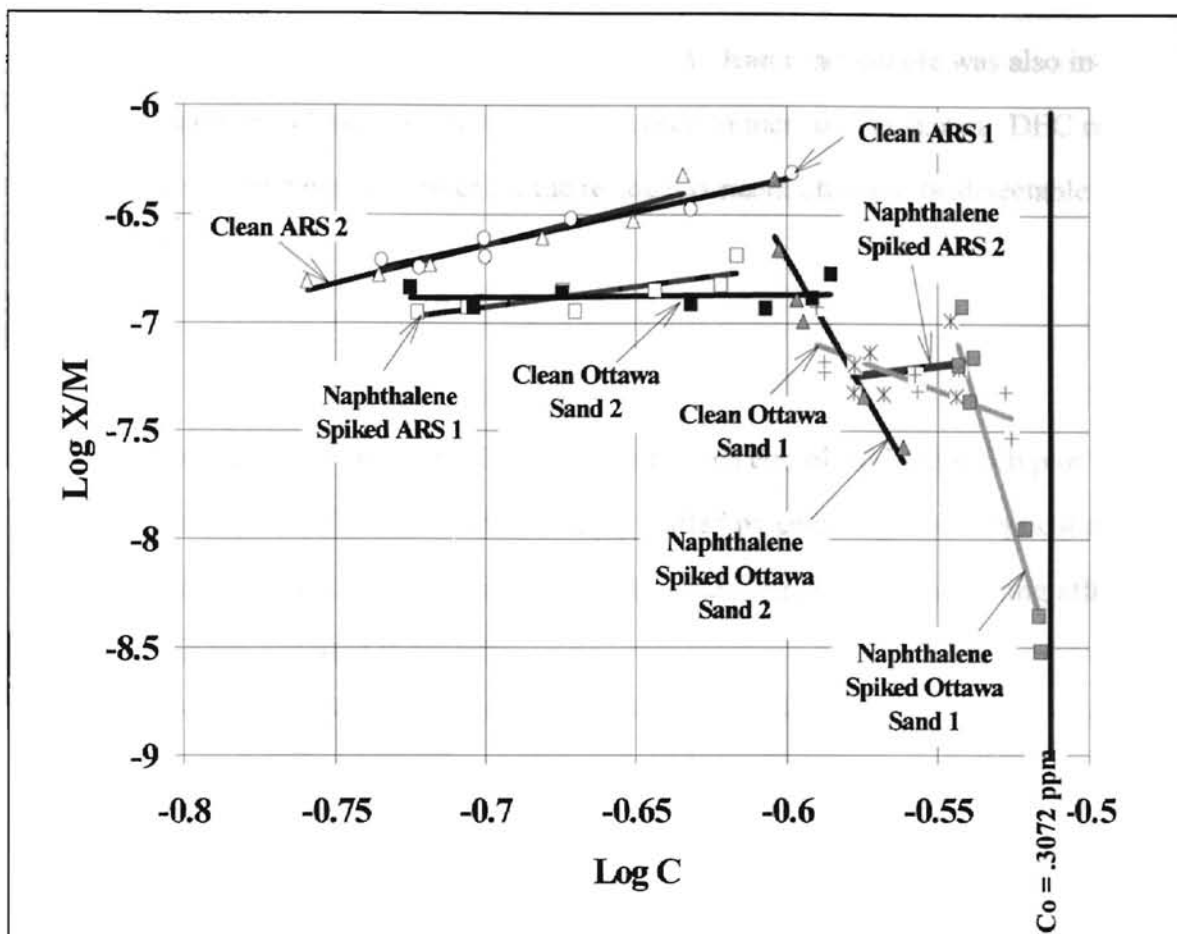


Figure 5.3: Composite Freundlich isotherm plots comparing ARS adsorption to Ottawa sand adsorption. ARS is a more efficient adsorbent and yields better repeatability.

### Non-Specific Adsorption of Dextran-Eosin Conjugate on Arkansas River Sand Spiked with Arab Medium Crude Oil

The adsorption tests with DEC on naphthalene-spiked sand indicated that adsorption was inhibited in proportion to the naphthalene concentration on the sand. DEC adsorption served as an assay for adsorbed naphthalene. This led to the idea of testing this as a potential assay technique for a qualitative analysis for less specific contaminants to soils, such as total petroleum hydrocarbons (TPH).

Adsorption isotherms were performed on ARS spiked with Arab Medium Crude oil using DEC as the adsorbate. Samples were spiked, as described in the previous chap-

ter, to a percent by weight range of 1.07 to 0.07%. A clean sand sample was also included. Preliminary adsorption tests indicated a need to increase the starting DEC concentration to one ppm eosin in order for the residual concentrations to be detectable above background.

## Results

Figure 5.4 shows the results of the isotherms in a combined Freundlich plot. Suspensions or emulsions of crude oil are not easily settled by centrifugation. Optical clarity is decreased proportional to the crude oil content in the sample. Light scattering affects of the suspensions distorted the results.

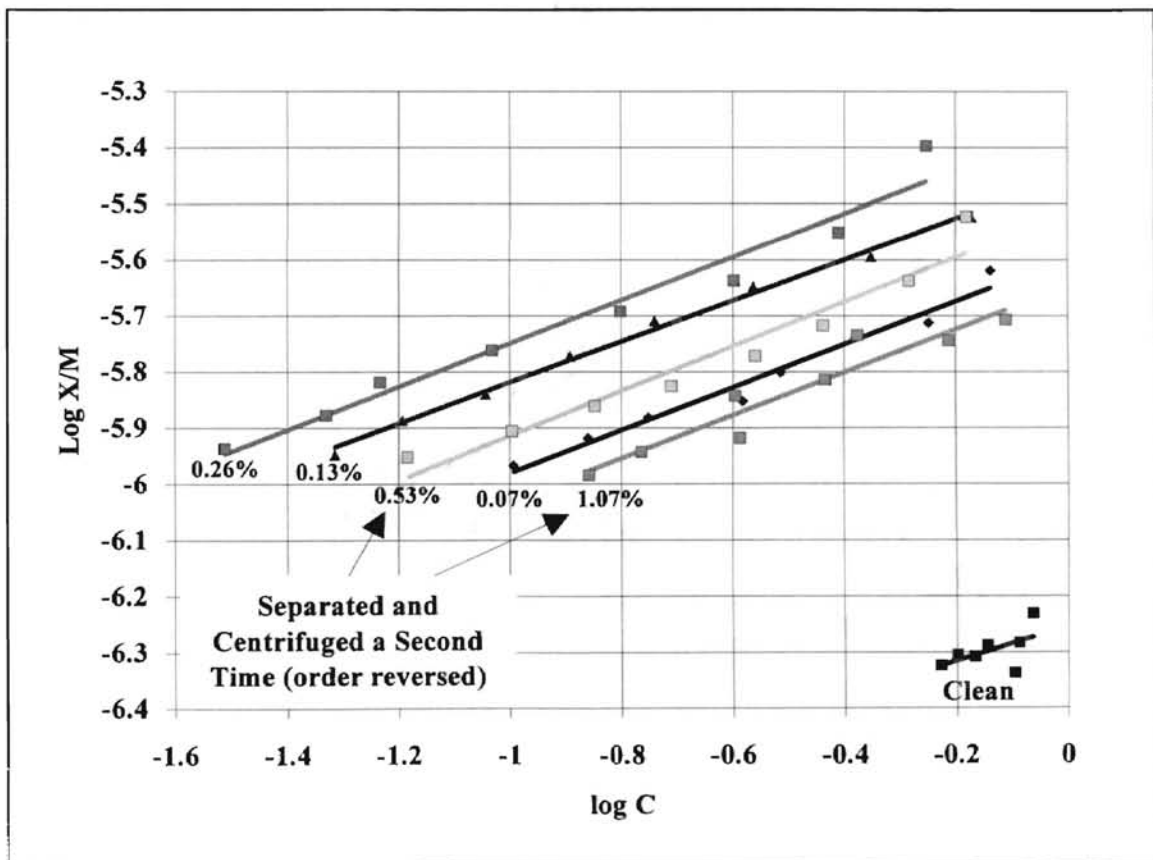


**Figure 5.4:** Freundlich isotherm plots of ARS spiked with Arab crude oil at a range of percents by weight. Colloidal suspensions and emulsions suppressed the fluorescent signals by scattering. The higher the percent crude oil present in the sand, the greater the scattering from the suspensions, giving a false indication of increased adsorption with increased crude oil content.

The samples with 0.53% and 1.07% crude oil were centrifuged a second time resulting in less scattering which altered the apparent relationship to the other isotherms. Increasing the time in the centrifuge would result in increased settling. However, since this would result in diminishing returns, a more practical approach was taken. The isotherms were repeated using an anionic polymer, diethylamine-epichlorhydrin, in an additional step to settle the suspensions. After the standard isotherm procedures were performed through centrifugation, two milliliters of the supernatant were extracted from each vial and placed in separate vials containing 1 drop (.012 grams) of the anionic polymer. This was gently agitated and centrifuged. This procedure cleared the supernatant of suspensions leaving only the residual DEC in solution. The supernatant was scanned to measure the residual concentration. These results are shown in Figure 5.5.

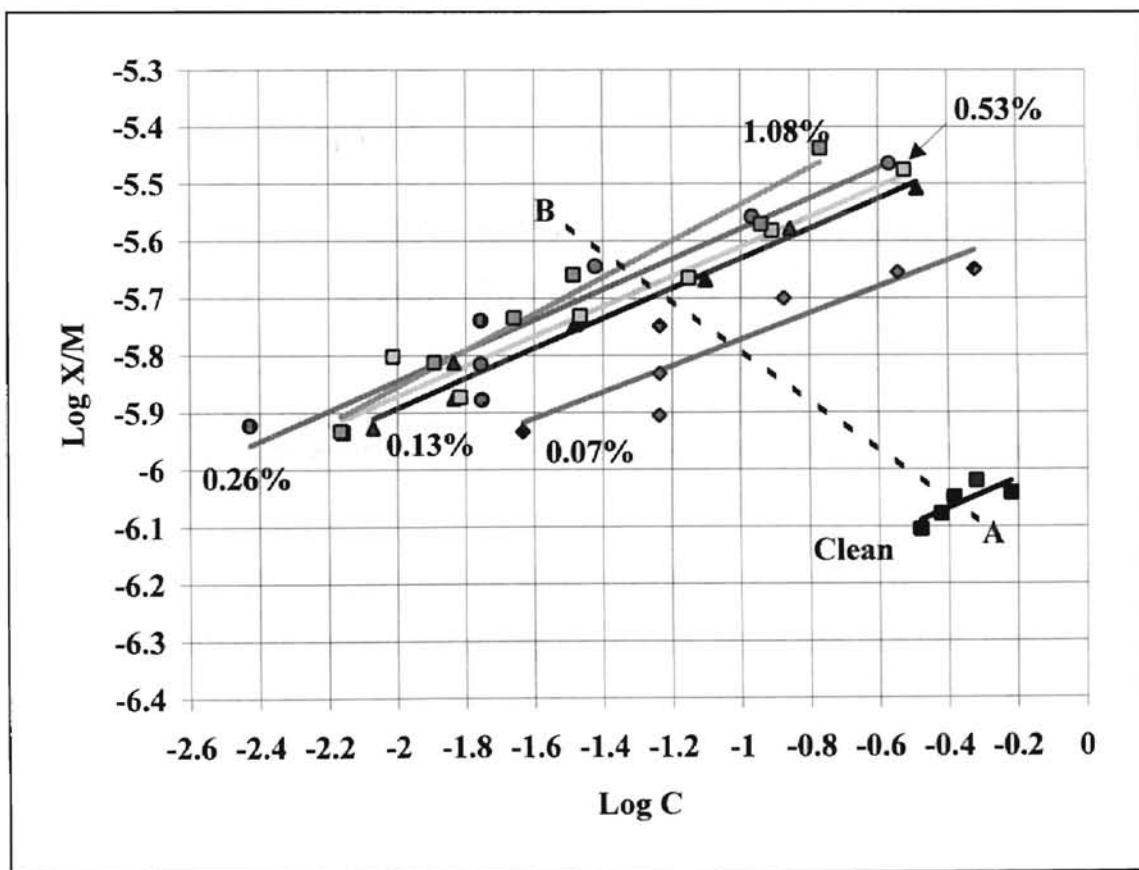
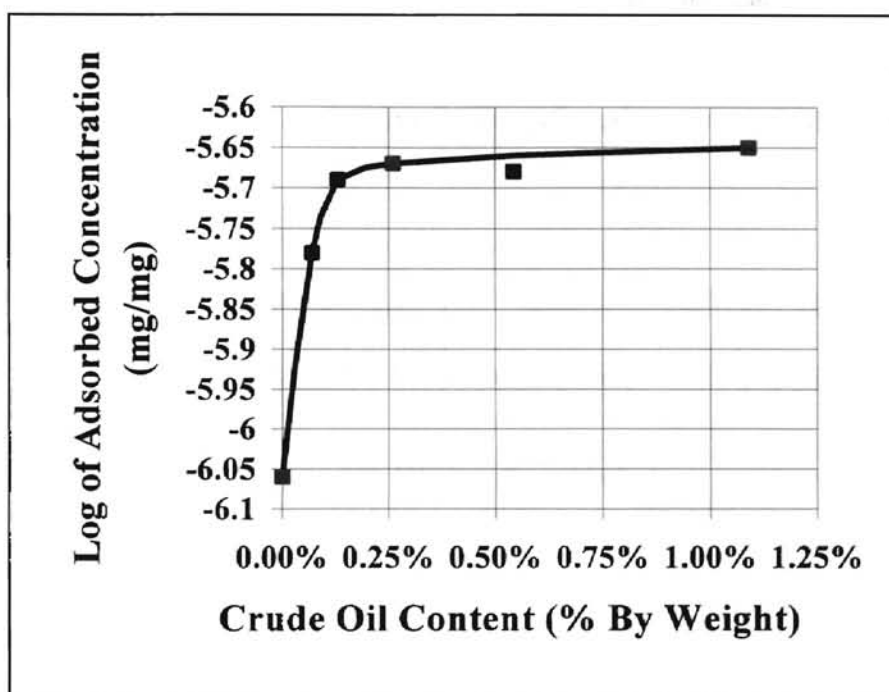


Figure 5.5: Freundlich isotherm plots of ARS spiked with Arab medium crude oil at a range of percents by weight. An anionic polymer was employed to settle suspensions.

The indication from the second test is that adsorption of the DEC increases as the crude oil content increases. However, there is an apparent limit to adsorption beyond which increasing the crude oil content alone will no longer increase adsorption. Figure 5.6 is a graph of the regression line values at the intersections of line **AB**. This line is a slice through the approximate midpoints of the regression lines and displays the 3rd dimension of the data.



**Figure 5.6:** Crude oil content in percent by weight vs. Log of adsorbed concentration. Values are extracted from the intersections of the regression lines and line **AB** in figure 5.5.

Figure 5.6 displays an apparent upper limit to adsorption. A first order relationship between crude oil content and adsorption of DEC exists only in a very narrow range of crude oil content. Beyond this, the relationship quickly becomes very nearly zero order. Potential exists for utilizing this technique for a qualitative measurement of TPH only within the range of the first order relationship. This was not explored further in this investigation.

## Discussion

Inhibited adsorption described in the earlier tests were based on a very simple model using a single PAH (naphthalene) for the spiking material. Naphthalene, being essentially electrically neutral and hydrophobic (low solubility) (Verschueren, 1983), forms a barrier to electrostatic adsorption and DEC, being more hydrophilic (high solubility), is effectively blocked from adsorption by the naphthalene. According to the GC analysis, Arab Medium Crude oil contains many more aliphatics, particularly paraffins, than aromatics. DEC adsorption is not inhibited by the presence of these complex organic compounds but is actually stimulated. The GC analysis of Arab Medium Crude oil is displayed in the appendix.

### Specific and Non-Specific Adsorption of Anti-Naphthalene Antibody on Clean Arkansas River Sand and Arkansas River Sand Spiked with Naphthalene.

From the adsorption tests using DEC as the adsorbate, it was learned that the presence of naphthalene on the surface of the adsorbent inhibited DEC adsorption by limiting free surface area and forming an electrostatically neutral barrier. The following experiments were designed to determine whether the anti-naphthalene antibody will bind specifically with the adsorbed naphthalene and remain in solid phase, overcoming the inhibition to adsorption.

Standard isotherm protocol as described in Chapter IV was employed. Non-specific adsorption was tested using clean ARS while specific adsorption was tested using ARS spiked with naphthalene according to the procedures described in Chapter IV.

EITC-labeled anti-naphthalene antibody provided by SDI was used as the adsorbate. The time required to reach equilibrium was tested with a single vial containing 2.4 grams of sand and 3 ml of a 1 mg/l solution of antibody (based on EITC Concentration). The vial was agitated and scanned at 20 min intervals. During this test, quenching of the fluorescent signal was observed (Molecular Probes, 1993). The quenching was much



greater than had been anticipated. To compensate, the starting EITC concentration was increased to 1 mg/l. Clean sand isotherms were run separately to test for repeatability. This was followed by one isotherm on naphthalene-spiked sand.

## Results

Isotherm data for anti-naphthalene antibody is displayed in Figure 5.7. The curve is concave upward and does not indicate a maximum adsorption limit. Regression analysis of the linear plots gave nearly equal  $r^2$  values for the Freundlich and the high Langmuir plots (0.82 versus 0.80). The Low Langmuir slope is reversed from the norm and does not fit the theoretical curve displayed in Chapter II, Figure 2.3. The BET isotherm has an  $r^2$  value of 0.4. It is inconclusive whether anti-naphthalene antibody fits a multilayer or a monolayer model, however, the concave upward shape does not suggest a limit to adsorption at these low concentrations.

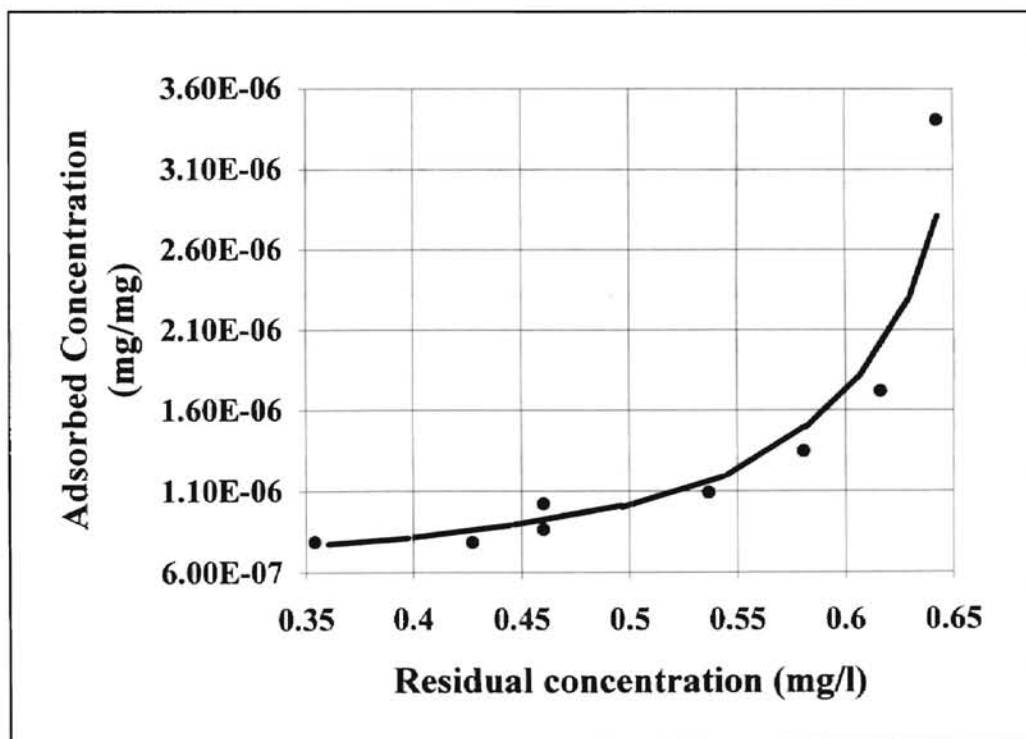


**Figure 5.7:** Isotherm data for anti-naphthalene antibody on clean ARS. A concave upward pattern is displayed.

Figure 5.8 is a composite Freundlich plot of two clean sand isotherms and one on sand spiked with naphthalene. The two clean sand isotherms differ from each other by only 5.67% of the average ppm adsorbed, while the isotherm on the naphthalene-spiked sand differs from the clean sand isotherm by 16.89% of the average ppm adsorbed. This clearly displays inhibited adsorption.

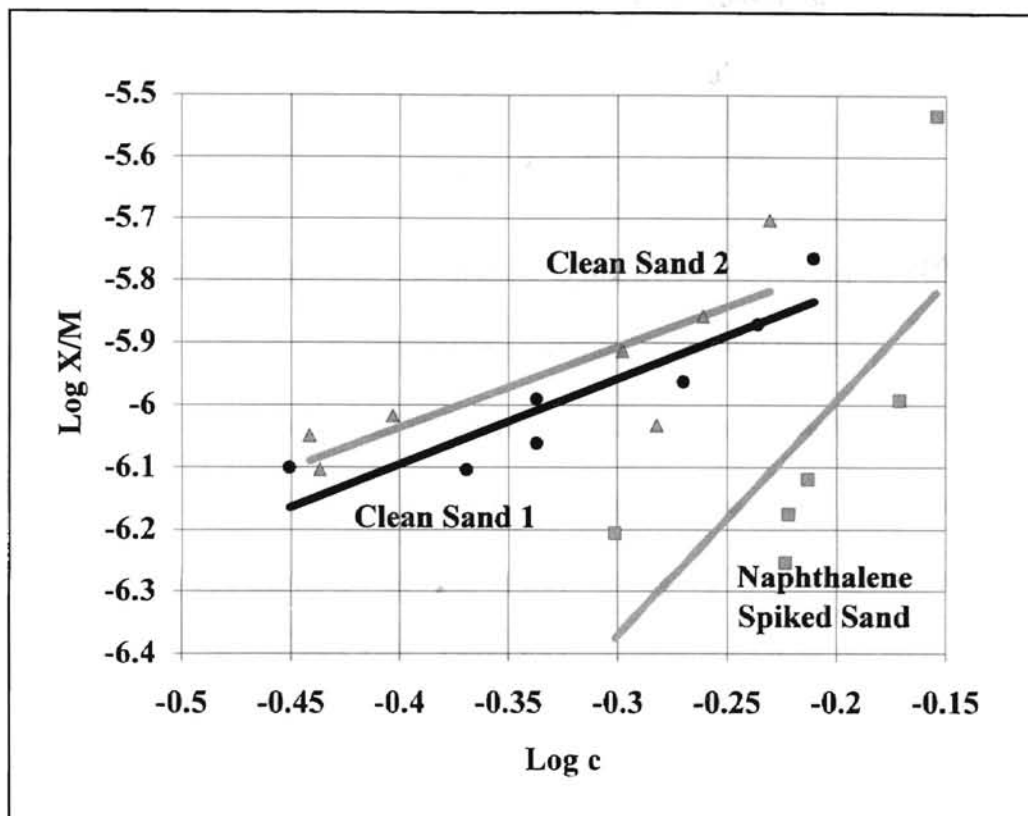


**Figure 5.8:** Composite Freundlich plots comparing three isotherms of Anti-naphthalene antibody on ARS.

Change in Free Energy. The standard change in free energy in calories per mole of a system at equilibrium is defined as

$$\Delta G^{\circ} = -RT \ln K$$

where  $K$  is the equilibrium constant (Sawyer and McCarty, 1978). For the isotherms that were performed using anti-naphthalene antibody on ARS, the equilibrium reaction can be written as



where  $Ab_L$  is the antibody in liquid phase and  $Ab_S$  is the antibody in solid or adsorbed phase. From Sawyer and McCarty (1978),  $K$  is defined as

$$K = \frac{[Ab_S]}{[Ab_L]}$$

The value of  $K$  is independent of expressing the concentrations as antibody-EITC conjugate or as EITC since the proportions are constant.  $K$  is evaluated as:

$$K = \frac{q \times 10^6}{C}$$

where  $q$  is in units of gm/gm and  $C$  is in units of mg/L. Multiplying  $q$  by  $10^6$  converts  $q$  to units of mg/kg, making both concentration values equivalent units.

Figure 5.9 is a cross plot of isotherm data from the adsorption of anti-naphthalene antibody on clean ARS and on ARS spiked with naphthalene. Lines of constant  $\Delta G^\circ$  values ranging from -900 cal/M to +200 cal/M were computed by solving for a range of  $q$  and  $C$  values for each constant  $\Delta G^\circ$ . These lines are displayed with the cross plot. Envelopes have been drawn around the two groupings of data. With the exception of one outlier from each grouping, all data falls into the two separate groupings. The  $\Delta G^\circ$  values related to adsorption on naphthalene-spiked sand are between -250 and +50 calories per mole, indicating a very low heat of adsorption.

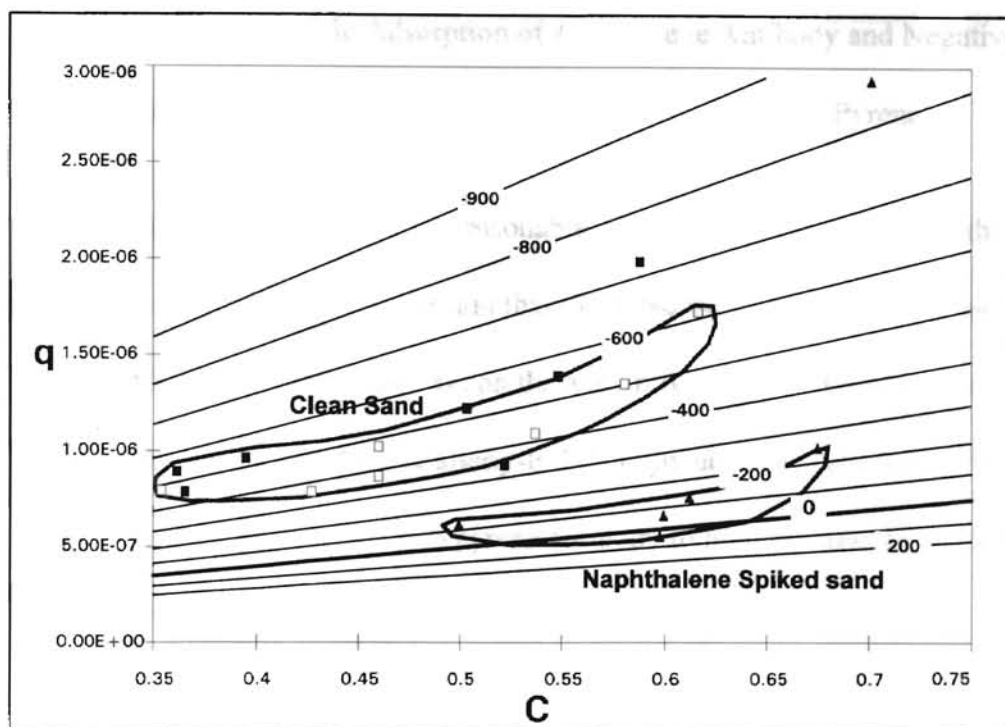


**Figure 5.9:** Cross plot of Anti-naphthalene antibody isotherm data with lines of equal  $\Delta G^\circ$  values in calories per mole.

### Discussion

The specificity of anti-naphthalene antibody for naphthalene did not overcome the inhibition to adsorption observed with DEC adsorption in the presence of naphthalene. This experiment does not rule out the possibility of a small degree of specific binding since a non-reactive control antibody was not used as a basis of comparison. SDI made available a "negative control" antibody that is non-reactive with PAH molecules according to ELISA results. Test results comparing adsorption of the negative control antibody with anti-pyrene antibody on pyrene spiked sand follow.

## Specific and Non-Specific Adsorption of Anti-Pyrene Antibody and Negative Control Antibody on Arkansas River Sand Spiked with Pyrene

It was determined that ARS is a reasonable adsorptive media for testing the anti-naphthalene and anti-pyrene antibodies and that the presence of low solubility and electrically neutral PAH's, such as naphthalene, on the adsorptive media inhibited non-specific adsorption of both the DEC and the antibody-EITC conjugate. The following procedure is designed to test the ability of the anti-pyrene antibody to bind specifically with pyrene that is adsorbed to the soil surfaces.

ARS was spiked with pyrene using the procedure described in Chapter IV. Polyclonal Anti-pyrene rabbit antibodies tagged with EITC were provided by SDI along with negative control antibodies also tagged with EITC. Negative control antibodies are identical to the anti-pyrene antibodies with the exception that they are non-reactive with PAH molecules. Reactivity characteristics were tested by SDI using ELISA protocol. Protocol design is shown in the appendix.

### Results

Two adsorption isotherms were run concurrently using equal concentrations of each antibody as the adsorbate, and pyrene spiked ARS as the adsorbent. Freundlich plots and High Langmuir plots of these isotherms are shown in Figure 5.10 and 5.11 below. The adsorption characteristics of the two antibodies are nearly identical.

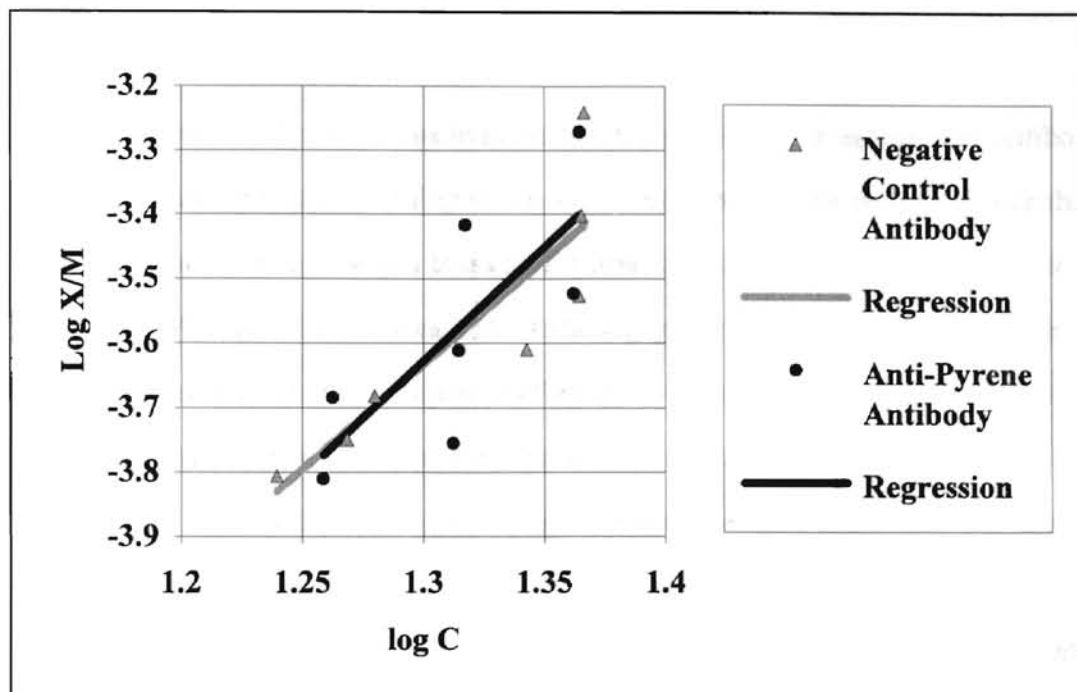


Figure 5.10: Freundlich isotherms of Anti-Pyrene antibody vs. Negative Control antibody on pyrene spiked ARS.

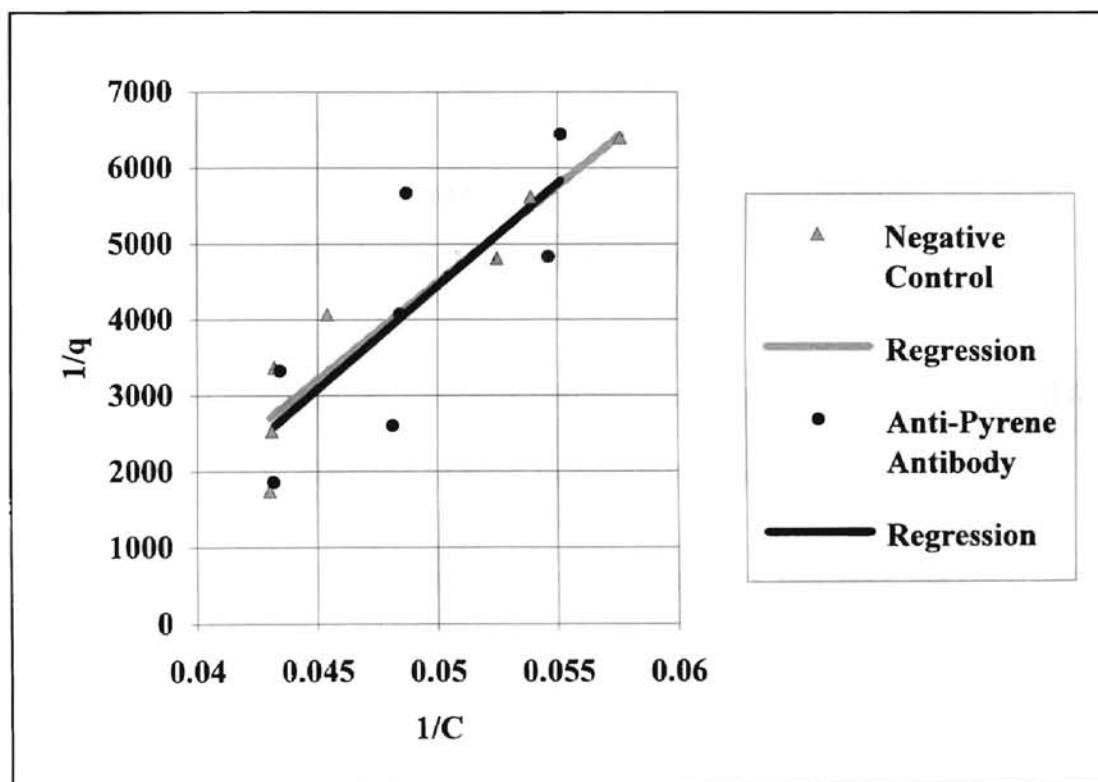


Figure 5.11: Langmuir high plot of Anti-Pyrene antibody vs. negative control antibody on pyrene spiked ARS

## Discussion

The results of the isotherms indicate that the specificity of anti-pyrene antibody for pyrene does not enhance its ability to adsorb to sand spiked with pyrene. Since the bonding force for antibody-antigen bonding is proportional to  $1/d^2$  for electrostatic forces and to  $1/d^7$  for Van der Waals forces, the interacting groups must be close to the point of bumping together and rotating into place before these forces become significant (Roitt, Brostoff, and Male, 1985). The flat structure of the PAH molecule adsorbed to soil particle surfaces is not accessible to the complementary structure of the antibody and the forces of attraction are not strong enough to lift the pyrene molecule from the soil surface. This situation can be illustrated by imagining picking up a dime from a flat surface while wearing mittens. If the dime were standing on edge the task would be easily achievable, however, this is not a likely state for a dime nor for a pyrene molecule adsorbed to soil. This suggests that immunoassay for pyrene in solid phase is not possible due to the physical nature of the required antibody-antigen bond. This result very likely extends to all PAH's that adsorb to surfaces leaving the epitope (handle) inaccessible. These observations are in retrospect to the negative results of the tests but would not have negated the need for performing the tests to prove their validity.

### Evaluation of Commercially Available Immunoassay Field Test Kits Developed for Analysis of PAH Contamination to Soil

A few commercially available immunoassay test kits have been marketed that claim to be accurate in testing for PAH contamination in soils and water. Two of the soil test kits, from Quantix Systems (Cinnaminson, New Jersey), and EnSys, Inc. (Research Triangle Park, North Carolina), were tested. Quantix claims to be able to give an exact reading in ppm from a hand held dual beam reflectometer (included in the kit). The

EnSys RIS<sup>c</sup>® test system was designed to give the levels in terms of a range from 1 to 10 or 10 to 100 ppm with a portable dual beam photometer (sold separately). The test procedures for these kits required an extraction step using the solvents isopropanol or methanol, respectively, prior to beginning the assay. These kits were tested for accuracy first by using ARS spiked to known levels of pyrene and second by adding measured amounts of naphthalene, pyrene, or anthracene directly to the extraction solvent.

### Quantix Systems

Kit Design. The Quantix kit is designed as a portable workstation in a vinyl carrying case. All necessary supplies and instruments fit neatly into slots and holes in the workstation. The work table surface is designed to assay five samples at one time. The opened lid contains additional storage for assay kit supplies, and a set of index cards with abbreviated operating instructions are easily accessible. The assay is a standard ELISA protocol where the sample being analyzed is competing for binding sites on the antibody with an enzyme labeled reference analyte. The antibodies are immobilized on the surface of polystyrene discs approximately five millimeters in diameter. Figure 5.12 is a detector showing two wells containing the polystyrene discs coated with the antibody. Assay solutions are dropped onto the discs in metered drops and excess solution is absorbed into the body of the detector below the discs. This detector snaps into the hand held reflectometer which compares the color intensity of the sample, S, with the reference sample, R, as a measure of the concentration. Calibration curves are selected from permanent memory in the reflectometer, depending on concentration range and type of pollutant being assayed.



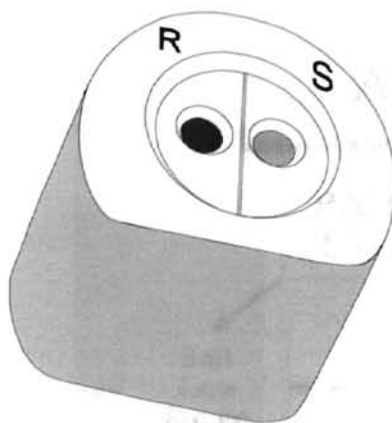


**Figure 5.12:** Quantix immunoassay detector.

The soil samples are taken with a tube with a syringe plunger. The tube is pushed into the soil until full and loosely packed. This soil sample represents an average of 10 grams of soil. By pressing the plunger, the soil sample is transferred into an extraction solution of 10 mg of isopropanol. The instructions call for mixing the soil with the extraction solution for one minute and then letting it settle. A tube with a filter covering one end surrounded by a rubber gasket is plunged into the extraction tube to filter a small amount of analyte solution. On the other end is a dropper tip for dispensing the solution. At this point the assay proceeds with as with a liquid sample. Figure 5.13 is a process flow diagram for the Quantix system.

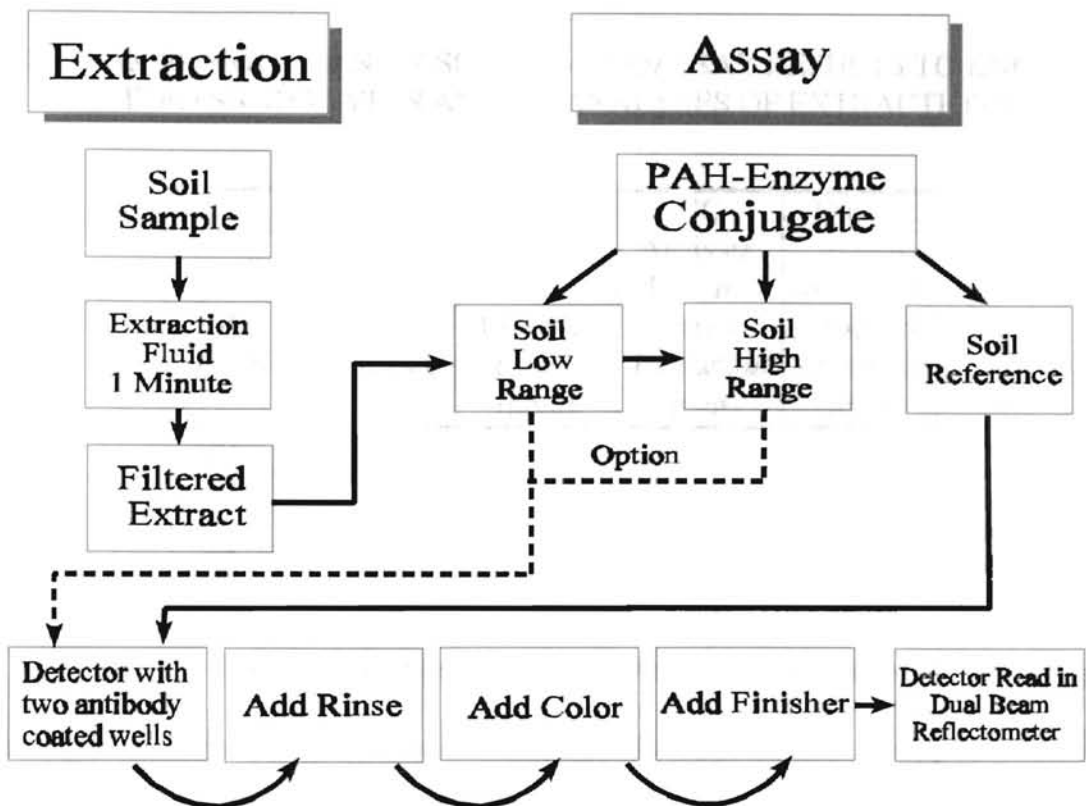


**Figure 5.13:** Process flow diagram for the Quantix field test kit. Five samples can be tested simultaneously.

Results. Arkansas River Sand spiked with pyrene was used to test the soil analysis system for PAH's. Table VII is a comparison of three types of analyses on three spiked samples. The GC analysis on the methylene chloride extraction is believed to be the more accurate analysis based on the intended spiking levels of 17.13 and 10.21 ppm.

TABLE VII

## COMPARISON OF QUANTIX SOIL IMMUNOASSAY RESULTS TO KNOWN SPIKED SAND LEVELS AND GC ANALYSES OF EXTRACTIONS

Spiked ARS Sample	Spiking level using pyrene spiking procedure (ppm)	GC Analysis, Methylene Chloride Extraction (ppm)	GC Analysis, Iso-propanol Extraction (ppm)	Quantix System Assay - Iso-propanol Extraction (ppm)
#1	97.58	-	-	42.6
#1	97.58	-	-	46.6
#2	17.13	15.234	3.958	1.60
#3	10.21	8.497	4.516	6.10

Methylene chloride extraction was not used to test spiked sample #1. The isopropanol extraction was not as efficient as methylene chloride extraction for pyrene on soil. This partially accounts for a low Quantix System assay value. Since extraction efficiency is a variable in the accuracy of the assay, tests on three different PAH's were performed by assuming 100% extraction efficiency. This was accomplished by adding the PAH directly to the extraction solution in known quantities. Table VIII on the following page summarizes those results.

TABLE VIII

## COMPARISON OF QUANTIX SOIL IMMUNOASSAY RESULTS TO KNOWN PAH CONCENTRATIONS IN SOLUTION

PAH	Known Concentration (ppm)	Quantix Assay Concentration (ppm)	Percent Error	Average Percent Error by PAH
Naphthalene	68	17.0	75.00%	79.81%
Naphthalene	247	38.0	84.62%	
Pyrene	108	86.0	20.37%	
Pyrene	108	61.0	43.52%	
Pyrene	108	61.0	43.52%	
Anthracene	66	0.8	98.79%	
Anthracene	72	1.2	98.33%	

The second and third test on pyrene was performed using a new package of assay supplies and the assayed concentration changed from 86.0 ppm to 61.0 ppm, as shown in Table VIII. A new package could have come from a different batch during manufacture of the kit supplies. This could explain the change in results and could indicate a quality control problem in manufacture. Repeated testing using the same supplies showed good precision in assay results although the accuracy was far less than desirable. Agitation for one minute was not adequate to dissolve the PAH's in the isopropanol. Naphthalene dissolved in slightly over one minute while pyrene took 15 to 20 minutes. Anthracene had to be placed on a shaker for several hours before completely dissolving.

Discussion. The Quantix work station is very well designed and very easy to use and ideal for field conditions. The immunoassay results without extraction showed good precision although accuracy was very low. The antibody clearly displayed a higher affinity for pyrene than for naphthalene or anthracene. Field use of the kit would require calibration by laboratory analysis. As the proportionate concentrations of PAH's change, the calibration will certainly be affected. The extraction technique using the soil sample

syringe and isopropanol solvent increases the variability in the test results. Soil samples should be weighed and mixed more thoroughly with the solvent. Methylene chloride is not miscible in water. This makes extraction of moist soils difficult. Vibrating mixers such as the Thermolyne Maxi Mix 1, help in breaking up and thoroughly mixing the soil with the solvent. Anhydrous magnesium sulfate powder could be used to sequester the moisture and improve extraction efficiency of methylene chloride.

A soil sample from a site undergoing remediation and known to be contaminated with PAH's was tested using the Quantix kit. The actual PAH content in this soil sample was unknown. The sample was very high in clay content and tended to remain in clumps. An attempt was made to break up the clay with a small stainless steel spatula. The assay indicated that the level of PAH contamination was below the limit of detection. It is very unlikely that the extraction was successful on this clay. The extraction method provided was useful only for very sandy soil with low clay content. It would have been more beneficial to use a blender to thoroughly mix the clay and the isopropanol.

#### EnSys RIS<sup>cc</sup>® Test System

Kit Design. The EnSys kit comes packaged in plastic trays that cannot be used as the work table. A separate test tube rack and flat table is necessary for running the tests. A portable scale is necessary for weighing the soil sample, and a positive displacement pipette with disposable tips is needed to dispense 30 µl of various solutions.

The soil extraction step is handled similarly to the Quantix System, however, the 10 grams of soil is weighed and a 20 ml methanol extraction solution is used. The assay design is a standard ELISA protocol, as with the Quantix System. Before the assay begins, the test solution is serially diluted two times to create a 1, 10 and 100 ppm sample. This means that each of these samples will be compared to a reference and be determined to be either greater than or less than their respective dilution values. Two

references are prepared using a supplied PAH. Five test tubes at a time are used for one test sample, making it difficult to run more than one sample at a time. Enzyme-labeled PAH substrate is added to each of the five test tubes and each of these test tubes are poured into clear test tubes containing the antibody immobilized on the bottom surface. The solutions are allowed to react for 10 minutes and then washed out vigorously with a wash solution. A color developer is added and then a stop solution. The final solutions are various shades of a clear yellow solution. The darkest reference solution is chosen and the other is discarded. The remaining three are compared to the reference in the portable photometer. The photometer reads either high or low for each of the three samples. This narrows the ppm concentration to either less than 1 ppm, between 1 and 10 ppm, between 10 and 100 ppm, or greater than 100 ppm. Following is a process flow diagram of the EnSys assay system.

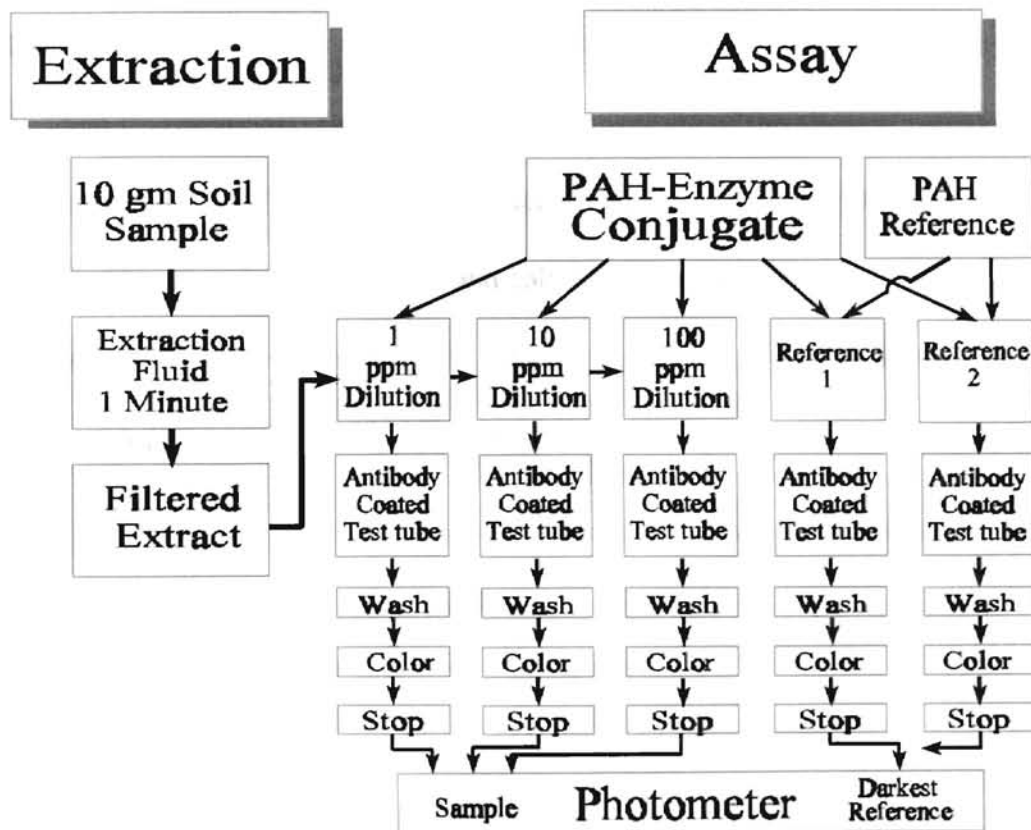


Figure 5.14: Process flow diagram of the Ensis RIS<sup>®</sup> kit. Only one test can be run safely at a time.

The IBM spectrophotometer was used with the RIS<sup>®</sup> kit rather than purchasing the portable photometer. The wavelength was set to 450 nanometers and values of absorbance for the three dilutions relative to the reference solution was read as per instructions given by the EnSys technical staff. Negative absorbance equated to a low reading while positive absorbance equated to a high reading.

Test Limitations. Due to a limited number of available test supplies, soil extraction accuracy was not tested. The handling of test tubes, solutions, and pipettes, and the timing of procedures allowed for potential accidents and errors for inexperienced operators. Errors further limited the number of tests that could be run. All tests were made by direct spiking of the extraction solution to insure a known concentration of test solution. Since this assay was designed as a total PAH indicator, the sensitivity to individual PAH's varies. Table IX shows the sensitivity of the assay to various PAH's. When individual PAH's are tested, the detection ranges (1,10, and 100 ppm) must be multiplied by the value in the right hand column of the table. For example, when testing a pyrene spiked sample, the sensitivity ranges become 3.5, 35, and 350 ppm. EnSys advertises a 95% accuracy with this system.

TABLE IX

PAH RIS<sup>®</sup> SOIL TEST SENSITIVITY TO PAH COMPOUNDS

PAH Compound	*Concentration Necessary to Result in Positive Test (ppm)
2 Rings	
Naphthalene	200
3 Rings	
Acenaphthene	8.1
Acenaphthylene	7.5
Phenanthrene	1.0
Anthracene	0.81
Fluorene	1.5
4 Rings	
Benzo[a]anthracene	1.6
Chrysene	1.2
Fluoranthene	1.4
Pyrene	3.5
5 Rings	
Benzo[b]fluoranthene	4.6
Benzo[k]fluoranthene	9.4
Benzo[a]pyrene	8.3
Dibenzo[g,h,i]perylene	>200
6 Rings	
Indeno[1,2,3-cd]pyrene	11
Benzo[g,h,i]perylene	>200

\*Data provided by EnSys, Inc.

**Results.** Two tests were run correctly on pyrene at 76 ppm and tests using anthracene at 47 and 48 ppm were run procedurally correct. Pyrene standards were 3.5, 35, and 350 ppm. Both tests registered correctly between 35 and 350 ppm. The ranges for anthracene were 0.81, 8.1, and 81 ppm. The first test on anthracene was in error, registering greater than 81 ppm while the second registered correctly between 8.1 and 81 ppm.



Use of the IBM spectrophotometer to read the relative absorbance values allowed a more critical analysis of the results. If the assay registered with 100% accuracy, a plot of the relative absorbance values against the detection range values expressed logarithmically would yield a straight line that intersects the zero relative absorbance line at the log of the exact concentration (EnSys, 1994). A linear regression through the three real data points will give an evaluation of how close this assay is reading the true value, or at least how repeatable the results are. Following are tabulations of the data and cross plots of the data along with their linear regressions.

TABLE X  
PYRENE ANALYSIS #1 at 76 PPM  
ASSAYED CONCENTRATION BETWEEN 35 AND 350 PPM

ppm	log ppm	Relative ABS <sub>450nm</sub>	Linear Regression
3.50	0.544	-0.0658	-0.0714
35.00	1.544	-0.0371	-0.0261
350.00	2.544	0.0248	0.0192
*131.72	2.120		0

\*Theoretical concentration from assay; i.e. concentration where relative absorbance of the sample is equal to the reference.

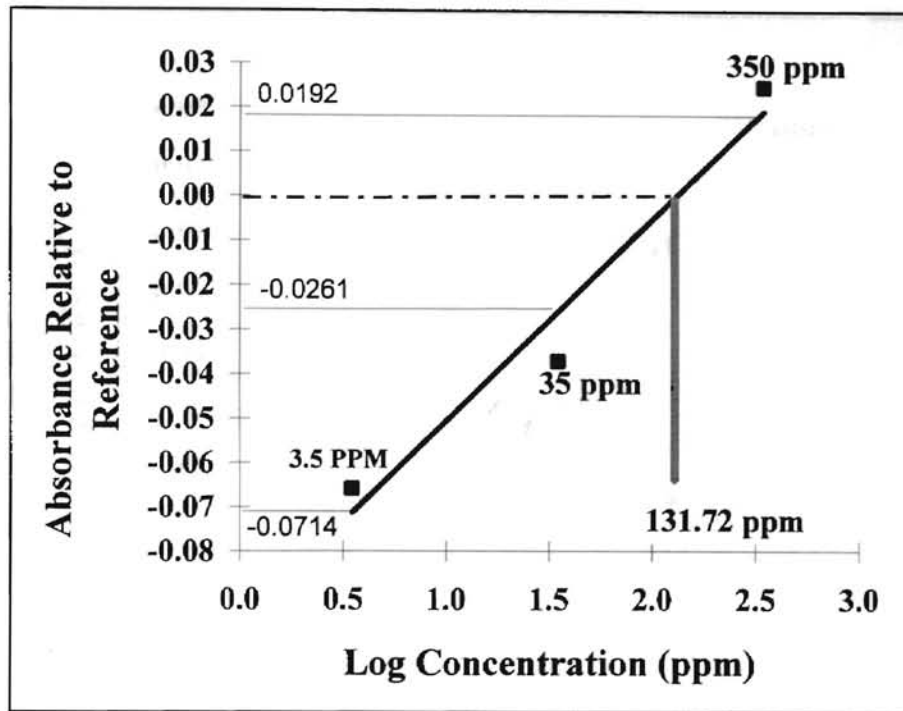


Figure 5.15: EnSys RIS<sup>®</sup> test data for first pyrene sample at 76 ppm. Test registers correctly between 35 and 350 ppm.

TABLE XI

PYRENE ANALYSIS #2 at 76 PPM

ASSAYED CONCENTRATION BETWEEN 35 AND 350 PPM

ppm	log ppm	Relative ABS <sub>450nm</sub>	Linear Regression
3.50	0.544	-0.103	-0.1114
35.00	1.544	-0.066	-0.0490
350.00	2.544	0.022	0.0134
*213.69	2.330		0

\* Theoretical concentration from assay; i.e. concentration where relative absorbance of the sample is equal to the reference.

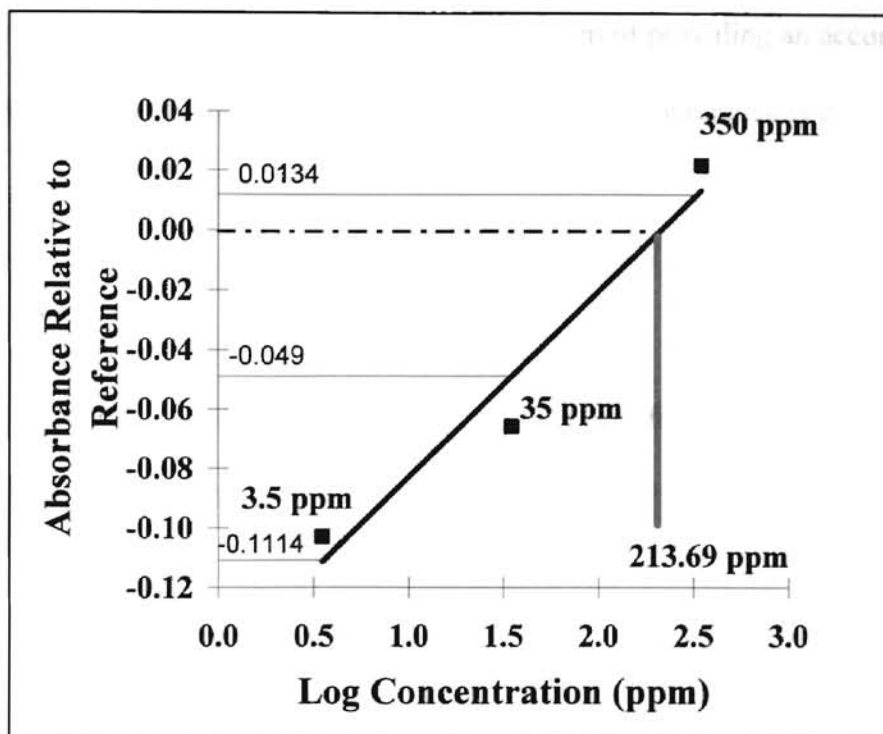


**Figure 5.16:** EnSys RIS<sup>®</sup> test data for second pyrene sample at 76 ppm. Test registers correctly between 35 and 350 ppm.

Both tests indicated the concentrations correctly between 35 to 350 ppm, which is the advertised accuracy of the assay. However, the concentrations indicated by reading the actual absorbance were in error by 73% and 181% respectively. When the detection ranges are left at 1, 10, and 100, the test still registers correctly and the error changes to a -50% and -20% respectively. The first test on anthracene was outside the window, registering greater than 81 ppm. The computed value was 590 ppm. The second test was within the detection limits of 8.1 to 81 ppm. The computed value was 70 ppm which is an error of 46%.

Discussion. The EnSys RIS<sup>®</sup> test kit is cumbersome and not easily usable under field conditions. The few tests that were run correctly did not fully evaluate the kit, how-

ever, the evidence suggests that the manufacturers claim of providing an accurate assay 95% of the time is true. The user would have to be satisfied with results given in broad ranges.

### Summary

Two commercially available immunoassay systems for the detection of PAH's in soil were tested. The Quantix System workstation, and the EnSys RIS<sup>®</sup> system. Both system were designed to be used under field conditions.

The EnSys system gives the results expressed in ranges. The ranges are less than 1 ppm, between 1 and 10 ppm, between 10 and 100 ppm, and greater than 100 ppm. EnSys advertises 95% accuracy when using this system. The extraction solvent (methanol) was spiked directly to simulate 100% extraction efficiency. Only four tests were run, two using pyrene and two using anthracene. Three test results were within the proper range of the spiked sample. This is not enough to confirm the 95% accuracy claim. Cross plotting relative absorbance against the log of the detection ranges, and doing a linear regression gave the theoretical exact concentration where the regression line crossed the zero relative absorbance line. This value varied widely between identical samples tested. The procedures were more complicated than the Quantix system and the handling of test tubes and timing of steps left room for mistakes. Field use requires a table, scale and portable photometer.

The Quantix system was designed as a portable work station in a carrying case. Everything that is needed to run the tests are included in the work station, including a

hand held reflectometer for reading the results. The system gives the results as a single number in parts per million. Seven tests were run by spiking the extraction fluid (isopropanol) directly to simulate 100% extraction efficiency. Samples tested were naphthalene, pyrene, and anthracene. At least two tests were run on each spiked sample. Nearly all results were repeatable with good precision, though the accuracy was very low, particularly for anthracene. The repeatability of the tests indicate that the results could be calibrated for a particular test site with a few laboratory tests. The extraction procedures could be improved for better accuracy using mechanical mixing and/or methylene chloride with anhydrous magnesium sulfate powder to sequester the moisture in the sample, provided this has no adverse impact on the antibody. Extraction using methylene chloride with anhydrous magnesium sulfate powder was not tested with the antibody. Despite the poor extraction system, two tests on pyrene spiked sand gave very close to the same result.

## CHAPTER VI

### CONCLUSIONS

The isotherm experiments demonstrated that antibodies specific to certain polycyclic aromatic hydrocarbons could not bind to their respective antigens while the antigens were bound to soil surfaces. This conclusion is substantiated by four main points documented in literature. These points are, (a) antibodies and antigens must have lock-in-key complementary shapes in order to bind, (b) the attractive forces in antibody-antigen binding (hydrogen bonds, electrostatic, Van der Waals, hydrophobic) are weak individually but become strong once in place due to the multiplicity of binding sites, (c) antigens must be accessible to the antibody's binding sites in order to bind, and (d) PAH molecules are structurally flat and are not accessible while bound to soil surfaces.

Very little is written concerning solid phase immunoassay. The poster presentation at Analytica '94 referenced by Stave (1994) and discussed in the literature review, indicated that solid phase immunoassay for more complex molecules with an accessible epitope is possible. Removing the *Fc* fragment and using only the *Fab* fragments of the antibodies reduced non-specific adsorption and increased the sensitivity of the assay.

Several isotherm tests were run in preparation for testing the antibodies and two commercially available immunoassay kits were tested. Following is a brief summary and conclusion for each of these tests.

## Dextran Eosin Conjugate Adsorption on Arkansas River Sand

Adsorption isotherms using dextran-eosin conjugate (DEC) on clean Arkansas River sand (ARS) and ARS spiked with varying amounts of naphthalene were performed to establish the antibody testing methodology. These isotherms showed a decreased adsorption ability of the sand spiked with naphthalene in proportion to the amount of naphthalene present. Naphthalene being electrically neutral, adsorbs hydrophobically and forms a barrier to adsorption where it is present.

## DEC Adsorption on Ottawa Sand

Isotherms using Ottawa sand as the adsorbent demonstrated that Ottawa sand has significantly less adsorptive capacity than ARS. Ottawa sand spiked with naphthalene showed a trend reversal in residual DEC concentration. This trend reversal occurred because desorption of the naphthalene was greater at lower sand dosages, leaving more available space for DEC adsorption.

## DEC as an Indicator for Total Petroleum Hydrocarbons

The use of DEC as an indicator for TPH was considered due to the results of the isotherms with naphthalene-spiked sand. Using DEC as an indicator for TPH is complicated by the complexity of the possible contaminants. Although DEC adsorption was inhibited by naphthalene adsorption, the presence of Arab crude oil which contains more aliphatics, particularly paraffins, than aromatics, actually caused an increase in adsorption of DEC. A first order relationship between crude oil content and adsorption of DEC exists only in a very narrow range of crude oil content. Only in this range is a qualitative measurement possible.

## Anti-naphthalene Antibody and Anti-Pyrene Antibody Adsorption

Isotherm comparisons using anti-naphthalene antibody as the adsorbate showed significantly less adsorption of the antibody from solution when the sand was spiked with naphthalene as did the DEC adsorption experiments. Increasing the naphthalene spiking level further decreased antibody adsorption. A negative control antibody determined by SDI to be non-reactive to PAH's was used in an isotherm comparison with anti-pyrene antibody on pyrene-spiked sand. The results showed essentially no difference between the adsorption of the two antibodies.

## Commercially Available PAH Test Kits

Two commercially available PAH-specific immunoassay field test kits were tested for accuracy and ease of use. The results of the tests were poor at best. EnSys, Inc. claims a 95% accuracy for its kit, which gives its answer in terms of broad ranges. The limited number of tests that were performed could not confirm this claim since the one failure represented a large percentage of the number of tests. The result given in broad ranges limits its value. The Quantix system gave results as a single number in ppm that proved to be consistent in subsequent tests, although much lower than the actual values. Consistency of results make it possible to calibrate the test for a specific site. The Quantix system is the easier to use under field conditions and allows five samples to be run at one time. Both kits require extraction of soil samples prior to testing, which influences the accuracy. The extraction procedures were inadequate as was shown by trying to dissolve some typical PAH's in the solvent and by trying to extract from a clay soil. Costs for these two test kits are comparable at approximately \$500 for ten samples.



## BIBLIOGRAPHY

- Adamson, A. W. (1976). *Physical Chemistry of Surfaces*. 3rd ed., John Wiley & Sons, New York, N. Y., 698 pp.
- Benefield, Larry D., Judkins, Joseph F., and Weand, Barron L., (1982). *Process Chemistry for Water and Waste Water Treatment*. Prentice Hall, Inc., Englewood Cliffs, N. J., 510 pp.
- Brock, Thomas D., and Madigan, Michael T. (1988). *Biology of Microorganisms*. 5th ed., Prentice-Hall, Inc. Englewood Cliffs, N. J.
- Brock, Thomas D., and Madigan, Michael T. (1991). *Biology of Microorganisms*. 6th ed., Prentice-Hall, Inc. Englewood Cliffs, N. J., 874 pp.
- EnSys, Inc. (1994). Personal communications with technical staff.
- GIBCO BRL (1994). *Life Technologies, Inc. Catalogue*. P.O. Box 6009, Gaithersburg, MD 20897-8405.
- Guilbault, G. G. (1967). *Fluorescence: Theory, Instrumentation, and Practice*. Marcel Dekker, Inc., New York, N. Y.
- Guilbault, G. G. (1973). *Practical Fluorescence: Theory, Methods and Techniques*. Marcel Dekker, Inc., New York, N. Y.
- Hahn, A., Frumel, F., Haisch, A., Henkelmann, G., Hock, H. (1992). *Immunolabelling of Atrazine Residues in Soil*. 7. Pflanzenemahr. Bodenk. 155, 203-208.
- Harris, D.A., and Bashford, C. L., Eds. (1988). *Spectrophotometry & Spectrofluorimetry: A Practical Approach*. IRL Press, Washington D.C.
- Harlow, Ed I., Lane, David P. (1988). *Antibodies: A Laboratory Manual*. Cold Spring Harbor Laboratory, Cold Spring Harbor, N. Y., 726 pp.
- Hiemenz, P. C. (1977). *Principles of Colloid and Surface Chemistry*. Marcel Dekker, Inc., New York, N. Y., 592 pp.

- Hines, A. L., and Maddox, R. N. (1985). *Mass Transfer: Fundamentals and Applications*. Prentice-Hall, Inc. Englewood Cliffs, New Jersey.
- Kolodziej, Kent K. (1994). *Investigation by Solid Phase Fluorimetry of Rodamine-B Adsorption on Solid Surfaces*, Thesis Report, Oklahoma State University.
- Krahn, M. M., Ylitalo, J. J., and Chan, S. (1991). Rapid, Semi-quantitative Screening of Sediments for Aromatic Compounds using Sonic Extraction and HPLC/Fluorescence Analysis. *Marine Environmental Research*, 31, 175-196.
- Langmuir, I. (1918). Adsorption of Gases on Plain Surfaces of Glass, Mica, and Platinum. *Journal of American Chemical Society*, 40, 1361.
- Look, D. C., Jr., and Sauer, H. J., Jr., (1986). *Engineering Thermodynamics*. PWS Publishers, Boston, Massachusetts.
- Manes, M. (1980). The Polanyi Adsorption Potential Theory and its Applications to Adsorption from Water Solution onto Activated Carbon. In I. H. Suffet and M. J. McGuire, Eds. *Activated Carbon Adsorption of Organics from the Aqueous Phase. Volume I*. (pp. 43-64). Ann Arbor Science Publishers, Inc., Ann Arbor, MI.
- Manes, M., and Hofer, J. E. (1968). Application of the Polanyi Adsorption Potential Theory to Adsorption from Solution on Activated Carbon. *The Journal of Physical Chemistry*, 73 (3), 584-590.
- Molecular Probes, Inc. (1994). Personal communications with technical support staff.
- National Research Council (1983). *Identifying and Estimating the Genetic Impact of Chemical Mutagens*, National Academy Press, Washington, D. C.
- Roitt, I. M., Brostoff, J., and Male, D. K. (1985). *Immunology*. Gower Medical Publishing Ltd., London, 382 pp.
- Sawyer, C.N., and McCarty, P.L. (1978). *Chemistry for Environmental Engineering*, 3rd ed., McGraw-Hill, Inc.
- Stave, J. (1994). Strategic Diagnostics, Inc., Personal communications.
- Thomas, C. (Ed.) (1989). *Taber's Cyclopedic Medical Dictionary*. Philadelphia: F. A. Davis.
- Udenfriend, Sidney (1962). *Fluorescence Assay in Biology and Medicine*. 3rd ed., Academic Press, New York, N.Y.

Veenstra, J. N., (1993). Class notes.

Verschueren, K. (1983). *Handbook of Environmental Data on Organic Chemicals*. 2nd ed., Van Nostrand Reinhold, New York, N. Y.

APPENDIX A

ISOTHERMS

TABLE XII

## ANTI-NAPHTHALENE ANTIBODY ON CLEAN ARS

Sample No.	Ab-EITC Sol. (grams)	Ab-EITC Sol. (ml)	Sand Dosage (grams)	Emissions Curve Area (v-nm)	Residual Concentration (mg/l EITC)	Adsorbed Concentration (gm/gm)
Co	0		0	0.365	1	
1	2.968	2.968	2.417	0.129	0.354	7.93E-07
2	2.982	2.982	2.165	0.156	0.427	7.89E-07
3	2.988	2.988	1.857	0.168	0.460	8.69E-07
4	2.993	2.993	1.579	0.168	0.460	1.02E-06
5	3.010	3.010	1.276	0.196	0.537	1.09E-06
6	2.980	2.980	0.926	0.212	0.581	1.35E-06
7	2.956	2.956	0.658	0.225	0.616	1.72E-06
8	2.999	2.999	0.314	0.235	0.643	3.41E-06

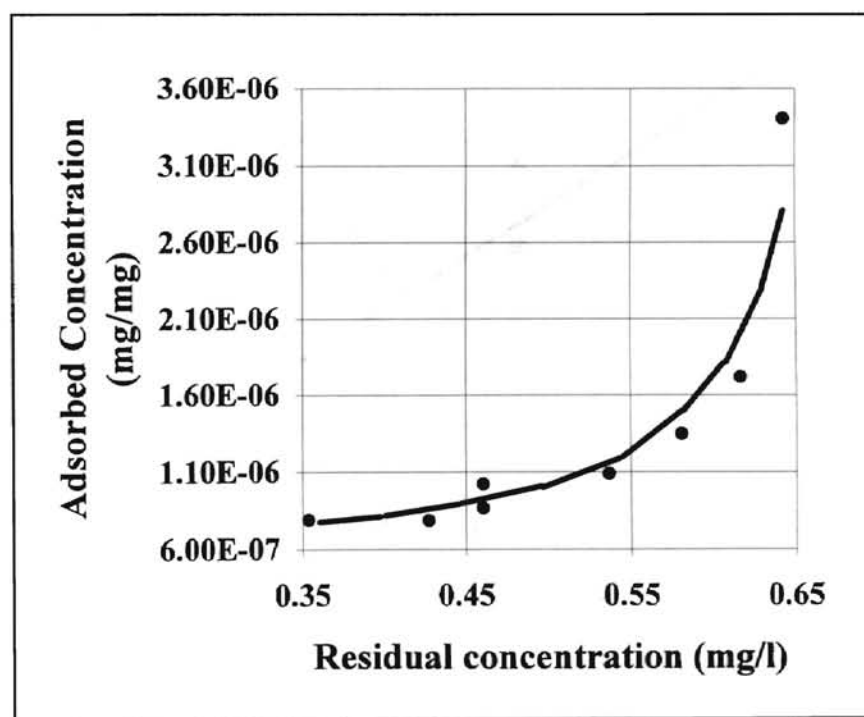


Figure A.1: Cross plot of isotherm data for anti-naphthalene antibody on ARS.

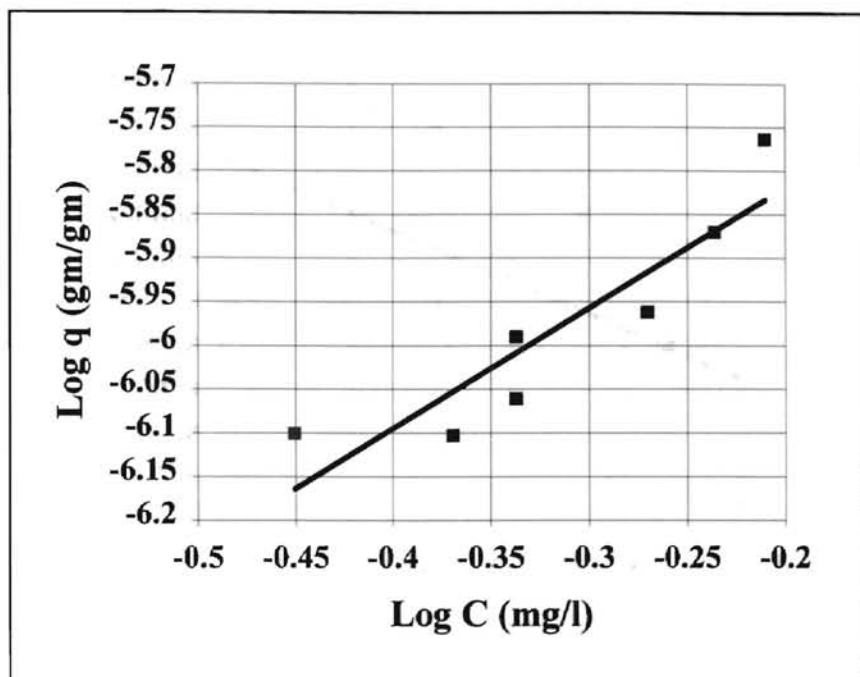


Figure A.2: Freundlich isotherm of anti-naphthalene antibody.  $r^2 = 0.83$

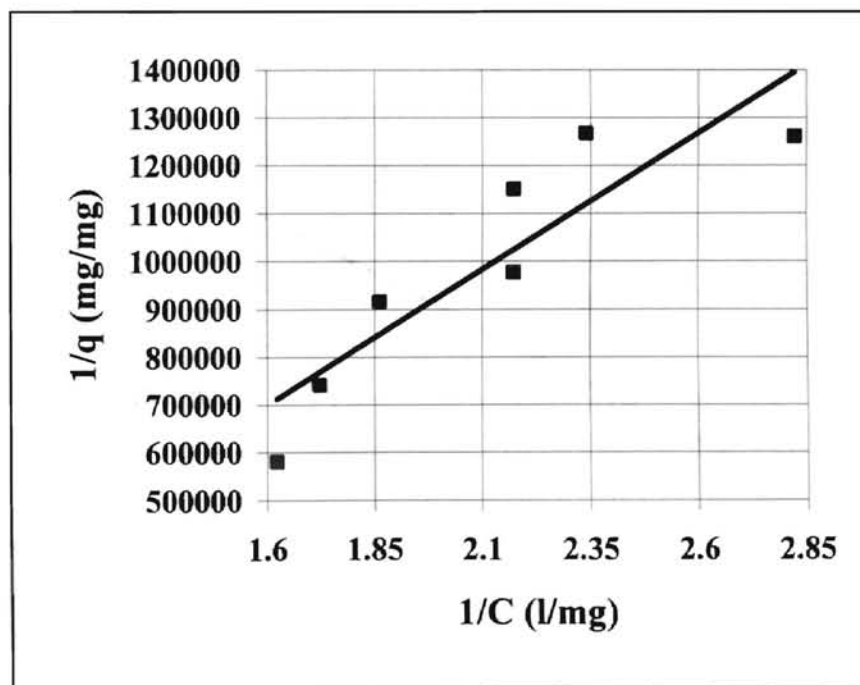


Figure A.3: Langmuir high isotherm of anti-naphthalene antibody on ARS.  $r^2 = 0.8$

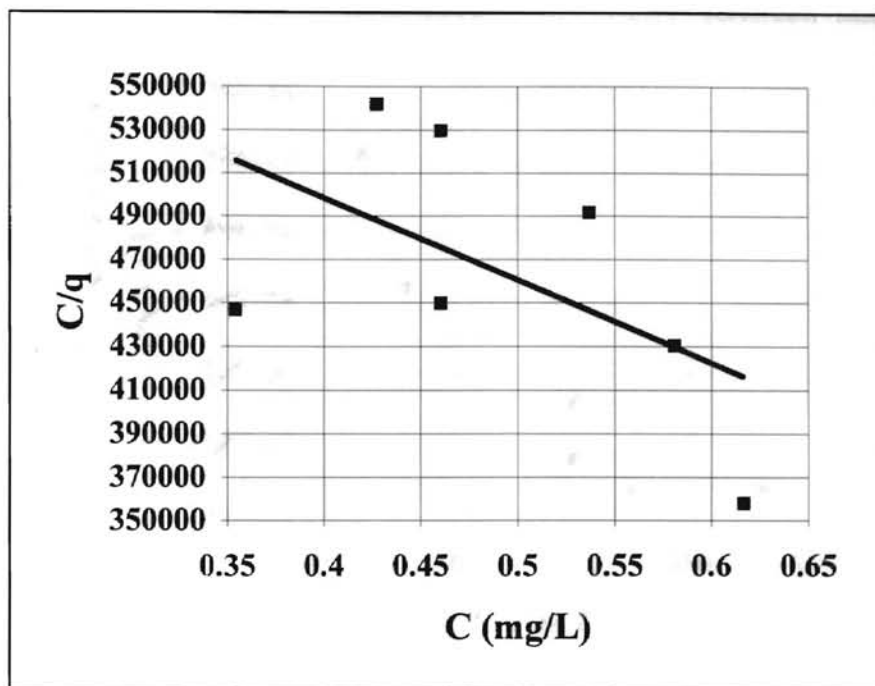


Figure A.4: Langmuir low isotherm of anti-naphthalene antibody on ARS.  $r^2 = 0.30$

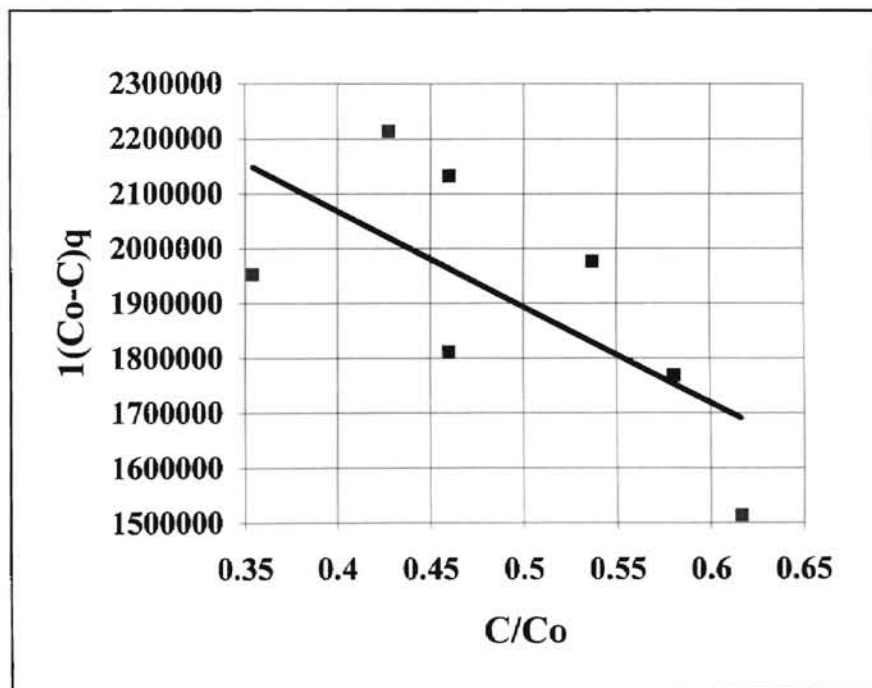


Figure A.5: BET isotherm of anti-naphthalene antibody on ARS.  $r^2 = 0.46$

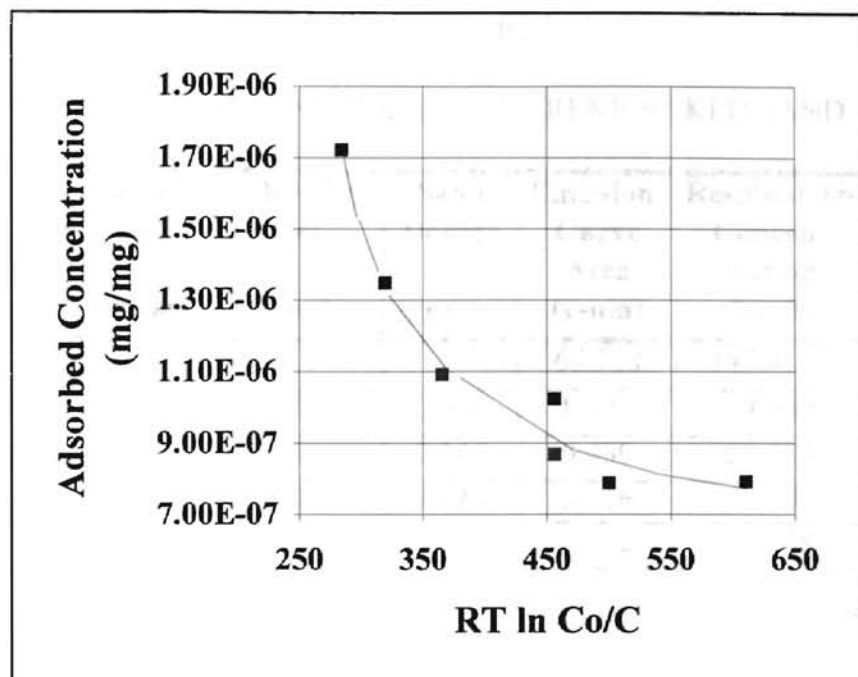


Figure A.6: Polanyi adsorption theory characteristic curve of anti-naphthalene adsorption isotherm on ARS.



TABLE XIII

## ANTI-PYRENE ANTIBODY ON PYRENE SPIKED SAND

Sample No.	Ab-EITC Sol. (grams)	Ab-EITC Sol. (ml)	Sand Dosage (grams)	Emissions Curve Area (v-nm)	Residual Ab Concentration (mg/l)	Adsorbed Concentration (gm/gm)
Co	0		0	67.768	147.4131	
1	2.983	2.939	2.450	8.339	18.140	1.55E-04
2	3.026	2.981	2.146	9.439	20.532	1.76E-04
3	3.006	2.962	1.848	8.416	18.307	2.07E-04
4	3.023	2.978	1.539	9.492	20.648	2.45E-04
5	3.018	2.973	1.232	10.586	23.027	3.00E-04
6	3.005	2.960	0.977	9.551	20.776	3.84E-04
7	3.009	2.964	0.686	10.646	23.158	5.37E-04
8	3.013	2.968	0.305	9.605	20.893	1.23E-03

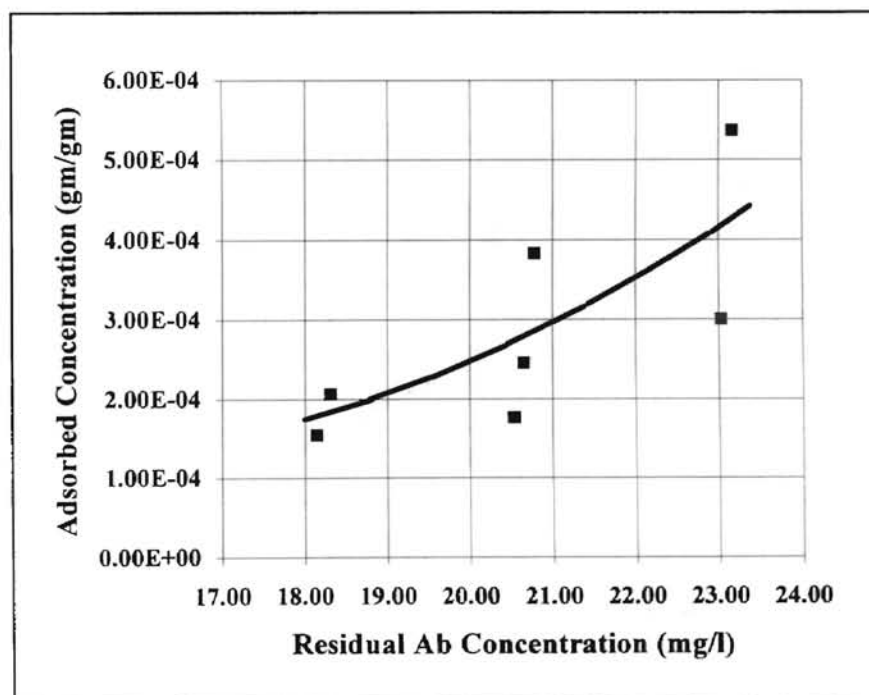


Figure A.7: Cross plot of isotherm data for Anti-Pyrene antibody on pyrene spiked ARS

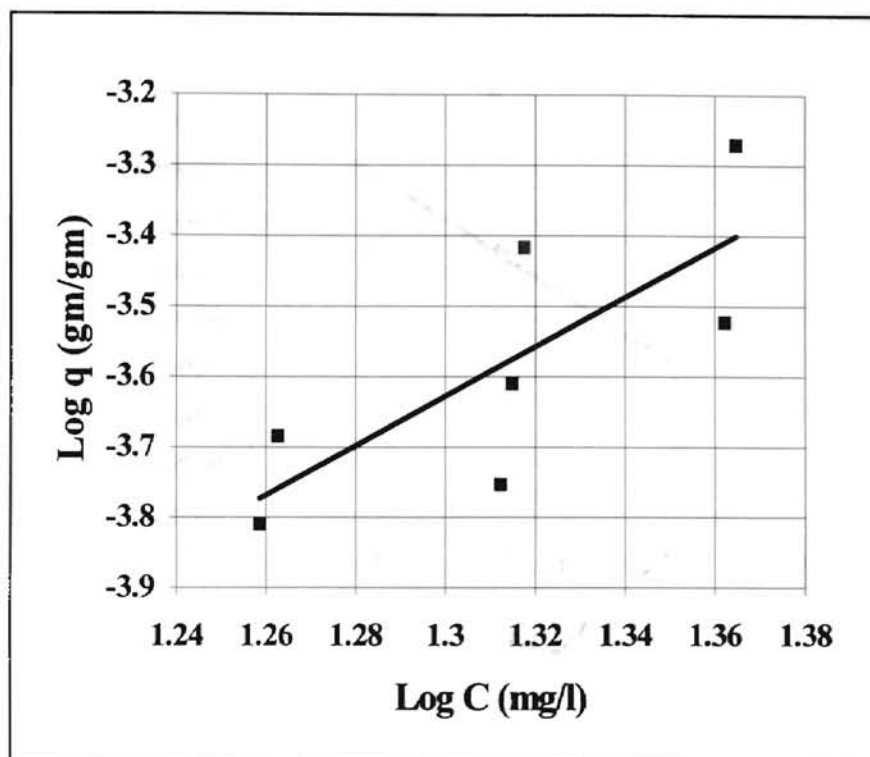


Figure A.8: Freundlich isotherm plot of Anti-Pyrene antibody on ARS spiked with Pyrene.  $r^2 = 0.60$

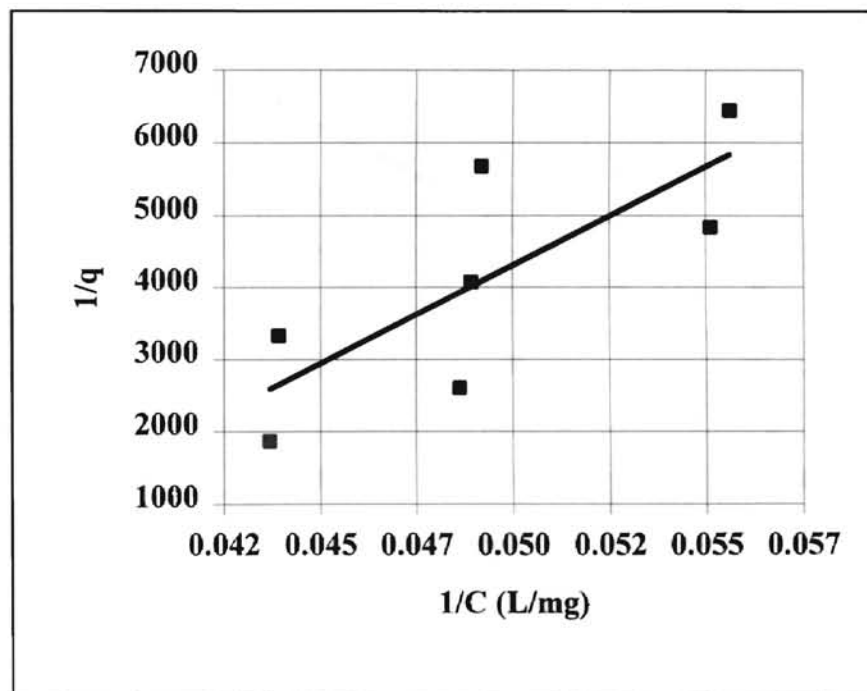


Figure A.9: High Langmuire isotherm of Anti-Pyrene antibody on ARS spiked with pyrene.  $r^2 = 0.61$

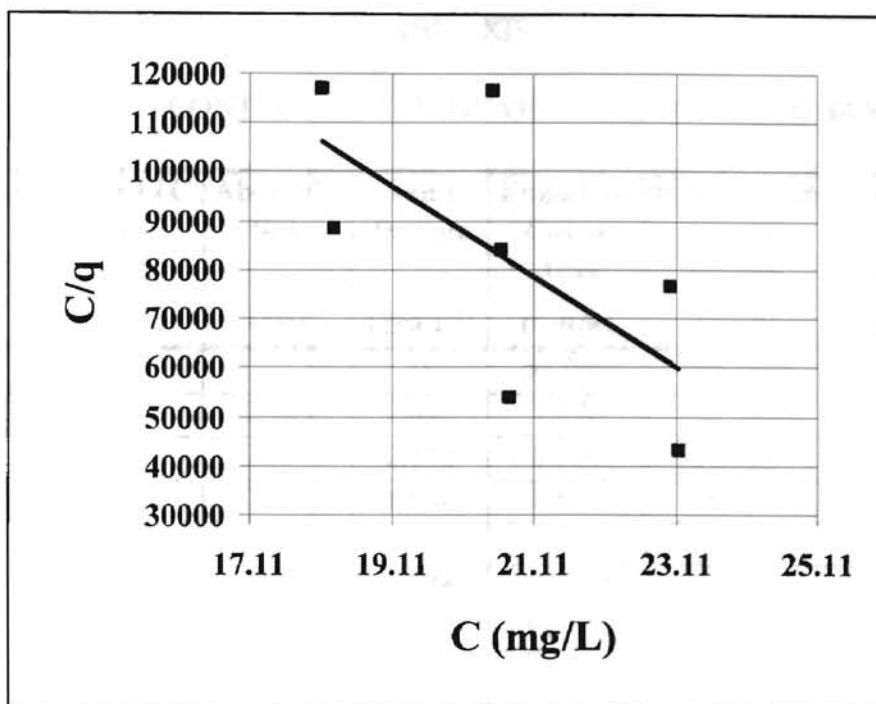


Figure A.10: Low Langmuire isotherm of Anti-Pyrene antibody on ARS spiked with pyrene.  $r^2 = 0.43$

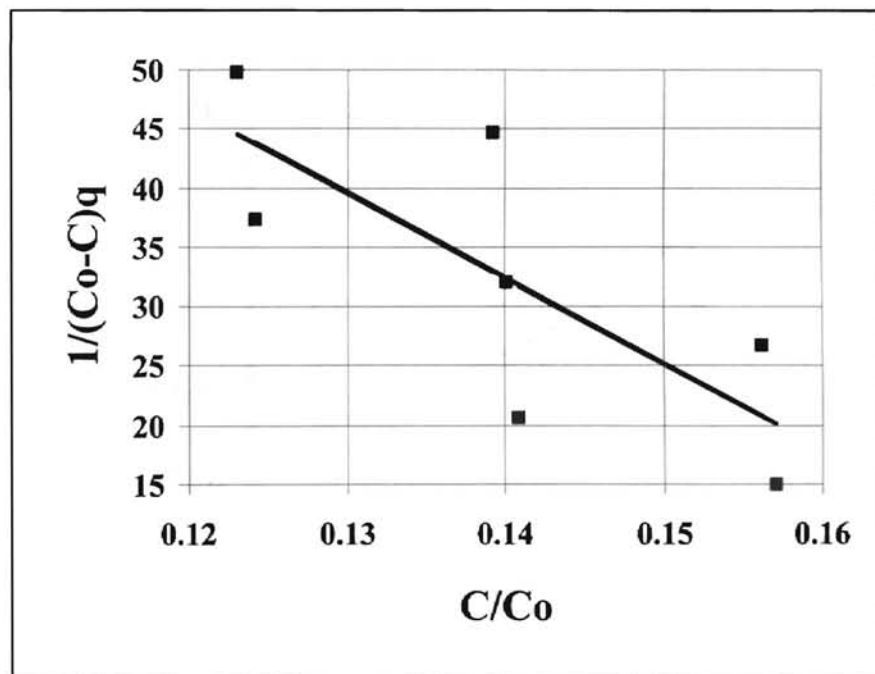


Figure A.11: BET isotherm of Anti-Pyrene antibody on ARS spiked with pyrene.  $r^2 = 0.59$

TABLE XIV

## NEGATIVE CONTROL ANTIBODY ON PYRENE SPIKED SAND

Sample No.	Ab-EITC Sol. (grams)	Ab-EITC Sol. (ml)	Sand Dosage (grams)	Emissions Curve Area (v-nm)	Residual Ab Concentration (mg/l)	Adsorbed Concentration (gm/gm)
Co	0		0	66.056	147.449	
Cont-1	2.991	2.943	2.448	7.776	17.357	1.56E-04
Cont-2	3.005	2.957	2.142	8.314	18.558	1.78E-04
Cont-3	3.024	2.975	1.838	8.537	19.056	2.08E-04
Cont-4	3.022	2.973	1.516	9.865	22.020	2.46E-04
Cont-5	3.006	2.958	1.238	10.369	23.145	2.97E-04
Cont-6	3.023	2.975	0.934	10.395	23.204	3.96E-04
Cont-7	3.020	2.972	0.642	10.416	23.250	5.75E-04
Cont-8	3.021	2.972	0.376	10.094	22.532	9.88E-04

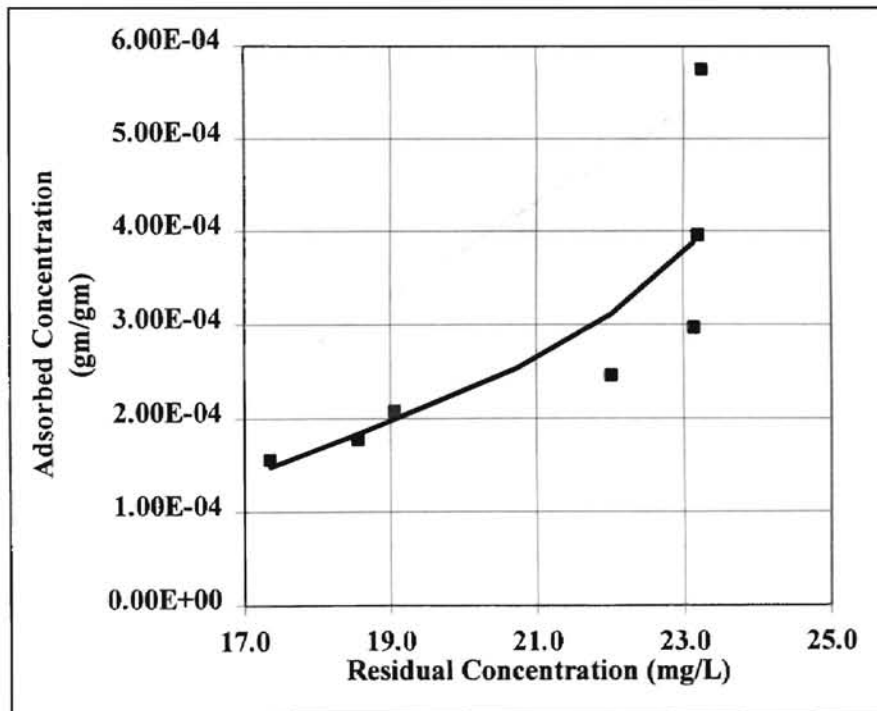


Figure A.12: Cross plot of isotherm data for Negative Control antibody on pyrene spiked ARS.

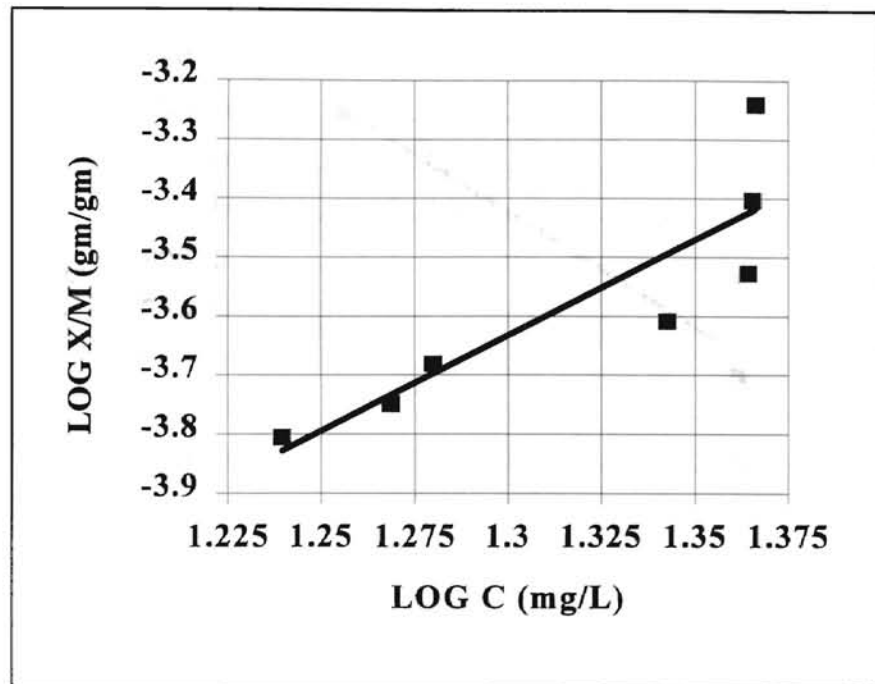


Figure A.13: Freundlich isotherm plot of Negative Control antibody on ARS spiked with Pyrene.  $r^2 = 0.76$

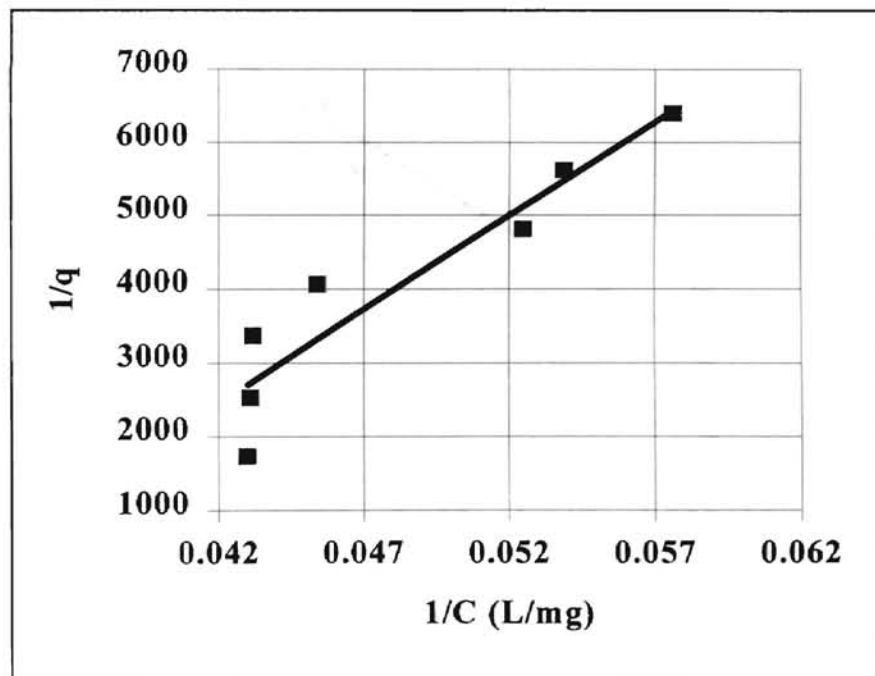


Figure A.14: High Langmuire isotherm of Negative Control antibody on ARS spiked with pyrene.  $r^2 = 0.88$

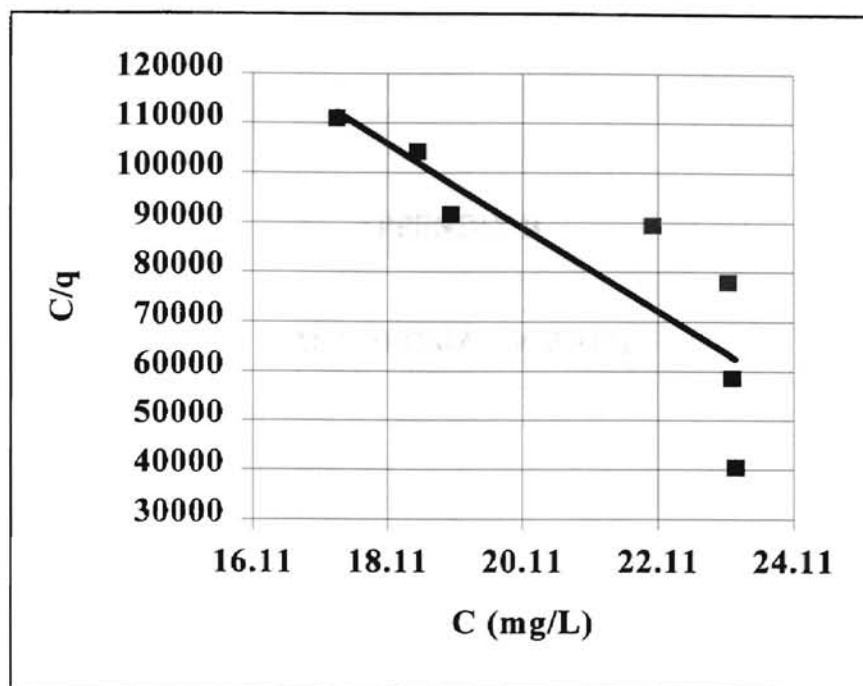


Figure A.15: Low Langmuire isotherm of Negative Control antibody on ARS spiked with pyrene.  $r^2 = 0.73$

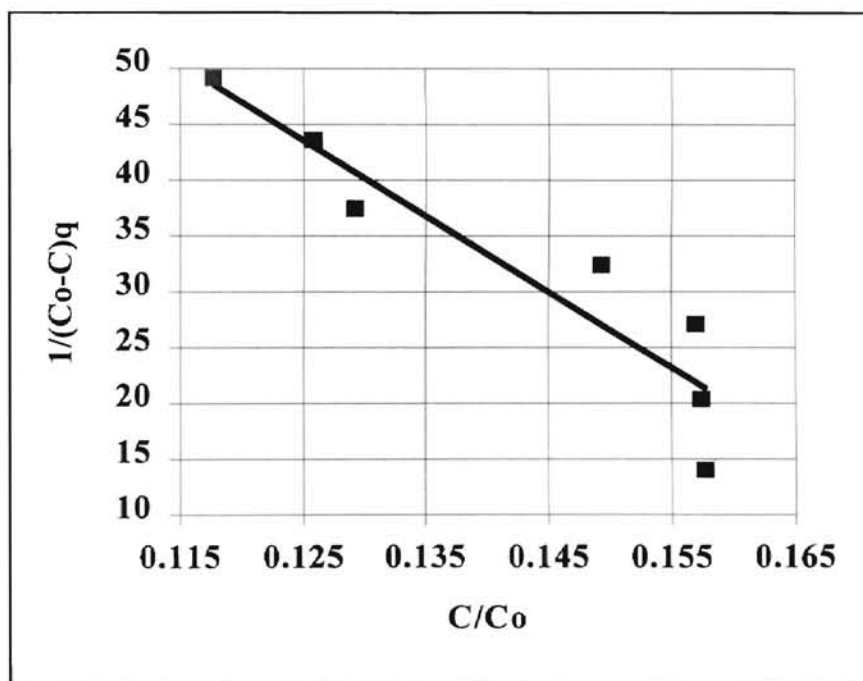


Figure A.16: BET isotherm of Negative Control antibody on ARS spiked with pyrene.  $r^2 = 0.87$

APPENDIX B

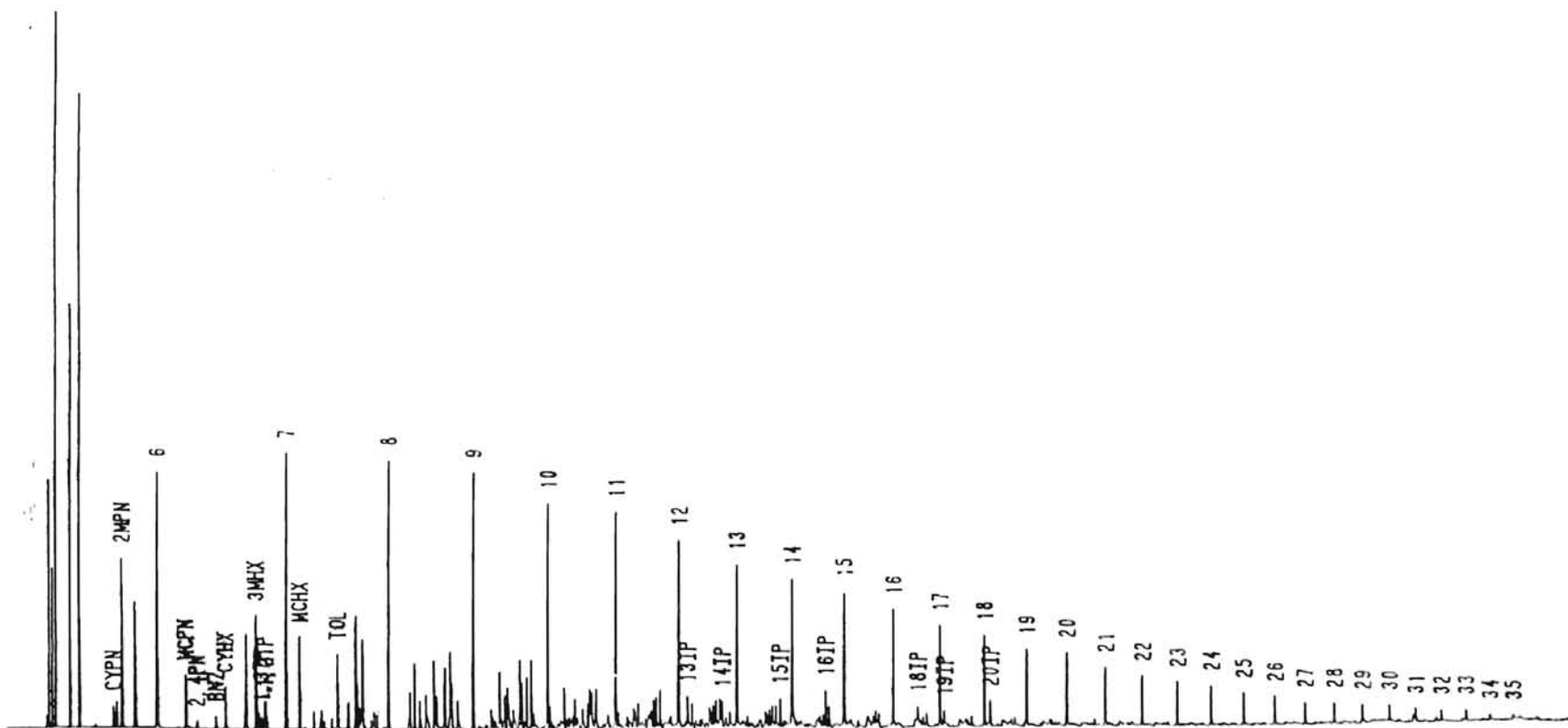
GAS CHROMATOGRAPH

# Geochemistry Analysis/Research

Analysis Name : [ANALYSES] 2 A040794, 2, 1.

ARAB MEDIUM CRUDE OIL      Amount : 0.500

66





APPENDIX C

ANTIBODY REACTIVITY DATA

PROVIDED BY STRATEGIC DIAGNOSTICS, INC.

January 6, 1994

Al Talley  
AMOCO

Dear Al:

Enclosed please find data demonstrating the reactivity of the antibody reagents we sent you to PAH along with a couple of figures illustrating the formats of the assays by which these data were derived. Let me know how you're doing.

Sincerely,

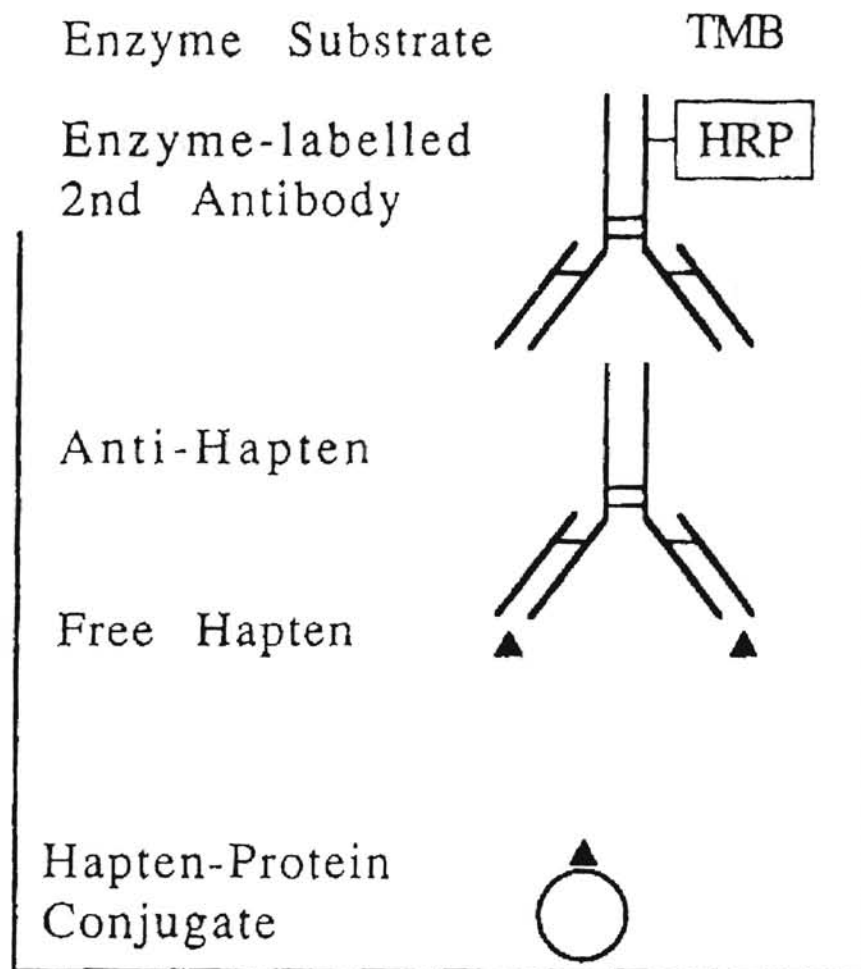
*James W. Stave*

James W. Stave

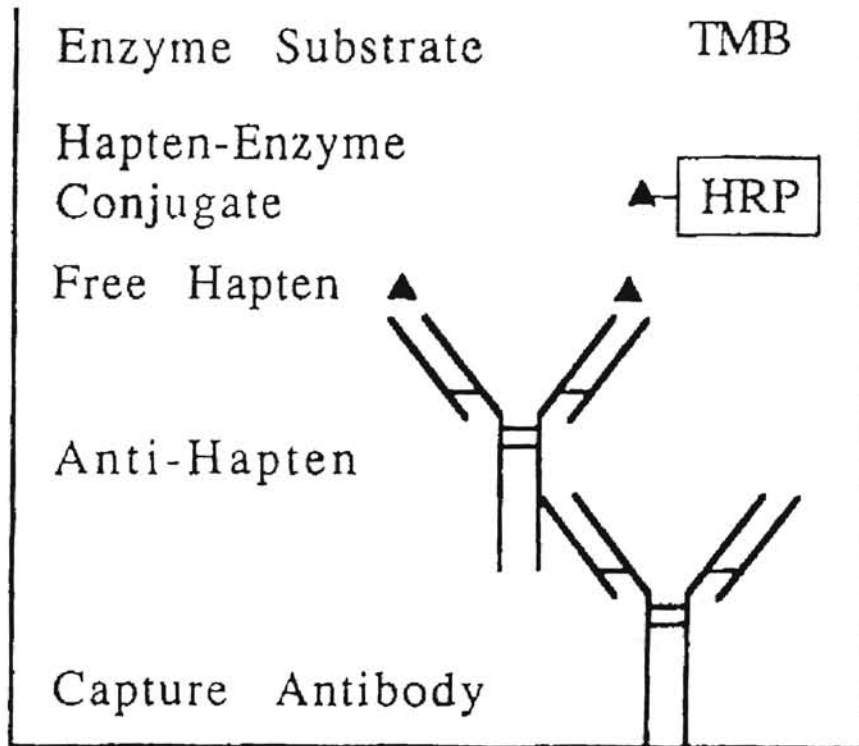


STRATEGIC DIAGNOSTICS INC. • 129 Sandy Drive • Newark, DE 19713-1147 • (302) 456-6789 • FAX (302) 456-6770

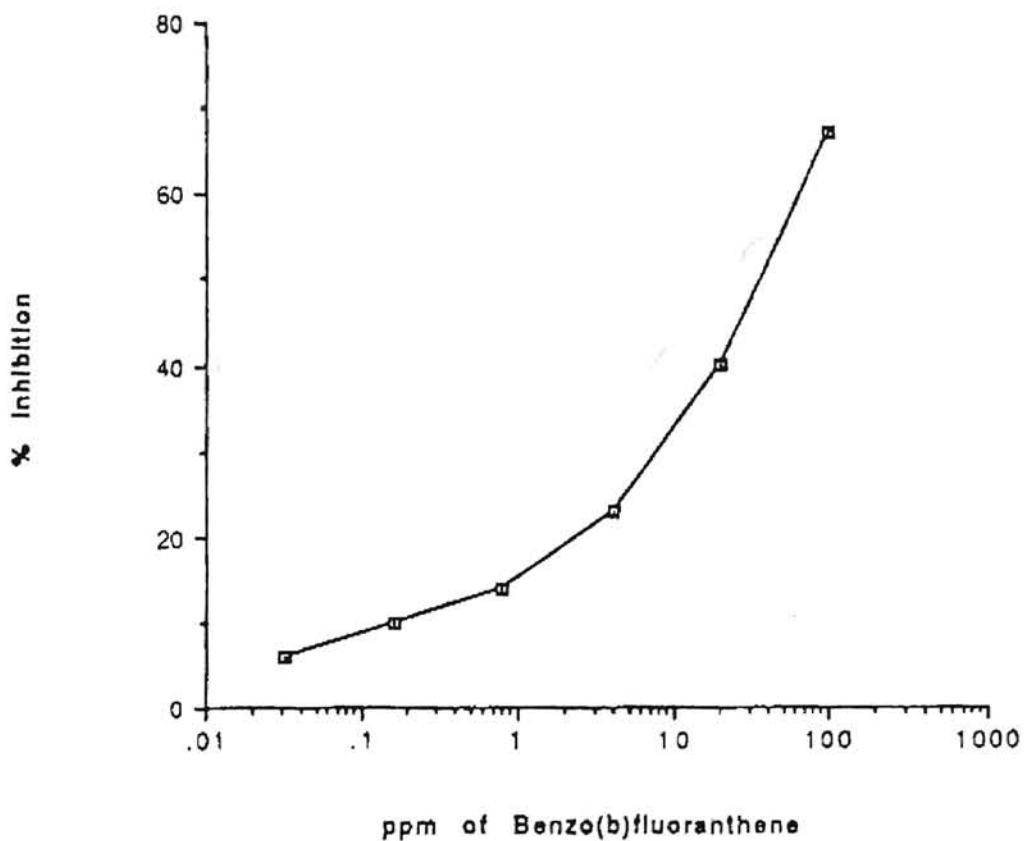
## Antigen-Coated Plate Competition ELISA



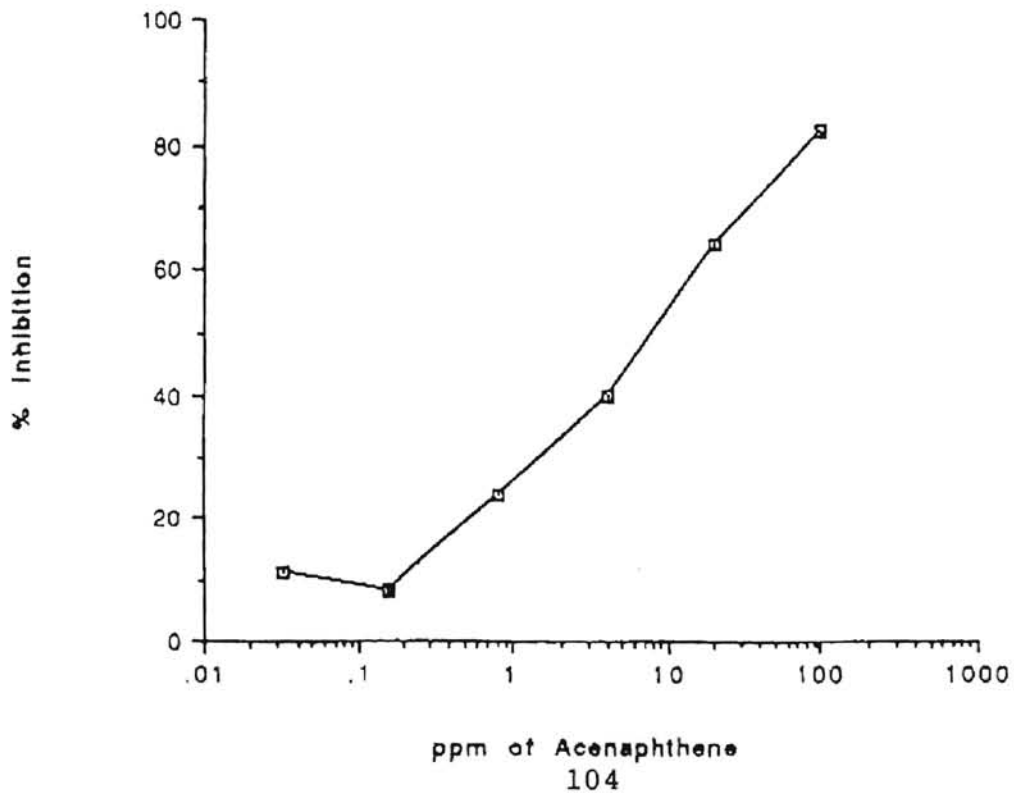
## Labelled Analyte Competition ELISA



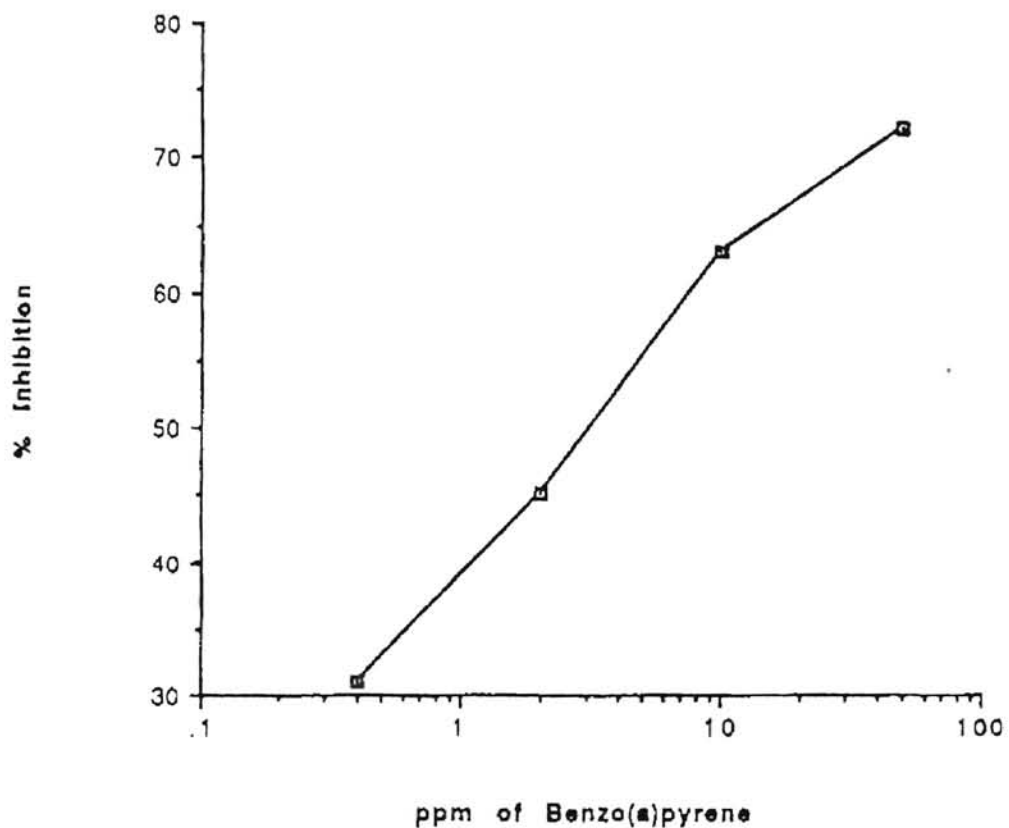
Benzo(b)fluoranthene Inhibition ELISA  
Antisera 186-8



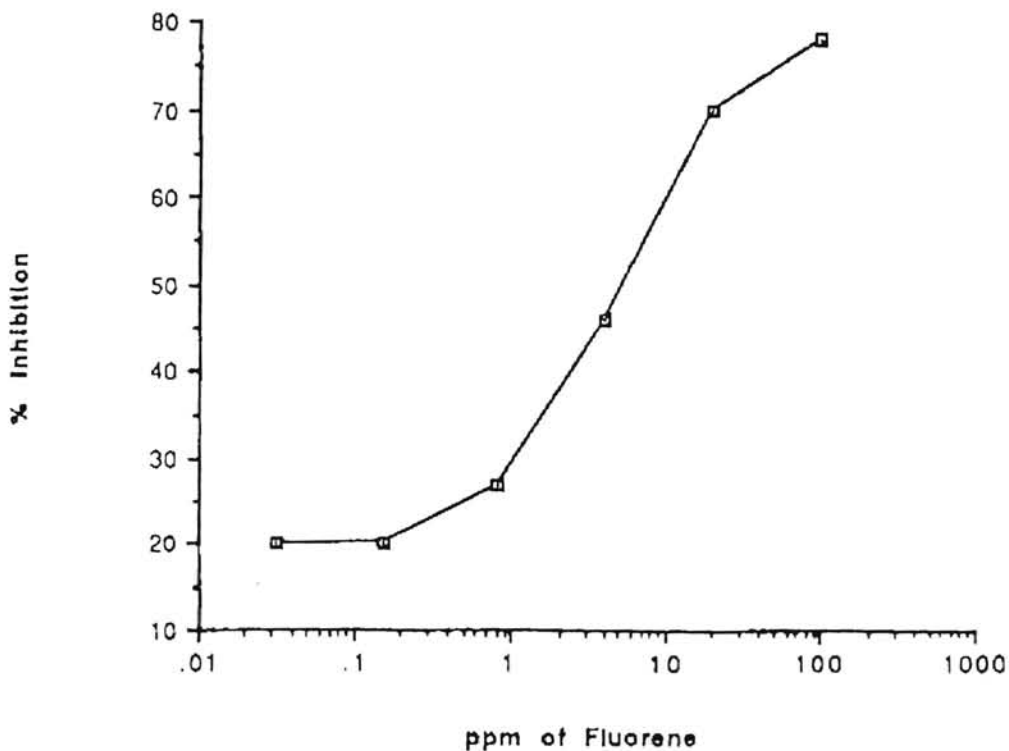
Acenaphthene Inhibition ELISA  
Antisera 186-8



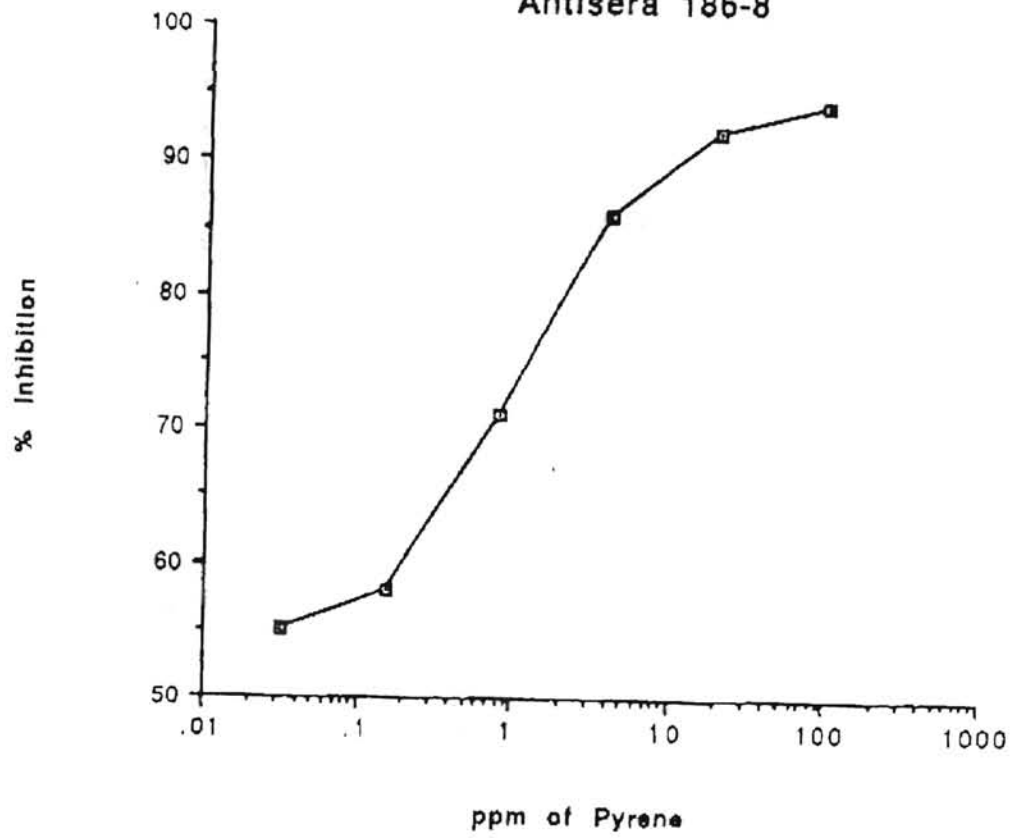
### Benzo(a)pyrene Inhibition ELISA 186-8 Antisera



### Fluorene Inhibition ELISA Antisera 186-8



Pyrene Inhibition ELISA  
Antisera 186-8



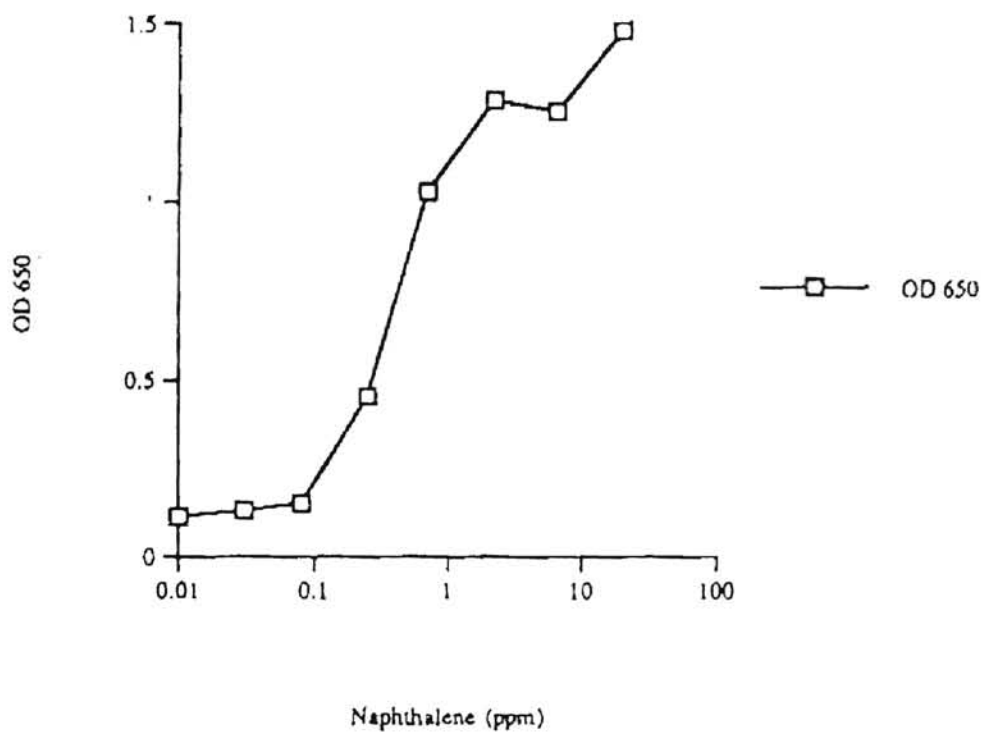
## Cross Reactivity Comparison

PAH	Pyrene-AP	Anthracene-AP	Fluorene-AP	Chrysene-AP
Pyrene	100	100	25	33
Fluorene	1	2.8	100	22
Fluoranthene	10	200		
Naphthalene	<1	25	1	28
Acenaphthylene	1	10	40	100
Benzo(a)anthracene*	1	1	3.3	16
Anthracene	<1	6.6	33	25
Benzo(a)pyrene*	2.5	100	160	20
Indenopyrene*	1	7.5	250	100
Benzo(k)fluoranthene*	<1	6.6	<1	<1
Dibenz(a,h)anthracene*	<1	ND	10	9
Benzo(g,h,i)perylene	<1	100	66	50
Chrysene*	<1	7.5	140	10
Benzo(b)fluoranthene*	<1	15	50	10
Acenaphthene	1	10	40	100
Phenanthrene	ND	ND	ND	ND
Dimethylnaphthalene				
Tetrahydroxynaph.				

\* Carcinogenic PAHs



## Naphthalene Inhibition of N1 Monoclonal



VITA 

Allen G. Talley

Candidate for the Degree of

Master of Science

Thesis: DETECTION OF BOUND POLYCYCLIC AROMATIC  
HYDROCARBON RESIDUALS IN SOILS THROUGH DIRECT  
IMMUNOASSAY: A FEASIBILITY STUDY

Major Field: Environmental Engineering

Biographical:

Education: Graduated from Olathe High School, Olathe, Kansas in May 1964; received Bachelor of Science degree in Geophysics from Kansas State University, Manhattan, Kansas in May 1969. Completed the requirements for the Master of Science degree with a major in Environmental Engineering at Oklahoma State University in May 1996.

Experience: Entered the United States Air Force as Second Lieutenant in 1969; served as Aircraft Maintenance Officer and was honorably discharged as Captain in 1973; employed by Texaco, Inc. as an exploration geophysicist in 1973, promoted to Exploration Project Manager; left Texaco to join Robinowitz Oil Company as Exploration Manager from 1981 to 1983; employed by Santa Fe Minerals in 1983 as Senior Geophysicist and served as District Geophysicist from 1985 to 1991; formed G&G Associates, Inc., Geological and Geophysical consultants from 1991 to 1994; employed by Williams Energy Ventures as Environmental/Geophysical Engineer in 1994; employed by Williams Field Services as Environmental/Geophysical Engineer in 1995 and Senior Environmental Specialist, 1996 to present.

Professional Memberships: Sigma Gamma Epsilon Geologic Honorary, Society of Exploration Geophysicists, Institute of Hazardous Materials Management.